Molecular Therapy
Original Article

Safety, Tumor Reduction, and Clinical Impact of Zika Virus Injection in Dogs with Advanced-Stage Brain Tumors

Carolini Kaid,[1] Raquel Azevedo dos Santos Madi,[2] Renato Astray,[3] Ernesto Goulart,[1] Luiz Carlos Caires-Junior,[1] Thiago Giove Mitsugi,[1] Ana Carolina Ramos Moreno,[4] Maria Fernanda Castro-Amarante,[4] Lennon Ramos Pereira,[4] Bruna Felício Milazzotto Maldonado Porchia,[5] Thais Oliveira de Andrade,[1] Vivian Landini,[1] Daniel Soares Sanches,[6] Carolina Gonçalves Pires,[6] Rubens Koji Oliveira Tanioka,[2] Marcia C.L. Pereira,[1] Igor Neves Barbosa,[1] Cristina O. Massoco,[7] Luís Carlos de Souza Ferreira,[4] Oswaldo Keith Okamoto,[1,8] and Mayana Zatz[1]

[1]Human Genome and Stem Cell Research Center (HUG-CEL) Institute of Biosciences, University of São Paulo, Cidade Universitária, São Paulo 055080-090, Brazil; [2]Hospital Veterinário Granja Viana, Granja Viana 06345-410, Brazil; [3]Butantan Institute, São Paulo 05503-900, Brazil; [4]Vaccine Development Laboratory, Biomedical Sciences Institute, Department of Microbiology, University of São Paulo, São Paulo 05508-900, Brazil; [5]Laboratory of Tumor Immunology, Department of Immunology, Institute of Biomedical Sciences, University of São Paulo, São Paulo 05508-900, Brazil; [6]Veterinary Pathological Anatomy Center. São Paulo 05376-070, Brazil; [7]Department of Pathology, School of Veterinary Medicine and Animal Science, University of São Paulo, São Paulo 05508-270, Brazil; [8]Hemotherapy and Cellular Therapy Department, Hospital Israelita Albert Einstein, São Paulo 05652- 900, Brazil

Malignant brain tumors are among the most aggressive cancers with poor prognosis and no effective treatment. Recently, we reported the oncolytic potential of Zika virus infecting and destroying the human central nervous system (CNS) tumors *in vitro* and in immunodeficient mice model. However, translating this approach to humans requires pre-clinical trials in another immunocompetent animal model. Here, we analyzed the safety of Brazilian Zika virus ($ZIKV^{BR}$) intrathecal injections in three dogs bearing spontaneous CNS tumors aiming an anti-tumoral therapy. We further assessed some aspects of the innate immune and inflammatory response that triggers the anti-tumoral response observed during the $ZIKV^{BR}$ administration *in vivo* and *in vitro*. For the first time, we showed that there were no negative clinical side effects following $ZIKV^{BR}$ CNS injections in dogs, confirming the safety of the procedure. Furthermore, the intrathecal $ZIKV^{BR}$ injections reduced tumor size in immunocompetent dogs bearing spontaneous intracranial tumors, improved their neurological clinical symptoms significantly, and extended their survival by inducing the destruction specifically of tumor cells, sparing normal neurons, and activating an immune response. These results open new perspectives for upcoming virotherapy using ZIKV to destroy and induce an anti-tumoral immune response in CNS tumors for which there are currently no effective treatments.

INTRODUCTION

Central nervous system (CNS) tumors are mostly malignant with a world incidence rate of 3.5 million (GLOBOCAN 2018). Despite aggressive current therapies, including surgery, radiation, and chemotherapy, the most common forms of adult and pediatric primary brain tumors remain lethal.[1] The treatment is not effective and surviving patients present important side effects that affect their quality of life.[2] Therefore, novel treatment options are urgently needed.

Since the approval of the first oncolytic virotherapy, T-VEC, in 2015, the search for viruses capable of infecting and destroying cancer cells has been growing. Recently, the Zika virus (ZIKV) has been reported as an oncolytic virus that infects and destroys cancer cells from CNS tumors. In glioblastoma, a study showed that ZIKV can oncolysis murine brain tumors and infect human glioblastoma (GBM) stem-like cell lines but at high concentrations of the virus.[3]

Our group demonstrated for the first time that the Brazilian ZIKV ($ZIKV^{BR}$) also has oncolytic activity against human embryonal CNS tumor cell lines, resulting in a massive tumor cell death 3 days after infection.[4] Furthermore, in a pre-clinical study in BALB/c nude mice bearing orthotopic human embryonal CNS tumor xenografts, we showed that a single intracerebroventricular injection of $ZIKV^{BR}$ significantly increased survival, decreased tumor burden, and reduced metastasis with a complete remission in some animals.[4] However, before translating this approach to humans, several questions need to be addressed in particular about safety and ZIKV oncolytic potential in a larger immunocompetent animal model for CNS tumors.

In cancer research, canine clinical trials have been performed before or in parallel with human clinical trials to assess safety, novel drug

Received 29 November 2019; accepted 6 March 2020;
https://doi.org/10.1016/j.ymthe.2020.03.004.

Correspondence: Mayana Zatz, Human Genome and Stem Cell Research Center (HUG-CEL) Institute of Biosciences, University of São Paulo, Cidade Universitária, São Paulo 055080-090, Brazil.
E-mail: mayazatz@usp.br

Table 1. Dogs' Characteristics

Dogs	Breed	Sex	Age	Body Weight	Diagnosis Prior to ZIKV Treatment[a]	Tumor Location
PIRATA	Pitbull	male	13	26 Kg	multicentric tumor / Meningioma	right ventrolateral region /Right frontoparietal lobe
MATHEUS	Boxer	male	8	32 Kg	oligodendroglioma	the right intra-axial parietal lobe
NINA	Dachshund	female	12	6.4 Kg	meningioma	left intra-axial parietal lobe

[a]Diagnosis was based on a combination of clinical signs and characteristic appearance on MRI. Tumor biopsy for histopathological diagnosis was confirmed post-mortem.

efficiency, and pharmacokinetics.[5] Canine intracranial malignancies develop spontaneously in older dogs with an intact immune system.[6] Human and canine primary brain tumors present clinical and high histological similarities, allowing the translation of canine clinical trials into new therapies.[7] Furthermore, dogs' spontaneous gliomas share key molecular and histopathological features with human gliomas that are absent in rodents.[8] In addition, the significant homology of the immune system and social environment between dogs and humans highlights the translational potential of a veterinary clinical trial using dogs with spontaneous intracranial tumors for a ZIKV oncolytic therapy.[9,10]

Intracranial neoplasia in dogs is prevalent in older and larger breed dogs, such as Boxer, Pug, and Bulldog but can also occur in other races.[11] The wide variability in dogs' breed, sizes, ages, and type of CNS tumors turns difficult to design a controlled study with a large and uniform group of animals. Furthermore, brain tumor diagnosis by magnetic resonance imaging (MRI) in dogs usually is identified in advanced stages and the type of tumor confirmed only during the autopsy. Despite these difficulties, immunocompetent dogs with naturally occurring brain tumors represent the best candidates for oncolytic ZIKV therapy studies because various publications indicate that oncolytic viruses can replicate and lyse canine cancer cells in culture.[12]

Here, we report our observations on the effect of ZIKV^{BR} injections in dogs severely disabled due to large brain tumors. Intrathecal injections of ZIKV^{BR} particles showed no side effects associated to ZIKV infection, reduced tumor size and significantly improved neurological clinical symptoms, extending survival. Additionally, the high influx of monocytes and microglia into the tumor microenvironment, as well as the *in vitro* activation of monocytes in co-cultures with tumor cells and ZIKV^{BR}, strongly suggests the immunotherapeutic potential of ZIKV in brain tumors.

RESULTS

Case One

The study included three dogs with different characteristics as summarized in Table 1. The first case was a 13-year-old male Pitbull dog presenting with seizure and total decubitus. A neurological examination revealed stupor consciousness levels, left decubitus position, total absence of locomotion, left nasal sensitive deficiency, bilateral papilledema, and postural reaction deficits indicating a lesion involving the left thalamo cortex and the brain stem. The MRI images confirmed two lesions, the first a possible multicentric tumor in the brain white matter in the left frontoparietal lobe region and the second a possible meningioma in the right ventrolateral side of the brain stem (Data S1). The complete blood count (CBC) showed low levels of leukocytes indicating an immunodeficiency clinical condition (Data S2).

First, we tested ZIKV^{BR} infection in the Pitbull dog by intrathecal injection of 1×10^6 viral particles. In adult humans, the main symptoms of ZIKV systemic infection are arthralgia, fever, myalgia, and generalized weakness.[13] We expected to see in the dogs the same symptoms as observed in the adult humans, as well as unspecific symptoms associated with other pathogens infection, namely vomiting, joint pain, and diarrhea. However, the dogs did not show any of these or other new clinical symptoms after ZIKV injection. On the contrary, all dogs improved their clinical neurologic symptoms. No clinical symptoms of viral infection were observed, and the Pitbull dog restored its capability to eat independently, raise and support the head 1 week after ZIKV^{BR} infection, and stand with support (Video S1). 18 days after the ZIKV injection, the Pitbull dog showed a sudden clinical worsening, pneumonia, and complications secondary to prolonged decubitus and was submitted to euthanasia, as requested by the owners. The necroscopic examination confirmed a left ventricle hypertrophic cardiomyopathy as its major disease. Importantly, an X-ray exam performed 2 days before ZIKV injection showed an increased cardiac silhouette suggesting cardiomegaly and therefore unlikely to be caused by ZIKV injection.

ZIKV^{BR} RNA quantified by RT-PCR in peripheral blood was found at day 3 in a decreased amount (4.446 copies/μL) when compared to the injected concentration of ZIKV at day 0 (1×10^6 particles) and it decreased until zero viral copies 9 days after ZIKV injection (Figure 1A). Viral titer in cerebrospinal fluid (CSF) was positive (182.18 copies/ μL) 1 week after ZIKV injection and decreased to zero at day 14 (Figure 1B). However, we observed higher levels of viral RNA in urine (1,357.56 copies/μL), kidney (4,636.44 copies/μL), and prostate (1,357.82 copies/μL) but particularly in testicles (1.08×10^8 copies/μL), which has been described before in human and mice models supporting a sexual transmission of ZIKV (Figure 1B).

Post-mortem confocal immunofluorescence (IF) analysis confirmed ZIKV^{BR}-positive immunolabeling in two CNS regions, the frontal lobe and the medulla (Figures 1C and 1D). Importantly, a more refined histopathological analysis on slides stained by hematoxylin and eosin (H&E), as well as immunohistochemistry (IHC) and IF, showed no ZIKV^{BR} infection in neurons from all CNS regions

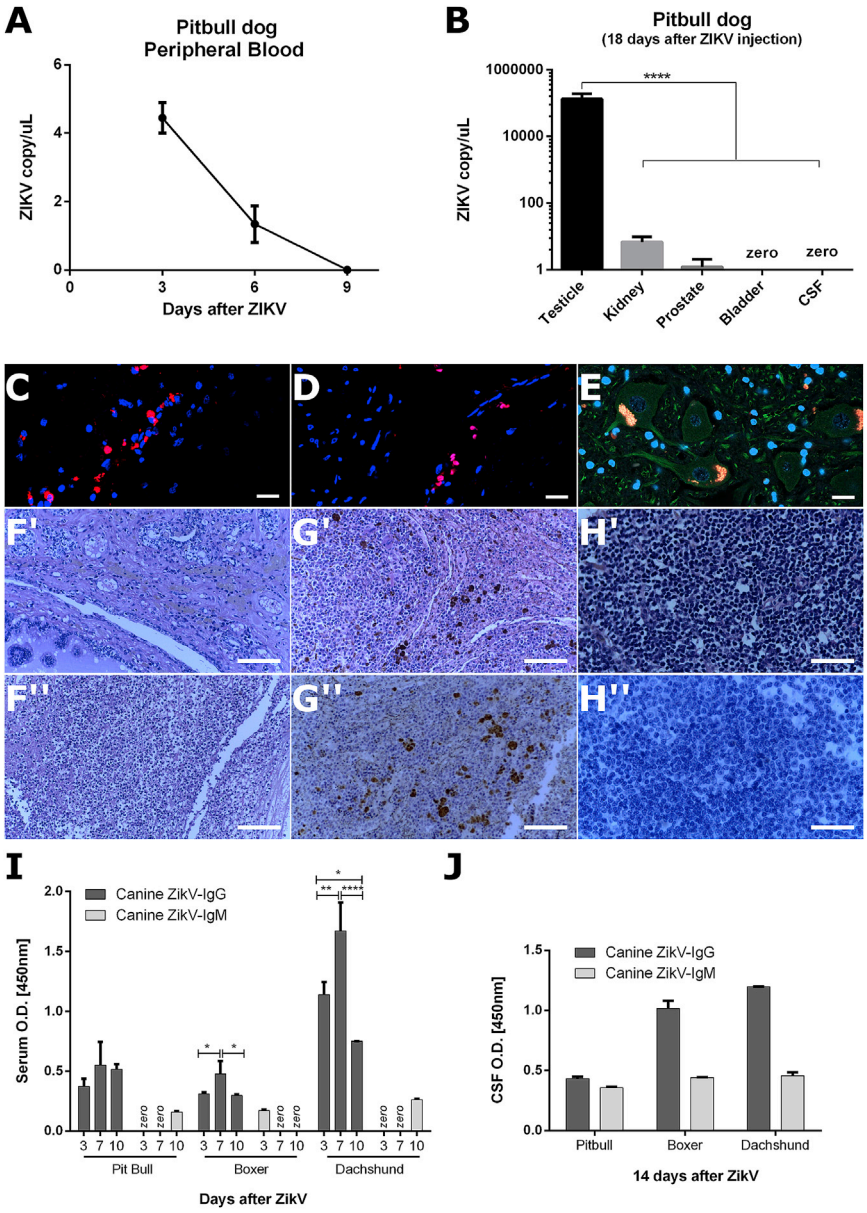

Figure 1. Safety of ZIKV^{BR} Intrathecal Injection in Dogs

(A) Viral RNA copies of peripheral blood serum at 3, 6, and 9 days after ZIKV^{BR} intrathecal injection in Pitbull immunosuppressed dog. (B) Viral titer in testicle, kidney, prostate bladder, and CSF samples at euthanasia in Pitbull dog, 18 days after ZIKV^{BR} injection (****$p < 0.0001$). (C and D) Representative images of frontal lobe (C) and medulla (D) CNS tissues IF immunolabeling for ZIKV^{BR} (red), and nuclei DAPI (blue). Scale bar, 20 μm. (E) Representative images of neurons from CNS tissues IF immunolabeling for ZIKV^{BR} (red), β3-tubulin cytoplasmatic (green) protein, and nuclei DAPI (blue). Yellow staining in neuron image (E) shows unspecific staining for lipofuscin accumulation. Scale bar, 20 μm. (F) H&E representative images of urologic tissues: prostate (F′) and testicle (F″). Scale bar, 100 μm. (G) Representative spleen tissue of H&E (G′) and IHC immunolabeling for ZIKV^{BR} (brown) and hematoxylin (blue) (G″). Scale bar, 100 μm. (H) Representative lymph node tissue of H&E (H′) and IHC immunolabeling for ZIKV^{BR} (brown) and hematoxylin (blue) (H″). Scale bar, 500 μm. The brown areas in H&E preparation of spleen (G′) and lymph node tissue (H′) suggests a hemosiderin accumulation. Canine ZIKV-IgG and ZIKV-IgM quantification by ELISA in peripheral blood serum (I) and CSF (J) dog samples. (*$p < 0.05$; **$p < 0.01$; ***$p < 0.001$; ****$p < 0.0001$, two-way ANOVA with Bonferroni multiple comparison test. Three technical replicas for each sample).

(Figure 1E; Figure S1). Urologic tissue investigation revealed no specific viral lesion (Figure 1F). Additionally, the testicles' IHC showed a degenerated and necrotic tissue, unabling ZIKV^{BR} immune staining (Figure 1F″). Besides the CNS and the urologic system, spleen and lymph nodes tissues presented no specific ZIKV^{BR}-positive staining cells (Figures 1G–1H).

Case Two

Case 2 was a 9-year-old male Boxer dog with a history of three episodes of generalized tonic-clonic seizures, beginning 2 months prior to the evaluation, with pacing and behavioral changes (Table 2). The neurological examination suggested a neoplastic lesion in the right intra-axial frontal lobe (confirmed by MRI images; Data S1).

As previously observed in the Pitbull dog, no clinical symptoms of infection were detected after ZIKV^{BR} intrathecal administration and no ZIKV^{BR} RNA copies were found in peripheral blood, CSF, urine, and saliva samples in both dogs 3, 7, and 10 days after the injection (1×10^6 particles).

Clinically, the Boxer dog presented a notable improvement of neurological symptoms after ZIKV^{BR} treatment (Table 2). The dog was able to eat independently and recovered the ability to run, jump, climb stairs, play with a ball, and interact with owners (Video S2). Before ZIKV^{BR} injection, brain MRI showed a contrasting and non-contrasting tumor region of 8.7 and 5.52 cm^3, respectively (Figures 2A and 2B; Data S1). ZIKV^{BR} treatment showed a tumor pseudo-progression by induction of local inflammation and increase in the contrasting area (Figures 2A and 2B). Since no adverse effects had been observed, a second ZIKV^{BR} dose, ten times greater than the first dose, was given intrathecally at day 21, which led to a substantial tumor remission (Figure 2B).

At day 60, an inflammation was observed in the Boxer right testicle which was confirmed by ultrasonography examination and the testicles were surgically removed. The left testis presented normal size and no signs of inflammation. Microscopic evaluation revealed the presence of a leydigoma in the right testicle and an intratubular seminoma in

Table 2. Clinical Progression

	Boxer			Dachshund		
Neurologic Clinical Symptoms[a]	Prior ZIKV^{BR} Treatment	After 1st ZIKV^{BR} Dose (10^6 PFU)	After 2nd ZIKV^{BR} Dose (10^7 PFU)	Prior ZIKV^{BR} Treatment	After 1st ZIKV^{BR} Dose (10^6 PFU)	After 2nd ZIKV^{BR} Dose (10^7 PFU)
Seizures	3 per day	zero	2 events	zero	zero	zero
Altered mental status[b]	+++	+	–	+++	+	–
Circling to one side	+++	+	–	–	–	–
Compulsive pacing	++	+	+	–	–	–
Abnormal gait and posture (ataxia and paresis)	–	–	–	+++	+	–
Nasal sensitivity deficiency	–	–	–	++	++	–
Central blindness (cortical)	–	–	–	–	–	–
Pupillary size and symmetry deficiency	–	–	–	+	+	+
Pupillary reflexes	–	–	–	–	–	–
Palpebral reflexes	–	–	–	–	–	–
Contralateral menace deficit	R+++	R+	R+	L+	L–	L–
Contralateral decreased conscious perception	R +++	R+	R+	L+	L–	L–
Contralateral facial sensation deficit	R+++	R+	R+	L+/R+	L+/R+	L+/R+

[a]The score system applied for each neurologic clinical symptom is as follows: (–) normal, (+) mild, (++) moderate, (+++) severe. The letters R and E stand for lateralization in each the neurologic lesion appear, either to the right or to the left side of the body, respectively.
[b]Defined by 1 or more of the following clinical signs as follows: behavior change, dementia, dullness, and disorientation.

the left testicle. Despite the presence of tumor and ZIKV in both testes, just the right one showed severe inflammatory infiltrate, degeneration, and severe multifocal necrosis. Thus, probably, the presence of leydigoma tumor, rather than ZIKV virus, was the cause of the right testis inflammation.

3 months after the ZIKV^{BR} injection, the non-contrasting tumor area was reduced to a volume of fewer than 1 cm^3 (Figure 1B) and showed a substantial irregular tumor shape modification with a 1.96 cm^3 remission of total tumor area (Figure 2C). The tumor mass stabilized until day 120. However, an MRI performed at day 150 showed tumor expansion with increasing intracranial pressure and recapitulating some neurological symptoms present before the treatment. As requested by the owners and for ethical reasons, the Boxer dog was euthanized on day 153. Post-mortem histopathological tumor exam confirmed the diagnosis of oligodendroglioma based on cell markers profile: positive staining for Olg2, CD56, S100, and Ki67 markers, and negative staining for GFAP, Sinaptofisin, Neurofilament, and NSECK-Pan markers[14,15] (Figure S2). Extensive necrosis, cellular debris, and immune-cellular infiltration were observed in tumor mass histopathological analysis (Figure S3), including a central hole and macroscopic tissue degeneration (Figure 2D), probably induced by ZIKV anti-tumoral effect since these features are unexpected in untreated oligodendroglioma.[14] Confocal IF analysis confirmed consistent ZIKV^{BR} infection in the tumor border tissue (Figures 2E and 2F). Besides tumor loci, ZIKV^{BR}-positive normal cells were found restricted to the CNS vessel walls but no persistent infection was observed in other CNS tissues (Figures 2G and 2H). No evidence of positive-ZIKV^{BR} staining in neurons from diverse CNS regions was found (Figure S1). The right testicle revealed a severe inflammatory infiltrate and neoplastic multi-focal areas in both testicles: a seminoma intratubular and a leydigoma in the left and right testicle, respectively. Although no detection of ZIKV^{BR} RNA by RT-PCR in the urine sample and testicle tissue was observed, IHC and IF analysis confirmed the ZIKV^{BR}-positive immunolabeling in the seminiferous epithelium and tumor cells (Figures 2I–2M).

Case Three

Case 3 was a 12-year-old Dachshund dog that had been misdiagnosed as carrying a highly suggestive glioma in the left frontal lobe by MRI image. A neurological examination revealed many alterations as described in Table 2. However, the most evident complaints were an ataxic gait, the inability to recognize the owners and feed independently, and head pressing. As case 2, the Dachshund dog was included in the clinical trial protocol to evaluate the safety, the potential oncolytic effect of ZIKV against CNS canine tumor, and its possible clinical effect.

As observed in the Boxer, the neurological symptoms showed a significant improvement in the Dachshund dog, (Table 2) and a tumor regression was also seen by MRI non-contrasting tumor volume decrease (3.344 cm^3) just 14 days after ZIKV^{BR} first injection (Figures 3A and 3B; Data S1). However, the Dachshund dog developed cerebral leukoencephalopathy characterized by peritumoral white matter tracts leading to brain pressure growth. These features were resolved

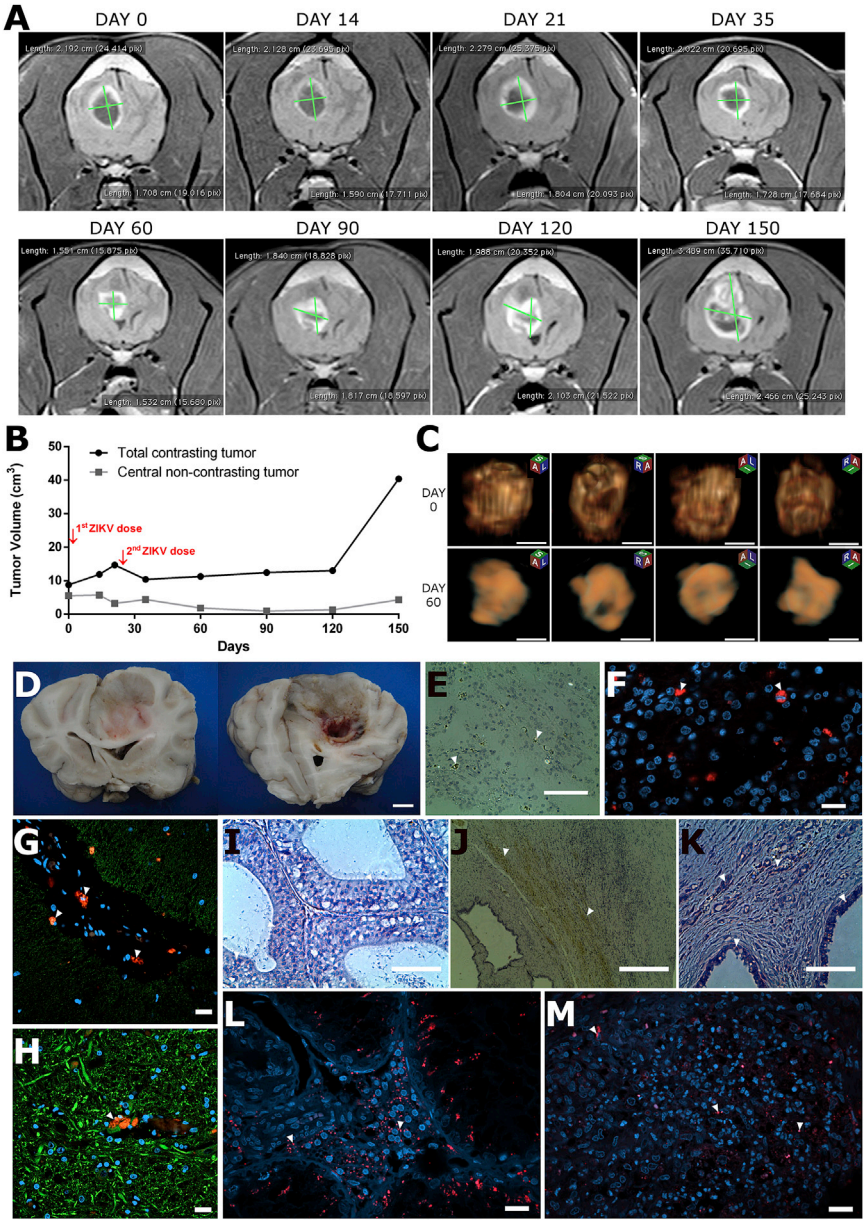

Figure 2. Tumor Remission after ZIKV^{BR} Treatment in Boxer Dog Bearing Oligodendroglioma

(A) Representative transversal tumor MRI at days 0, 14, 21, 35, 60, 90, 120, and 150 after clinical ZIKV^{BR} oncolytic treatment protocol beginning. (B) Tumor volume growth kinetics quantified by MRI analysis. (C) Representative 3D MRI analyses of four different dimensions at day 0 and 60 after ZIKV^{BR} first injection. Scale bar, 1 cm. (D) Post-mortem macro images of CNS tumor. Scale bar, 1 cm. (E–M) Representative images of tumor (E and F), cerebellum (G), medulla (H), left testicle (I), and right testicle bearing leydigoma (J–M) tissues. IHC (E, I–K) staining for H&E and ZIKV^{BR} (brown, white arrowhead), and IF (F–H, L and M) Immunolabeling for ZIKV^{BR} (red, white arrowhead), β3-tubulin cytoplasmatic (green) protein and nuclei DAPI (blue). Scale bar, 100 μm (E, I, and K), 20 μm (F–H, L and M), and 200 μm (J).

following the administration of corticosteroids anti-inflammatory doses and confirmed by contrasting tumor region decrease at day 21 (Figure 3B). After a tumor growth stabilization, we administrated a second ZIKV^{BR} dose (1×10^7 particles) at day 42. As seen after the first dose, the ZIKV^{BR} infection led to non-contrasting tumor regression of 2,084 cm^3 and contrasting area growth by ZIKV^{BR} inflammatory local response. Between days 60 and 78, the Dachshund dog presented a significant clinical improvement recovering the lost abilities to climb stairs, recognize the owners and their instructions, run, and play with toys (Video S3). Although there was an apparent tumor volume stabilization, the owners decided to stop the treatment after a third episode of cerebral leukoencephalopathy on day 78. As required by the owners and following the ethical guidelines, the Dachshund dog was euthanized on day 80. 3D MRI analysis performed at the end of the treatment showed a tumor remission of 5.53 cm^3 and a significant change in the tumor shape (Figure 3C). The brain macro images showed a necrotic and very disrupted tumor (Figure 3D). Although the tumor characteristics and localization suggested a glioblastoma by MRI imaging, the histopathological diagnosis of Dachshund tumor confirmed a rare intracranial meningioma showing positive staining for CK-Pan and Vimentin markers and negative staining for GFAP, Sinaptofisin, Neurofilament, NSE, S100, Olg2, PGP 9.5, and Ki67 markers[16] (Figure S2). Interestingly, although this was a rare case of meningioma developed inside the CNS, which technically makes it protected by the blood-brain barrier (BBB), it showed significant tumor remission after ZIKV treatment, which we considered very positive since it may broaden the effect of ZIKV against brain tumors. As observed in the Boxer dog, the IF ZIKV^{BR} staining showed viral presence limited to the tumor but mostly at the tumor border (Figures 3E and 3F) and no evidence of neuron virus infection (Figure S1), confirming the brain safety of ZIKV^{BR} therapy. Immune cell infiltration with intensive cell death was observed in tumor mass (Figures 3G and 3H).

ZIKV^{BR} Infection Modulates Immune System Recruitment and Activation

In an attempt to evaluate the immune response to ZIKV^{BR}, we quantified canine ZIKV-immunoglobulin G (IgG) and ZIKV-IgM antibodies in serum and CSF samples by ELISA. The early response of ZIKV-IgG was observed in the serum of all 3 dogs and presented higher amounts

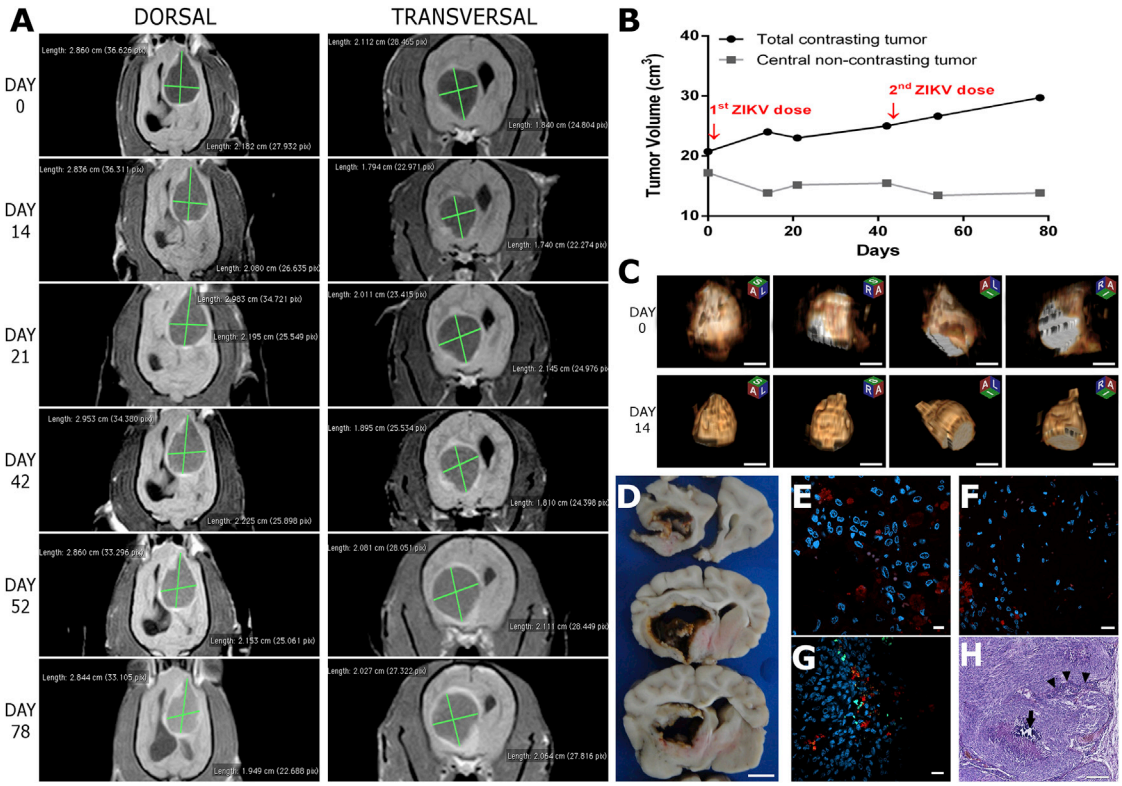

Figure 3. Tumor Remission after ZIKV^{BR} Treatment in Dachshund Dog Bearing a Rare Intracranial Meningioma

(A) Representative dorsal and transversal tumor MRI at days 0, 14, 21, 42, 52, and 78 after clinical ZIKV^{BR} oncolytic treatment protocol onset. (B) Tumor volume growth kinetics quantified by MRI analysis. (C) Representative 3D MRI analyses of four different dimensions at day 0 and 14 after ZIKV^{BR} first injection. Scale bar, 1 cm. (D) Post-mortem macro images of CNS tumor. Scale bar, 1 cm. (E–G) Representative images of tumor positive for ZIKV^{BR} (red), microglia marker (G) (green), and nuclei DAPI (blue). Scale bar, 10 μm (E) and 20 μm (F and G). (H) H&E representative image of the tumor highlighting the lymphocytes infiltration (white arrowhead) and necrosis area with calcium accumulation (black arrow). Scale bar, 100 μm.

7 days after the first ZIKV^{BR} injection (Figure 1I). In the two dogs (Boxer and Dachshund) the presence of ZIKV-IgG was more evident in CSF samples when compared to the Pitbull dog (Figure 1J). The production of ZIKV-IgM was also observed but at low levels in serum and CSF samples (Figures 1I and 1J).

Given the substantial involvement of the immunologic system in oncolytic virotherapy, we further investigated the concentration of the immune cytokine measured by multiplex assays in peripheral blood and CSF samples from the three dogs after ZIKV^{BR} injection. Despite the difference in time points of each sample, all three dogs commonly showed high levels of interleukin-8 (IL-8), KC-like, and MCP-1 in both serum and CSF samples after intrathecal ZIKV^{BR} injection (Figures 4A–4C). Since these three proinflammatory cytokines are required to initiate an effective inflammatory response by monocytic infiltration and activation,[17] we performed a non-contact co-culture with canine tumor cell line and canine monocyte to evaluate the paracrine effect of cytokine signaling after ZIKV^{BR} infection (Figure 4D) by a multiplex array.

First, we confirmed ZIKV modulatory properties in canine cells by infecting canine mesenchymal stem cell (ADSC) and a dog GBM cell line (D-GBM) in monolayer cultures against various multiplicity of infection (MOIs: 0.01, 0.1, 1, and 2). Figure S4 show that 72 h post-infection (hpi), ZIKV^{BR} induced significant growth reduction in D-GBM cell line at MOI 1 and MOI 2, but we did not detect cell death caused by direct ZIKV^{BR} infection in this cell line using until MOI 100 (Figures S4, 4C, and 4J). Interestingly, although immunostaining showed that 72 hpi the virus was capable of entering the cytoplasm of both canine cell lines (Figures S4D–S4F), only D-GBM produced viral genomic copies 72 hpi (Figures S4G and S4H). D-GBM cell infection was also demonstrated at MOIs 0.1, 1, and 2 by detection of E ZIKV^{BR} protein in the intracellular compartment after staining with 4G2 monoclonal antibody (mAb), using flow cytometry technique (Figure S4I). These viral genomic and protein detection assays indicate that ZIKV^{BR} had no effect in the normal canine cell line but supported its modulatory properties in glioblastoma tumor cell line as observed by the clinical improvement in the Boxer and Dachshund, as well as tumor remission.

After confirming D-GBM susceptibility to ZIKV^{BR}, we performed a non-contact co-culture assay with canine monocyte. In the absence of monocytes, multiplex assay in supernatant samples from

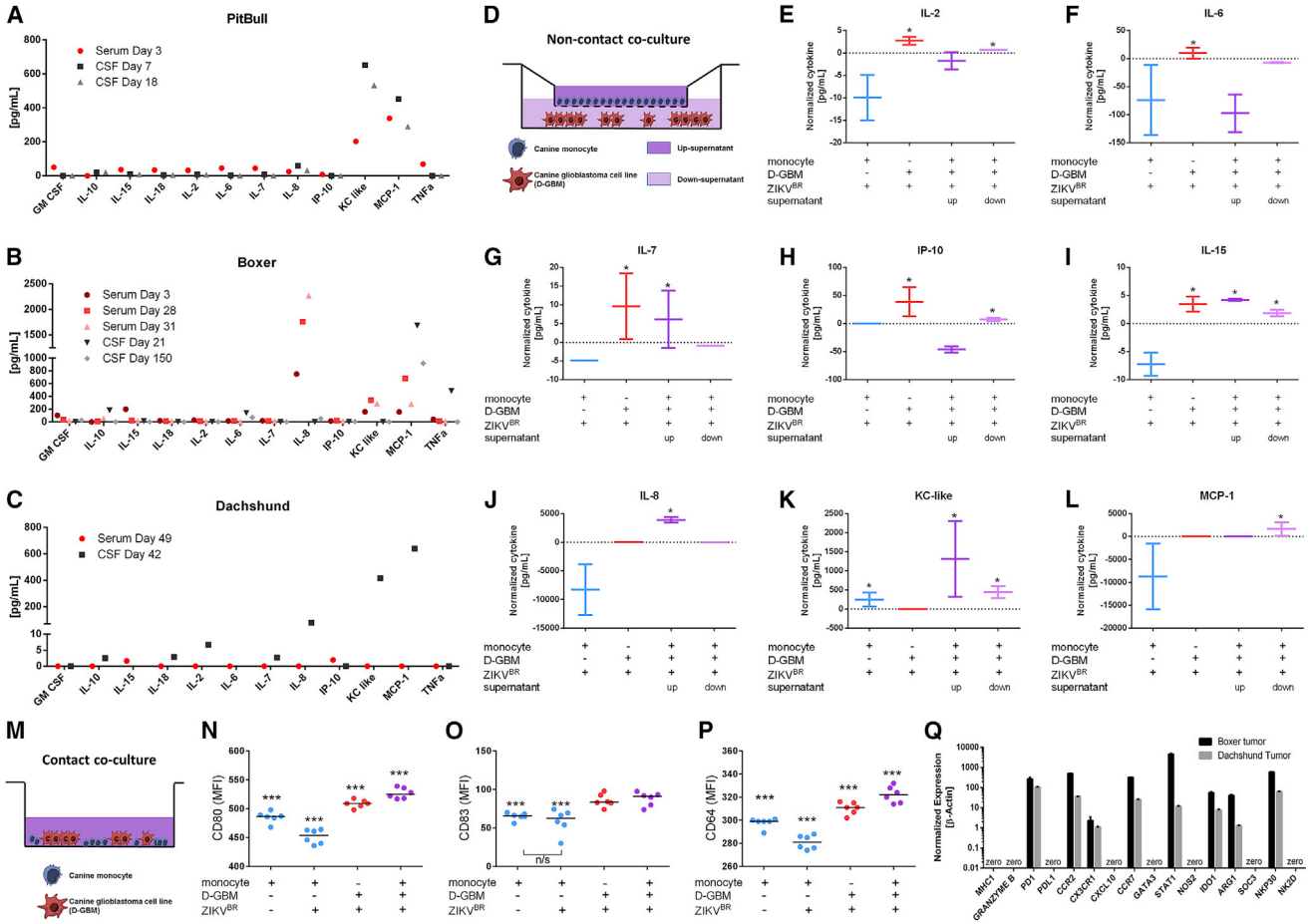

Figure 4. Canine Cytokine Profile Generated by Brain Tumors in the Presence of ZIKV^{BR} in Both *In Vivo* and *In Vitro* Models

(A–C) Cytokine profile in the serum and CSF of Pitbull (A), Boxer (B), and Dachshund (C) dogs at different time points after ZIKV^{BR} injection. (D) Schematic representation of canine monocyte and D-GBM non-contact co-culture assay. (E–L) Cytokines concentration in non-contact co-culture groups normalized by respective day mock condition. (M) Schematic representation of canine monocyte and D-GBM contact co-culture. (*p < 0.05, t test in comparison with correspondent MOCK group. Two technical replicas for each two biologic replica). (N–P) Evaluation of monocytes activation with CD80 (N), CD83 (O), and CD64 (P) positive cell quantification by flow cytometer. Gating strategy for the evaluation of canine monocytes in the co-culture assay detailed in Figure S5. (Q) qRT-PCR analysis of Boxer and Dachshund tumor tissue for lymphocyte T cells (*MHC*, *GRANZYME B*, and *PD1*), tumor cell receptor *PDL-1*, inflammatory monocyte (CCR2), microglia (CX3CR1), macrophage M1 (*CXCL10*, *CCR7*, *GATA3*, *STAT1*, *NOS2*, and *IDO1*), macrophage M2 (*ARG1* and *SOC3*), and NK cells (*NKP30* and *NK2D*), normalized by endogenous expression (Beta-Actin).

co-culture assay showed a significant increase of IL-2, IL-6, IL-7, IP-10, and IL-15 concentrations in D-GBM culture after ZIKV^{BR} (MOI 2) infection (Figures 4E–4I). In the presence of monocytes, IL-8, KC-like, and MCP-1 cytokine presented a significant upregulation after ZIKV^{BR} infection of the D-GBM cell line (Figures 4J–4L).

We further evaluated juxtracrine signaling by the evaluation of phenotypic changes in contact co-culture with D-GBM (Figure 4M). A significant increase of CD80- and CD63-positive cells were observed in co-cultured assay indicating activation of inflammatory monocytes in contact with infected D-GBM tumor cells (Figures 4N–4P). In order to combine these *in vitro* data with the results observed in treated dogs, we analyzed RNA expression of diverse immune mediators in post-mortem tumor samples by RT-PCR (Figure 4Q). PD-1 receptor was found expressed in the tumor microenvironment. All transcripts analyzed were found less expressed in Dachshund tumor when compared to Boxer tumor. The T cell proteins (MHC1 and Granzyme B), as well as tumor receptor PDL-1, were not expressed in both dogs. Among the others immune cell markers tested, we found high expression of macrophage transcription factor STAT1, the chemokines CCR7 and CCR2, and the NK cell marker NKP30. These cytokines and chemokine networks indicate a prevalence of monocyte/macrophage infiltrate pattern.

DISCUSSION

The main aspects that contribute to a poor prognosis in people with brain tumors are: (1) BBB physiologic isolation, (2) presence of cancer stem cells resistance to conventional therapy, and (3) the immune-privileged isolation of the brain.[18] Unfortunately, current therapies are not effective and cause important negative side effects.[1] Here we

show for the first time that intrathecal ZIKV^{BR} injections of 1 to 10 million virus particles in dogs represent a safe procedure since it did not trigger any negative clinical side effects in injected animals. More importantly, at autopsy, mature neurons from CNS regions showed no damage or any specific ZIKV^{BR}-positive staining either. Furthermore, ZIKV^{BR} intrathecal injections in two dogs bearing intracranial tumors showed a tropism toward the tumor border, infecting the neoplastic cells without spreading to other brain regions, inducing immune cell recruitment and resulting in substantial tumor remission. Despite the differences in races, sizes, age, and tumor kind between the two immunocompetent dogs treated here, both dogs improved clinical neurologic symptoms and had an overall survival with good quality of life of 80 and 150 days. This observation represents a significant increase of survival rate since the literature reports a survival of 24–33 days for dogs diagnosed with brain tumor.[19,20] It is also noteworthy that they had very large tumors and were in an advanced stage of the disease when brought to the veterinary clinic.

Current intracranial human tumors in animal models are limited to immunosuppressed mice that are less representative of human disease features and the response to the treatment.[21] On the other hand, immunocompetent dogs that spontaneously develop brain tumors are more similar to human gliomas and represent a stronger platform for validating successful therapeutic strategies when compared to mice models.[22] To our knowledge, the dogs reported here are the first to demonstrate the oncolytic effects of ZIKV^{BR} against brain tumor cells in a canine model and presented clinical symptoms similar to human clinical trials using other oncolytic virus against brain tumors.[21] The apparent observed tumor growth is actually an immune reaction in the tumor bed called pseudoprogression.[23] This inflammatory condition requires a fine adjustment between the repression of the intracranial pressure increment and the anti-tumoral effect of immune cells tumor infiltration caused by the viral presence. However, the possible leukoencephalopathy observed in the Dachshund dog represents no critical side effects since it can be treated with very low doses of corticoids. In competent mice models, the generated microgliosis is totally reversible 60 days after ZIKV injection or after anti-inflammatory drug administration.[24]

Based on these observations and the recently created Immunotherapy Response Assessment in Neuro-Oncology (iRANO) human criteria,[25] we identified contrasting and non-contrasting tumor areas. Immediately after ZIKV^{BR} administration, the contrasting region growth and the immune cell markers expression profile seem to reflect an anti-tumoral immunity response.[26] The interactions between oncolytic viruses and the immune system affect therapeutic outcomes by inducing an antitumoral immune response in most durable and late responses.[27] This antitumoral late response was observed in the Dachshund and Boxer dogs leading to clinical improvement and tumor remission up to 40 and even 100 days after the last ZIKV^{BR} injection, respectively.

Since ZIKV^{BR} prominently infects neural stem and progenitor cells (NPCs), as well as embryonal CNS tumors closely resembling NPCs at a molecular level,[4,28] it is not known whether the oncolytic virus anti-tumoral potential would be efficient in glial tumors and meningiomas. However, the significant observed tumor remission of 5.53 cm^3 in the meningioma Dachshund dog confirmed ZIKV^{BR} anti-tumoral immune regulation. As future approaches, a possible co-administration of ZIKV^{BR} and immune checkpoint inhibitors targeting PD-1, STAT1, and CCR2, found overexpressed in both Boxer and Dachshund tumors tissues, could enhance the anti-tumoral immune response.[29,30]

In the present study, our data suggest a general trend in the establishment of a prevalent cytokine/chemokine cluster led by increase of IL-8, KC-like, and MCP-1 at serum and CFS samples. It confirms the evolution of the inflammatory response after ZIKV^{BR} administration since these cytokines and chemokines constitute a family of secretory proteins that drive and control leukocyte migration.[31,32] Besides, the *in vitro* model more specifically paracrine effect shows a similar cytokine/chemokine pro-inflammatory pattern while the juxtracrine effect showed a mature phenotype of canine macrophage in contact with infected D-GBM cells (increase of CD80, CD83, and CD64).

Clearly, the presence of ZIKV^{BR} modulate tumor immune profiling and recruited immune cells to the tumor microenvironment in the two dogs. However, before translating this promising oncolytic/immunomodulatory therapy to humans, a concern to be taken in the application of ZIKV^{BR} as oncolytic therapy against brain tumors is the virus capability to infect and replicate in the testicle cells. Although some studies have reported flavivirus infection in domestic dogs, like dengue virus,[33] until now there is no scientific evidence that dogs could be a reservoir for ZIKV.[34] Here we report for the first time the ZIKV^{BR} capability to infect and replicate in canine urologic organs. In humans, ZIKV particles were detected in blood, saliva, urine, and semen up to 150 days after the initial symptoms, preserving the integrity and infectivity during replication in the male reproductive system.[35] Although the present canine pre-clinical study confirms the ZIKV^{BR} replication and shedding in the male reproductive system, this result does not represent a barrier to human oncolytic therapy since the virus sexual transmission can be physically prevented and ZIKV does not cause infertility in male patients.[35]

In short, here we show for the first time significant CNS tumor remission following ZIKV^{BR} intrathecal injections in two dogs bearing spontaneous intracranial tumors with an absence of clinical side effects associated with ZIKV infection. We also show that the two dogs followed for a longer time had a positive response following a second ZIKV injection, which opens the possibility of a protocol with multiple injections. Furthermore, the present results confirm the ZIKV^{BR} safety in a larger animal model and most importantly its potential as oncolytic virotherapy in different CNS tumors. Alternative treatment protocols involving multiple injection schemes, dose-escalation, and combination with drugs, may now be envisioned in further preclinical studies aiming at higher therapeutic efficacy. Our results open new perspectives for upcoming oncolytic

virotherapy using ZIKV strains to destroy CNS tumors as well as to induce an anti-tumoral immune response in CNS tumors for which there are currently no effective treatments.

MATERIALS AND METHODS

The Canine Clinical Trial Protocol

This clinical trial followed the International Ethical Guideline for Biomedical Research (CIOMS/OMS, 1985) and was approved by the Institutional Animal Experimentation Ethics Committee. Dogs were considered eligible for the oncolytic therapy if they were diagnosed by a veterinary neurologist with advanced CNS primary tumor with neural origin, excluding meningioma and other non-neural tumors (based on neurological symptoms and brain MRI), had adequate organs function (hematocrit >25% and renal/hepatic function), with no neural infection diseases, and whose owners were not pursuing chemotherapy or immediate euthanasia and consented to include the dogs in the clinical trial. Pre-treatment primary tumor size and location were obtained by brain MRI (Hitachi - Airis 0.3T Elite model) to establish a baseline for assessing tumor response. A 3D tumor reconstruction was carried out in 3 dimensions using a medical image reader program (Dicom - Radiant Viewer). Dogs received one intrathecal injection containing 1×10^6 PFU of $ZIKV^{BR}$ donated by Dr. Pedro Vasconcelos, Instituto Evandro Chagas, Brazil, established as described in Faria et al.[36] Viral titer in urine, saliva and peripheral blood sample were analyzed at 3, 7, and 9 days after $ZIKV^{BR}$ injection. 2 and 3 weeks after the oncolytic treatment, the dog was submitted to MRIs and clinical neurological symptoms analyses to evaluate the tumor response of the therapy. CSF viremia was performed at 14 and 21 days after $ZIKV^{BR}$ injection. Dogs' weight was monitored weekly along with the immunologic system and end-organ function by blood sample exams. A second $ZIKV^{BR}$ dose of 1×10^7 PFU was intrathecally injected when observed clinical neurological symptoms recurrence confirmed by tumor growth. More details about the clinical protocol and methodologies are described in the Supplemental Information.

Viral Burden Measurement

Blood serum, urine, saliva, and CSF samples were collected at specified time points after $ZIKV^{BR}$ treatment. Testicle, prostate, kidney, and bladder were recovered following euthanasia. Viral RNA extraction, cDNA synthesis, and viral RNA copies were quantified by qRT-PCR were performed as described in Kaid et al.[4] The viral burden is expressed as viral RNA equivalents per microliter of total RNA. RNA copy numbers in tissues were normalized per ng of total RNA. A comparison with a standard curve run in parallel as described above for qRT-PCR of *in vitro* assays was used.

Histopathology and IHC

Immediately after controlled euthanasia, all tissues were fixed with a 4% paraformaldehyde solution for 24 h at room temperature and paraffin sections with 4 um thickness were processed for H&E staining. Sections were deparaffinized for enzyme IHC and IF. All procedures for ZIKV IHC were performed using the anti-ZIKV NS2B antibody (Genetex) diluted at 1:100 and Vector Laboratory solutions following fabricant instructions.

Immunofluorescence

Tissue sections were blocked with 10% FBS, 5% bovine serum albumin (BSA), and 0.1% Triton X-100 in PBS for 1 h at room temperature and incubated at 4°C overnight with primary antibodies anti-Zika virus NS2B (GTX133308, Genetex, 1:500), anti-alpha-tubulin (NB100-690, Novus Biologicals, 1:200), anti-IBA1 (ab107159, Abcam, 1:200), and anti-CD14 (MCA1042, Serotec/BioRad, 1:500). Fixed mesenchymal and glioblastoma cells (3.7% formaldehyde for 30 min) were permeabilized (0.1% Triton X-100 in 1 PBS for 2 h) and blockaded (5% BSA in PBS) before primary antibody 4°C overnight incubation. Tissue and cell culture were incubated with secondary antibodies goat anti-rabbit IgG (A11037, Thermo Fisher Scientific) Alexa Fluor 594 and goat anti-mouse IgG Alexa Fluor 488 (A11001, Thermo Fisher Scientific) at a 1:1,000 dilution for 1 h at room temperature. Tissues and cell culture were counterstained with 1 μg/mL DAPI (4′,6-diamidino-2-phenylindole) for 2 min and microscope slides mounted in Vectashield medium (Vector Laboratories). All images were taken in a confocal microscope (Zeinss LSM 800).

ELISA Quantitative Canine ZIKV IgG and IgM Assay

ZIKV-IgG and ZIKV-IgM analysis were performed using the Canine Zika IgG/IgM ELISA kit (MyBioSource). Blood serum and CSF samples were collected at specified time points after $ZIKV^{BR}$ treatment. The blood serum was prepared after coagulation at 37°C/30 min and 2,000 RPM/8°C/10 min centrifugation. The protocol was followed according to the fabricant's instructions. Cut-off values were calculated as the average optical density (O.D.) of the negative control well plus 0.15 in samples (cut-off: ZIKV-IgG = 0.217333; ZIKV-IgM = 0.344333).

Canine Cell Culture

D-GBM[37] canine glioblastoma cell line was kindly provided by Dr. Michael Empl from the University of Veterinary Medicine Hannover, Germany. Mesenchymal stem cell-derived from normal canine adipose tissue (ADSC) were isolated and characterized as previously described.[38] All cells were cultivated in Dulbecco's modified Eagle's medium (DMEM) low glucose supplemented with 10% fetal bovine serum (FBS, Thermo Fisher Scientific), 100 U/mL Penicillin, 100 μg/mL Streptomycin, and 250 ng/mL Fungizone (Thermo Fisher Scientific) at 37°C at 5% CO_2 atmosphere.

Co-Culture Assay

For the non-contact co-culture, we used the 24 transwell cell culture plate (Corning) with 0.8 μm pore size. Briefly, 2×10^4 D-GBM cells were placed on the lower side and incubated for 24 h. Then, canine monocytes were isolated following the laboratory standard protocol.[39] On day 2, D-GBM were infected or not with $ZIKV^{BR}$ (MOI 2) on the lower side, and then canine 4×10^4 monocytes were placed on the upper side of the transwell. Cells were incubated for 48 h, and then supernatants (up and down) were removal for cytokines analysis.

For the contact co-culture, 1×10^5 D-GBM cells, $ZIKV^{BR}$ (MOI 2), or/and 2×10^5 canine monocytes were cultured in 6 well plates and incubated for 48 h. Next, the supernatants were separated for cytokine analysis, and the total cells were recovered for the evaluation of monocytes activation. For that, cells were stained with fluorescein isothiocyanate (FITC) anti-human CD14 (Biolegend), BV605 anti-human CD80 (Biolegend), PE anti-human CD83 (Biolegend), and PerCP-Cy5.5 anti-human CD64 (BD Biosciences) for 30 min at 4°C, followed by cell washings with PBS, 2% FBS. Cells were acquired by LSR Fortessa (BD Biosciences) flow cytometer and data were analyzed using the FlowJo software. Multicolor flow cytometry was performed using specific gating strategies (Figure S5), and the CD80, CD83, and CD64 mean fluorescence intensity (MFI) analyzes were performed within the CD14 gate.

Canine Cytokines Profile by Multiplex Assay

Peripheral blood serum and CSF samples were collected and centrifuged at 1,200 rpm for 10 min at room temperature. Supernatant samples isolated from co-culture assay were diluted two times. Cytokine profiles were determined using the MILLIPLEX MAP Canine Cytokine Magnetic Bead Panel (CCYTOMAG-90K Millipore) with an automated analyzer (Luminex 200, Luminex Corporation, Austin, TX, USA). The protocol was followed according to the manufacturer's instructions. The analytes were measured in technical and biological duplicate.

Immune Markers RT-PCR Profiling

Total RNA was extracted from tumor tissue using the RNeasy Mini Kit (QIAGEN), according to the manufacturer's instructions. A total of 1 μg of RNA was reverse transcribed with SuperScript IV Reverse Transcriptase Kit (Invitrogen) according to the manufacturer's instructions. Quantitative PCR was performed in a 7500 Real-Time PCR System Thermal Cycler (Applied Biosystems). Expression analysis of immune markers was performed with Platinum SYBR Green qPCR SuperMix-UDG (Life Technologies), using β-ACTINA as an endogenous control. Primer sequences are described in Table S1.

SUPPLEMENTAL INFORMATION

Supplemental Information can be found online at https://doi.org/10.1016/j.ymthe.2020.03.004.

AUTHOR CONTRIBUTIONS

C.K., E.G., L.C.C.-J., O.K.O., and M.Z. designed the study. R.A.S.M., T.O.A., V.L., and C.O.M. performed the clinical tests and analyzes. R.A.S.M. and R.K.O.T. performed MRI acquisition and analysis. D.S.S. and C.G.P. were responsible for histopathological exams. C.K., R.A., T.G.M., A.C.R.M., M.F.C.-A., L.R.P., B.F.M.M.P., M.C.L.P., and I.N.B. performed experimental work. C.K. performed data analyses. C.K., T.G.M., A.C.R.M., M.F.C.A., L.R.P., and C.O.M. produced the text and the figures. M.Z., O.K.O., and L.C.S.F. provided the leadership for the project.

CONFLICTS OF INTEREST

The authors declare no competing interests.

ACKNOWLEDGMENTS

We are extremely grateful to the dogs' owners, in particular Gladys Aparecida Bernadino dos Santos and her daughter Carolina, and for the generous contribution of Rosalia Raia, Carol Sandler, Adriana César Carvalho, Elizabete Piedade, Ester Hadassa Sandler, Irene Faiguenboim, Mariana Fischer, Paulo Sousa, Sergio Cipullo, and Simone Schapira Wajman. We also thanks Felipe Chica Lopes, the owner of the Hospital Veterinário Granja Viana (São Paulo, Brazil), where the dogs were maintained and treated. This study was financed in part by the FAPESP-CEPID (2013/08028-1); Coordenação de Aperfeiçoamento de Pessoal de Nível Superior - Brasil (CAPES) - Finance Code 001; CNPq, Brazil (309206/2011-1; 444722/2014-9); INCT-CETGEN, Brazil (573633/2008-8); and FINEP-CTC, Brazil (0108057900). C.K. is a fellow of FAPESP, São Paulo, Brazil (2018/16213-7).

REFERENCES

1. Gardeck, A.M., Sheehan, J., and Low, W.C. (2017). Immune and viral therapies for malignant primary brain tumors. Expert Opin. Biol. Ther. *17*, 457–474.
2. Guerreiro Stucklin, A.S., Ramaswamy, V., Daniels, C., and Taylor, M.D. (2018). Review of molecular classification and treatment implications of pediatric brain tumors. Curr. Opin. Pediatr. *30*, 3–9.
3. Zhu, Z., Gorman, M.J., McKenzie, L.D., Chai, J.N., Hubert, C.G., Prager, B.C., Fernandez, E., Richner, J.M., Zhang, R., Shan, C., et al. (2017). Zika virus has oncolytic activity against glioblastoma stem cells. J. Exp. Med. *214*, 2843–2857.
4. Kaid, C., Goulart, E., Caires-Júnior, L.C., Araujo, B.H.S., Soares-Schanoski, A., Bueno, H.M.S., Telles-Silva, K.A., Astray, R.M., Assoni, A.F., Junior, A.F.R., et al. (2018). Zika virus selectively kills aggressive human embryonal CNS tumor cells in vitro and in vivo. Cancer Res. *78*, 3363–3374.
5. Ruble, G.R., Giardino, O.Z., Fossceco, S.L., Cosmatos, D., Knapp, R.J., and Barlow, N.J. (2006). The effect of commonly used vehicles on canine hematology and clinical chemistry values. J. Am. Assoc. Lab. Anim. Sci. *45*, 25–29.
6. Schiffman, J.D., and Breen, M. (2015). Comparative oncology: what dogs and other species can teach us about humans with cancer. Philos. Trans. R. Soc. Lond. B Biol. Sci. *370*, 20140231.
7. Kimmelman, J., and Nalbantoglu, J. (2007). Faithful companions: a proposal for neurooncology trials in pet dogs. Cancer Res. *67*, 4541–4544.
8. Candolfi, M., Curtin, J.F., Nichols, W.S., Muhammad, A.G., King, G.D., Pluhar, G.E., McNiel, E.A., Ohlfest, J.R., Freese, A.B., Moore, P.F., et al. (2007). Intracranial glioblastoma models in preclinical neuro-oncology: neuropathological characterization and tumor progression. J. Neurooncol. *85*, 133–148.
9. Felsburg, P.J. (2002). Overview of immune system development in the dog: comparison with humans. Hum. Exp. Toxicol. *21*, 487–492.
10. Momozawa, Y. (2019). The potential of translational research in dogs in human medicine. Transl. Regul. Sci. *1*, 31–36.
11. Song, R.B., Vite, C.H., Bradley, C.W., and Cross, J.R. (2013). Postmortem evaluation of 435 cases of intracranial neoplasia in dogs and relationship of neoplasm with breed, age, and body weight. J. Vet. Intern. Med. *27*, 1143–1152.
12. MacNeill, A.L. (2015). On the potential of oncolytic virotherapy for the treatment of canine cancers. Oncolytic Virother. *4*, 95–107.
13. Hussain, A., Ali, F., Latiwesh, O.B., and Hussain, S. (2018). A Comprehensive Review of the Manifestations and Pathogenesis of Zika Virus in Neonates and Adults. Cureus *10*, e3290.
14. Koehler, J.W., Miller, A.D., Miller, C.R., Porter, B., Aldape, K., Beck, J., Brat, D., Cornax, I., Corps, K., Frank, C., et al. (2018). A Revised Diagnostic Classification of Canine Glioma: Towards Validation of the Canine Glioma Patient as a Naturally Occurring Preclinical Model for Human Glioma. J. Neuropathol. Exp. Neurol. *77*, 1039–1054.

15. Kishimoto, T.E., Uchida, K., Thongtharb, A., Shibato, T., Chambers, J.K., Nibe, K., Kagawa, Y., and Nakayama, H. (2018). Expression of Oligodendrocyte Precursor Cell Markers in Canine Oligodendrogliomas. Vet. Pathol. *55*, 634–644.

16. Motta, L., Mandara, M.T., and Skerritt, G.C. (2012). Canine and feline intracranial meningiomas: an updated review. Vet. J. *192*, 153–165.

17. Galán, A., Mayer, I., Rafaj, R.B., Bendelja, K., Sušić, V., Cerón, J.J., and Mrljak, V. (2018). MCP-1, KC-like and IL-8 as critical mediators of pathogenesis caused by Babesia canis. PLoS ONE *13*, e0190474.

18. Foreman, P.M., Friedman, G.K., Cassady, K.A., and Markert, J.M. (2017). Oncolytic Virotherapy for the Treatment of Malignant Glioma. Neurotherapeutics *14*, 333–344.

19. Heidner, G.L., Kornegay, J.N., Page, R.L., Dodge, R.K., and Thrall, D.E. (1991). Analysis of survival in a retrospective study of 86 dogs with brain tumors. J. Vet. Intern. Med. *5*, 219–226.

20. Moirano, S.J., Dewey, C.W., Wright, K.Z., and Cohen, P.W. (2018). Survival times in dogs with presumptive intracranial gliomas treated with oral lomustine: A comparative retrospective study (2008-2017). Vet. Comp. Oncol. *16*, 459–466.

21. Ranjan, S., Quezado, M., Garren, N., Boris, L., Siegel, C., Lopes Abath Neto, O., Theeler, B.J., Park, D.M., Nduom, E., Zaghloul, K.A., et al. (2018). Clinical decision making in the era of immunotherapy for high grade-glioma: report of four cases. BMC Cancer *18*, 239.

22. Bentley, R.T., Ahmed, A.U., Yanke, A.B., Cohen-Gadol, A.A., and Dey, M. (2017). Dogs are man's best friend: in sickness and in health. Neuro-oncol. *19*, 312–322.

23. Hodi, F.S., Hwu, W.-J., Kefford, R., Weber, J.S., Daud, A., Hamid, O., Patnaik, A., Ribas, A., Robert, C., Gangadhar, T.C., et al. (2016). Evaluation of Immune-Related Response Criteria and RECIST v1.1 in Patients With Advanced Melanoma Treated With Pembrolizumab. J. Clin. Oncol. *34*, 1510–1517.

24. Figueiredo, C.P., Barros-Aragão, F.G.Q., Neris, R.L.S., Frost, P.S., Soares, C., Souza, I.N.O., Zeidler, J.D., Zamberlan, D.C., de Sousa, V.L., Souza, A.S., et al. (2019). Zika virus replicates in adult human brain tissue and impairs synapses and memory in mice. Nat. Commun. *10*, 3890.

25. Okada, H., Weller, M., Huang, R., Finocchiaro, G., Gilbert, M.R., Wick, W., Ellingson, B.M., Hashimoto, N., Pollack, I.F., Brandes, A.A., et al. (2015). Immunotherapy response assessment in neuro-oncology: a report of the RANO working group. Lancet Oncol. *16*, e534–e542.

26. Chiocca, E.A., and Rabkin, S.D. (2014). Oncolytic viruses and their application to cancer immunotherapy. Cancer Immunol. Res. *2*, 295–300.

27. Chon, H.J., Lee, W.S., Yang, H., Kong, S.J., Lee, N.K., Moon, E.S., Choi, J., Han, E.C., Kim, J.H., Ahn, J.B., et al. (2018). Tumor microenvironment remodeling by intratumoral oncolytic vaccinia virus enhances the efficacy of immune checkpoint blockade. Clin. Cancer Res. *25*, 1612–1623.

28. Caires-Júnior, L.C., Goulart, E., Melo, U.S., Araujo, B.H.S., Alvizi, L., Soares-Schanoski, A., de Oliveira, D.F., Kobayashi, G.S., Griesi-Oliveira, K., Musso, C.M., et al. (2018). Discordant congenital Zika syndrome twins show differential in vitro viral susceptibility of neural progenitor cells. Nat. Commun. *9*, 475.

29. Zhang, Y., Jin, G., Zhang, J., Mi, R., Zhou, Y., Fan, W., Cheng, S., Song, W., Zhang, B., Ma, M., and Liu, F. (2018). Overexpression of STAT1 suppresses angiogenesis under hypoxia by regulating VEGF-A in human glioma cells. Biomed. Pharmacother. *104*, 566–575.

30. Vakilian, A., Khorramdelazad, H., Heidari, P., Sheikh Rezaei, Z., and Hassanshahi, G. (2017). CCL2/CCR2 signaling pathway in glioblastoma multiforme. Neurochem. Int. *103*, 1–7.

31. Deshmane, S.L., Kremlev, S., Amini, S., and Sawaya, B.E. (2009). Monocyte chemoattractant protein-1 (MCP-1): an overview. J. Interferon Cytokine Res. *29*, 313–326.

32. Zlotnik, A., and Yoshie, O. (2012). The chemokine superfamily revisited. Immunity *36*, 705–716.

33. Thongyuan, S., and Kittayapong, P. (2017). First evidence of dengue infection in domestic dogs living in different ecological settings in Thailand. PLoS One *12*, e0180013.

34. Kim, K. (2018). Seroconversion does not a reservoir host make: No scientific proof to date that dogs are a reservoir for Zika virus. Can. Vet. J. *59*, 93.

35. Oliveira, D.B.L., Durigon, G.S., Mendes, É.A., Ladner, J.T., Andreata-Santos, R., Araujo, D.B., Botosso, V.F., Paola, N.D., Neto, D.F.L., Cunha, M.P., et al. (2018). Persistence and Intra-Host Genetic Evolution of Zika Virus Infection in Symptomatic Adults: A Special View in the Male Reproductive System. Viruses *10*, 615.

36. Faria, N.R., Azevedo, R.D.S.D.S., Kraemer, M.U.G., Souza, R., Cunha, M.S., Hill, S.C., Theze, J., Bonsall, M.B., Bowden, T.A., Rissanen, I., et al. (2016). Zika virus in the Americas: Early epidemiological and genetic findings. Science *352*, 345–349.

37. Stoica, G., Lungu, G., Martini-Stoica, H., Waghela, S., Levine, J., and Smith, R., 3rd (2009). Identification of cancer stem cells in dog glioblastoma. Vet. Pathol. *46*, 391–406.

38. Gomes, J.P., Coatti, G.C., Valadares, M.C., Assoni, A.F., Pelatti, M.V., Secco, M., and Zatz, M. (2018). Human Adipose-Derived CD146^{+} Stem Cells Increase Life Span of a Muscular Dystrophy Mouse Model More Efficiently than Mesenchymal Stromal Cells. DNA Cell Biol. *37*, 798–804.

39. Okada, S.S., de Oliveira, E.M., de Araújo, T.H., Rodrigues, M.R., Albuquerque, R.C., Mortara, R.A., Taniwaki, N.N., Nakaya, H.I., Campa, A., and Moreno, A.C. (2016). Myeloperoxidase in human peripheral blood lymphocytes: Production and subcellular localization. Cell. Immunol. *300*, 18–25.

YMTHE, Volume *28*

Supplemental Information

Safety, Tumor Reduction, and Clinical Impact of Zika Virus Injection in Dogs with Advanced-Stage Brain Tumors

Carolini Kaid, Raquel Azevedo dos Santos Madi, Renato Astray, Ernesto Goulart, Luiz Carlos Caires-Junior, Thiago Giove Mitsugi, Ana Carolina Ramos Moreno, Maria Fernanda Castro-Amarante, Lennon Ramos Pereira, Bruna Felício Milazzotto Maldonado Porchia, Thais Oliveira de Andrade, Vivian Landini, Daniel Soares Sanches, Carolina Gonçalves Pires, Rubens Koji Oliveira Tanioka, Marcia C.L. Pereira, Igor Neves Barbosa, Cristina O. Massoco, Luís Carlos de Souza Ferreira, Oswaldo Keith Okamoto, and Mayana Zatz

SUPPLEMENTAL INFORMATION

Supplementary Figure S1: Absence of viral infection in canine neurons after $ZIKV^{BR}$ CNS infection.

Supplementary Figure S2: Immunohistochemistry assay for histopathologic tumor diagnosis.

Supplementary Figure S3: H&E representative images of Boxer dog tumor.

Supplementary Figure S4: $ZIKV^{BR}$ in vitro infection in canine cell lines.

Supplementary Figure S5: Gating strategy for the evaluation of canine monocytes in the co-culture assay.

Supplementary Table 1: Primers sequence for the quantitative PCR for canine immune mediators.

Supplementary Data 1: MRI Images. Representative images of all MRI from the Pitbull, Boxer, and Dachshund dogs post-contrast T1 and T2 weighted dorsal, transversal and sagittal planes.

Supplementary Data 2: Blood Exam Data. Detailed blood exam data from Pitbull, Boxer and Dachshund dogs before and during the clinical protocol.

Supplementary Video 1: Clinical outcome of the first case, the Pitbull dog, before and during the clinical protocol.

Supplementary Video 2: Clinical outcome of the second case, the Boxer dog, before and during the clinical protocol.

Supplementary Video 3: Clinical outcome of the third case, the Dachshund dog, before and during the clinical protocol.

Supplementary Methods

Inclusion Criteria for canine clinical trial protocol

Dogs were considered eligible for the oncolytic therapy if they were diagnosed by a veterinary neurologist with advanced CNS primary tumor with neural origin, excluding meningioma and other non-neural tumors (based on neurological symptoms and brain magnetic resonance images), had adequate organs function (hematocrit >25% and renal/hepatic function), with no neural infection diseases and whose owners were not pursuing chemotherapy or immediate euthanasia and consented to include the dogs in the clinical trial. Pre-treatment primary tumor size and location were obtained by brain magnetic resonance images (MRI) (Hitachi - Airis 0.3T Elite model) to establish a baseline for assessing tumor response.

Canine cell culture

D-GBM canine glioblastoma cell line were kindly provided by Dr. Michael Empl from University of Veterinary Medicine Hannover, Germany. Mesenchymal stem cell derived from normal canine adipose tissue (ADSC) were isolated and characterized as previously described[12]. All cells were cultivated in Dulbecco's Modified Eagle Media (DMEM) low glucose supplemented with 10% Fetal Bovine Serum (FBS, Thermo Fisher Scientific), 100 U/mL Penicillin, 100 µg/mL Streptomycin and 250 ng/mL Fungizone® (Thermo Fisher Scientific) at 37° C at 5% CO^2 atmosphere.

Immunofluorescence

Tissue sections were blocked with 10% FBS, 5% bovine serum albumin (BSA), and 0.1% Triton X-100 in PBS for 1 h at room temperature and incubated at 4°C overnight with primary antibodies anti-Zika virus NS2B (GTX133308, Genetex, 1:500), anti-Alpha-tubulin (NB100-690, Novus Biologicals, 1:200), anti-IBA1 (ab107159, Abcam, 1:200) and anti-CD14 (MCA1042, Serotec/BioRad, 1:500). Fixed mesenquimal and glioblastoma cells (3,7% formaldehyde for 30 minutes) were permeabilized (0.1% Triton X-100 in 1 PBS for 2-hour) and blockaded (5% bovine serum albumin in PBS) before primary antibody 4°C overnight incubation. Tissue and cell culture were incubated with secondary antibodies goat anti-rabbit IgG (A11037, Thermo Fisher Scientific) Alexa Fluor 594 and Goat anti-mouse IgG Alexa Fluor 488 (A11001, Thermo Fisher Scientific) at a 1:1000 dilution for 1 h at room temperature. Tissues and cell culture were counterstained with 1 µg/mL DAPI for 2 minutes and microscope slides mounted in Vectashield medium (Vector Laboratories). All images were taken in confocal microscope (Zeinss LSM 800).

In vitro ZIKV infection and detection by flow cytometry

D-GBM ($8x10^4$ cells/well) or VERO cells ($5x10^4$ cells/well) were seeded in 6-well plate and 96-well plate, respectively at the day before of infection in DMEM or MEM culture media supplemented with 10% FBS. At the day of infection, the media was replaced with plain culture media containing the virus at MOI of 0.1, 1, 2, 5 and 10. After 1 hour

at 37 °C/5% CO2, the virus was removed and the cells washed once with 100ul of plain media and incubated in media supplemented with 2% FBS for 24, 48 or 72 hours. The cells were harvested using 50ul of trypsin/EDTA 2.5g/L solution (Vitrocell/Embriolife) and moved to a V-bottom 96-well plate containing 50ul of 1X PBS/2% FBS. The cells were pelleted at 700xg/5min/4 °C and washed with 100ul of 1X PBS/2% FBS. After, the cells were fixed and permeabilized using the BD Cytofix/Cytoperm method (BD Biosciences). Briefly, the cells were incubated on ice/15 minutes with 50 ul of Cytofix solution and washed twice with 100ul of 1X Cytoperm solution. The cells were then stained with the primary antibody 4G2 (0.5ug/well) followed by the secondary antibody goat anti-mouse-Alexa Fluor® 488 at 1:800 (Thermo Fisher Scientific) for 30 minutes each and washed as described above. Finally, the cells were resuspended in 200 ul of 1X PBS/2% FBS. The cells were acquired by LSR FortessaTM Analyser (BD Biosciences) and the data were using the FlowJo Software to determine the presence of E ZIKV protein intracellularly.

Cell proliferation Assay (Cell Growth Curve)

To access $ZIKV^{BR}$ influence on the D-GBM cells growing, $5x10^3$ cells per well were seeded in 96-well plate at a day before of infection. The cells were infected with $ZIKV^{BR}$ at MOIs of 1, 10 and 100 and their growth were evaluated at different time points (24h, 42h, 72h, 96h, and 120 hours). The $ZIKV^{BR}$ permissive VERO cells were infected at the same conditions serving as control to the assay. The cells were maintained in DMEM (D-GBM) or MEM (VERO) media supplemented with 10% FBS at 37 °C/5% CO_2. The culture media was removed, and the cells washed once with 200ul of 1X PBS and fixed with 100ul of 70% ethanol for 10 minutes. After, the cells were incubated with 40ul of 0.5% gentian violet (Laborclin) for 30 minutes. The cells were then washed 5 times with 200ul of Milli-Q water and lysed with 100 ul of 10% acetic acid. After 30 minutes, the absorbance was measured at 540 nm using the Epoch microplate spectrophotometer[37] (BioTek Instruments Inc).

LIVE/DEAD D-GBM viability assay after in vitro ZIKV infection

D-GBM were seeded in 6-well plate (1×10^5 cells/well) at the day before of $ZIKV^{BR}$ infection in DMEM media supplemented with 10% FBS. After overnight cells incubation, the media was replaced with the culture media containing the virus at MOI of 0.1, 1, and 2. Cells were incubated for 72 hours for further cell viability analysis. For the positive control, cells were treated with a 20% DMSO culture media solution for 5 min prior to the cells labeling. Then, the total cells (adherent and floating cells) were harvested, washed, moved to a U-bottom 96-well plate and stained with the LIVE/DEAD™ Fixable Violet Dead Cell Stain Kit (#L34964), according to manufacturer's instructions. Finally, the cells were resuspended in 200 ul of 1X PBS/2% FBS and acquired by LSR FortessaTM (BD Biosciences) flow cytometer. Data were analyzed using the FlowJo software.

Supplementary Figures

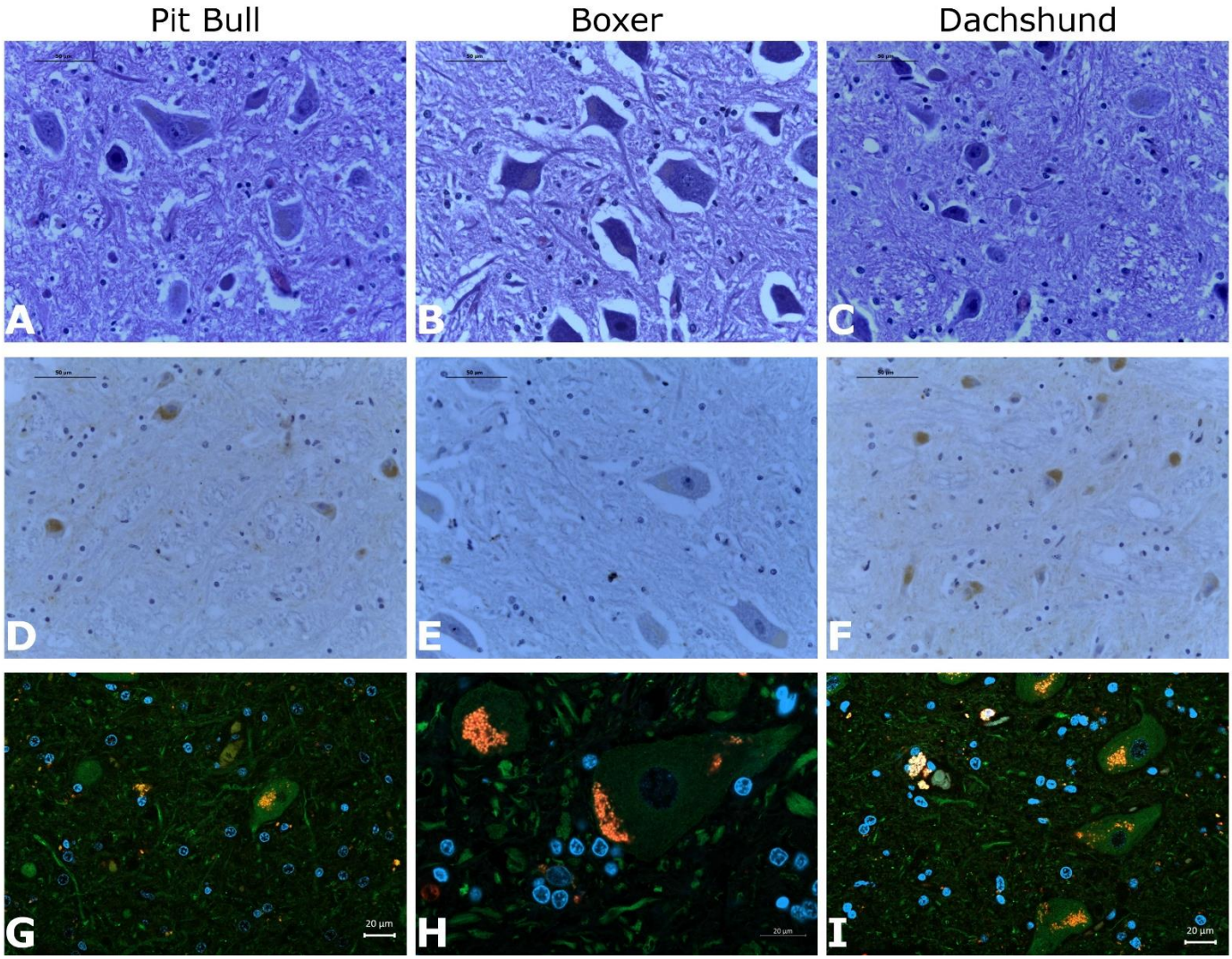

Supplementary Figure S1: Absence of viral infection in canine neurons after ZIKV^{BR} CNS infection. Representative images of neurons from CNS tissues H&E (A-C), immunohistochemistry immunolabeling for ZIKV^{BR} (D-F) and immunofluorescent immunolabeling (G-I) for ZIKV^{BR} (red), β3-TUBULIN cytoplasmatic (green) protein and nuclei DAPI (blue). Lipofuscin accumulation in neurons can be seen in post-mortem Pit Bull (A, D, G), Boxer (B, E, H) and Dachshund (C, F, I) in dogs CNS tissues samples after H&E and immunohistochemistry analysis, in brown, and in immunofluorescent analysis, in yellow, by unspecific-positive result for ZIKV^{BR} (red), β3-TUBULIN cytoplasmatic. Scale bar, 50 µm and 20 µm.

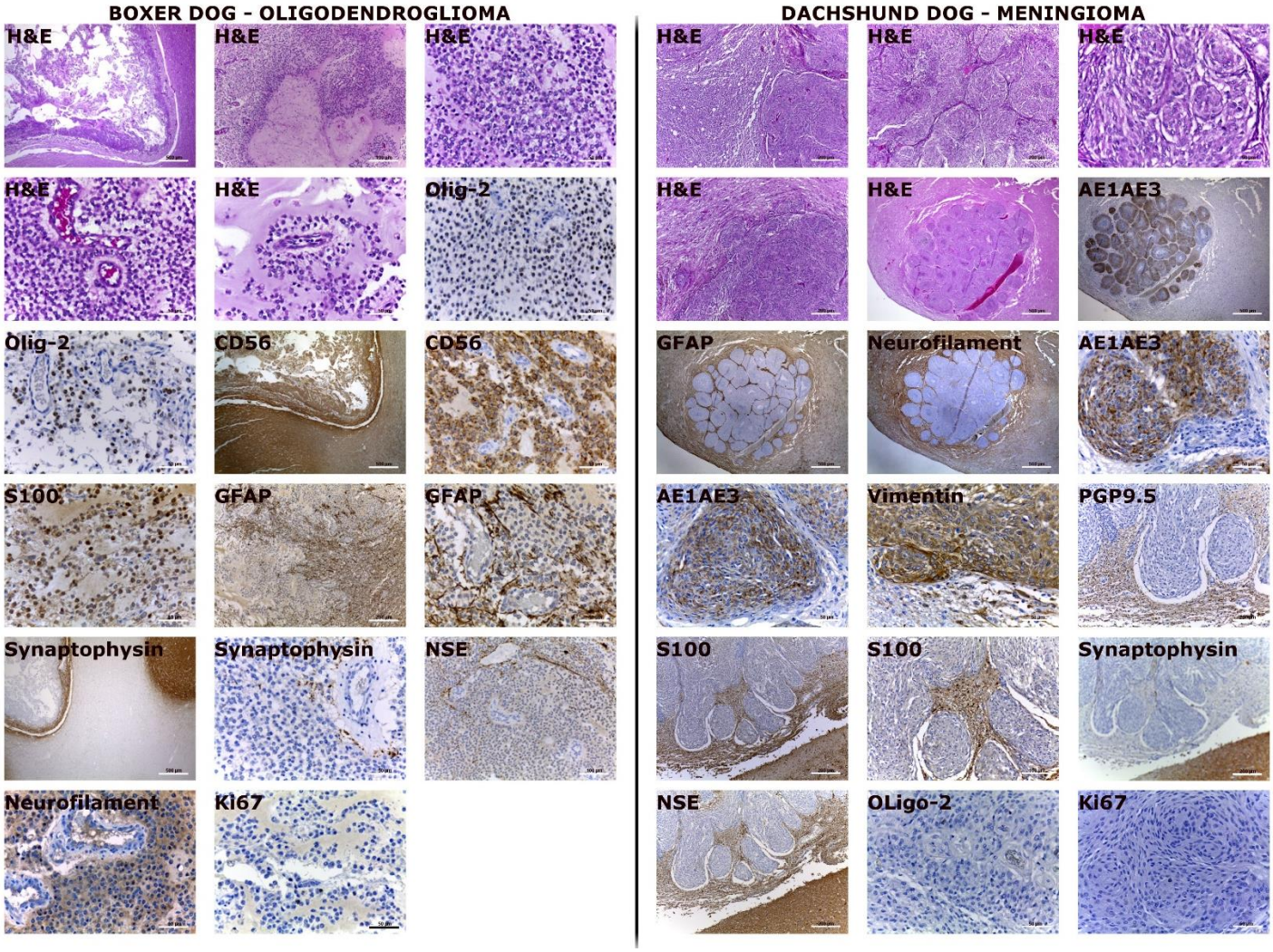

Supplementary Figure S2: Immunohistochemistry assay for histopathologic tumor diagnosis. Boxer dog: confirmed oligodendroglioma by positive immunolabeling in tumor cells for Olig2, CD56, S100, Ki67 and negative immunolabeling for GFAP, Synaptophysin, NSE and Neurofilament markers. **Dachshund dog:** confirmed meningioma by positive immunolabeling in tumor cells for CK Pan (AE1AE3), Vimentin and negative immunolabeling for GFAP, Synaptophysin, Neurofilament, NSE, S100, Olig2, PGP 9.5 and Ki67 markers.

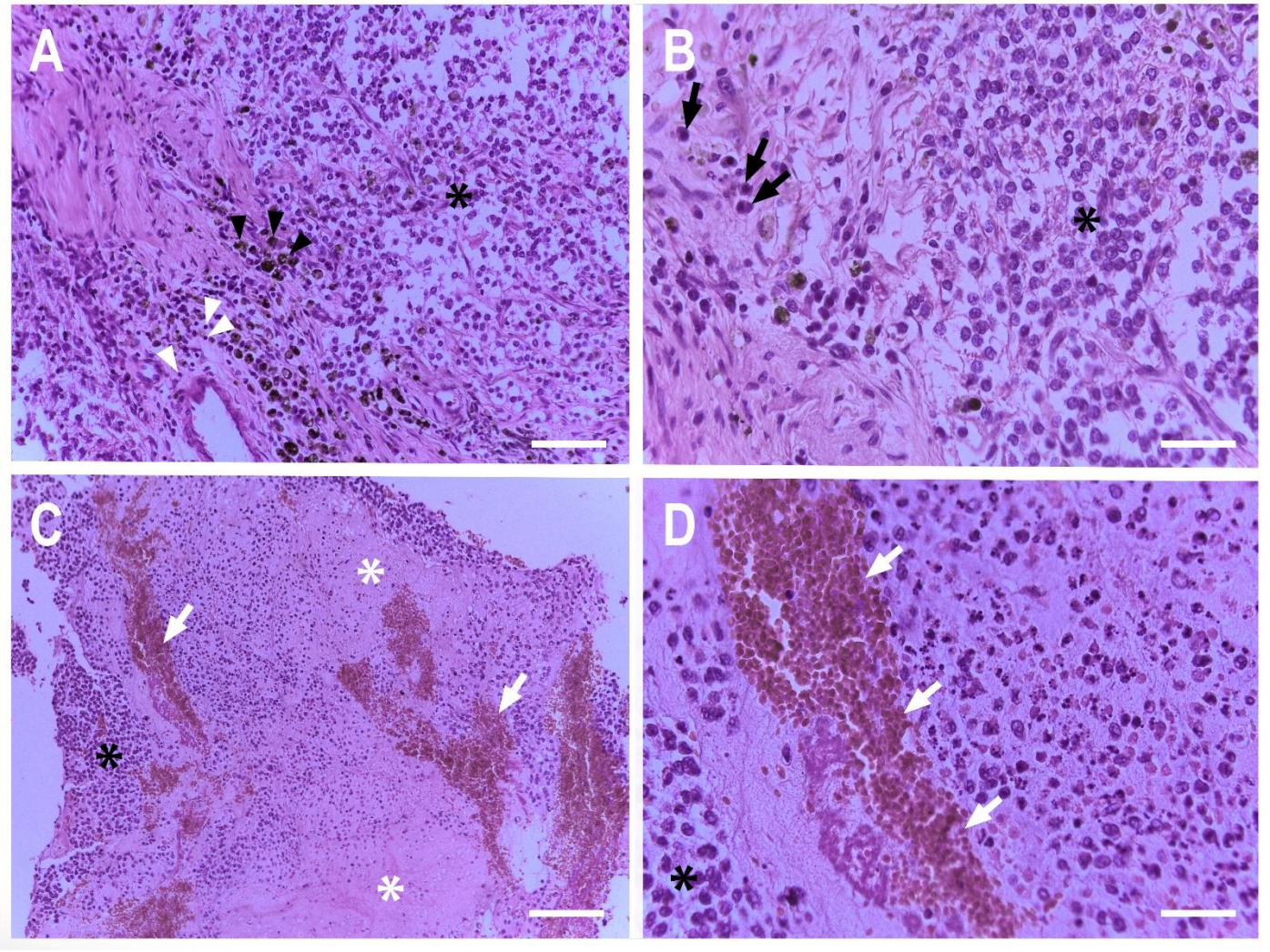

Supplementary Figure S3: H&E representative images of Boxer dog tumor. A and B, Macrophages (black arrowhead), Lymphocytes (white arrowhead) and plasma cell (black arrow) presence in the tumor (black asterisk). Scale bar, 100 µm (A) and 50 µm (B). C and D, Large necrosis area (white asterisk) with haemorrhage (white arrow) alongside remaining tumor cells (black asterisk). Scale bar, 200 µm (C) and 50 µm (D).

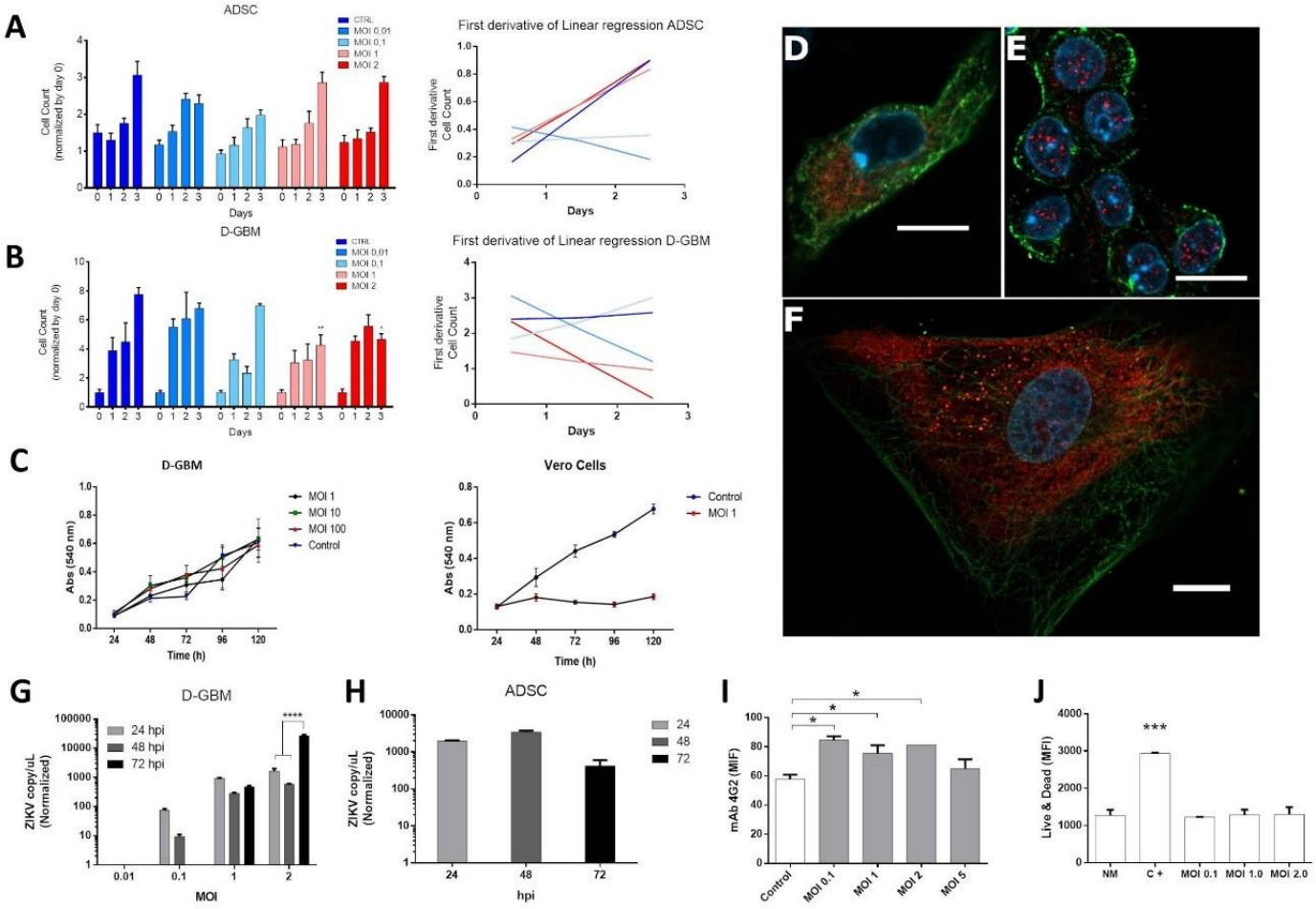

Supplementary Figure S4: ZIKV^{BR} in vitro infection in canine cell lines. A-B, Total cell number of canine mesenchymal stem cell (ADSC)(A) and dog glioblastoma cell line (D-GBM) (B) infected by ZIKV^{BR} at different MOI conditions at 24, 48 and 72 hpi. First derivative of linear regression graphic analysis is followed at right. (*p<0.05, **p<0.01). **C,** Evaluation of cell death induced by ZIKV infection (MOI 1, 10 or 100) in D-GBM and VERO cells for up to 120 hours. **D-F,** Immunolabeling positive of ZIKV^{BR} (red), β3-TUBULIN cytoplasmatic (green) protein and nuclei DAPI (blue) in MOI 2 at 72 hpi of D-GBM (D-E) and ADSC (F) cells. Scale bar, 10 µm. **G-H,** Viral genomic copies on culture supernatants at 24, 48 and 72 hpi in MOI 0.01, 0.1, 1 and 2 for D-GBM(G) and MOI 2 for ADSC(H). (****p<0.0001). **I,** Intracellular staining of E ZIKV protein using the mAb 4G2 by flow cytometry (*p<0.05). **J,** Cell viability of ZIKV-infected D-GBM cell culture evaluated 48h after infection by flow cytometry. (***p<0.001)

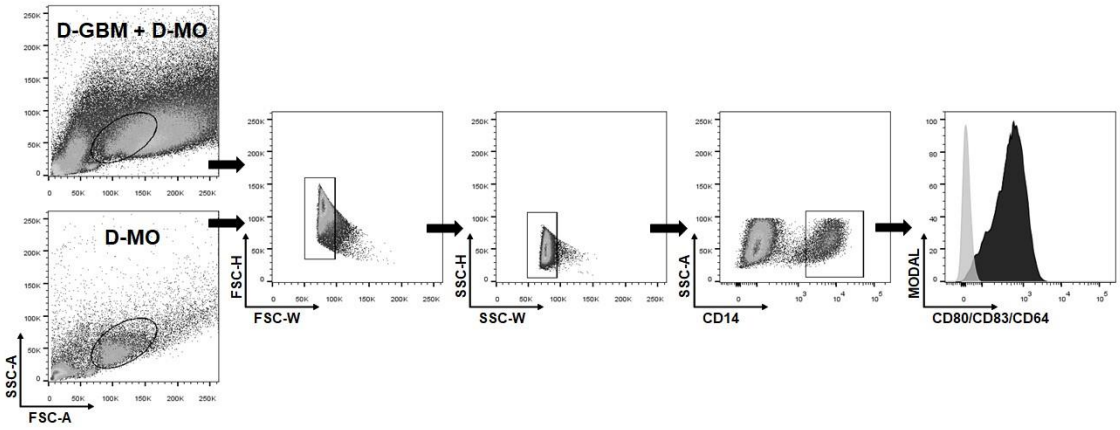

Supplementary Figure S5: Gating strategy for the evaluation of canine monocytes in the co-culture assay. Doublets were initially excluded from analysis by FSC and SSC parameters. D-GDM and monocytes were distinguished by $CD14^+$ expression. Cells were gated by the expression of $CD14^+$ and subsequently separated according to the $CD80^+$, $CD83^+$ and $CD64^+$ specific surface molecules expression and analyzed by mean of fluorescence intensity (MFI).

Supplementary Table 1: Primers sequence for the quantitative PCR for canine immune mediators

Canine Primers	Sequence
ZIKV	ZIKV 1086 forward: 5′-CCGCTGCCCAACACAAG-3 ZIKV 1162 reverse: 5′-CCACTAACGTTCTTTTGCAGACAT-3
MHC-1	forward 5′-CACCAACCTGTCCAAAGTTCC-3 reverse 5′-CCGGGCAGATCAAGAGAAGATA -3
GRANZYME B	forward 5′-GGAGAGATCATCGGGGGACATGA -3 reverse 5′-CTCCTGTTCCTTGATGTTGTGG-3
PD-1	forward 5′-ATGAGAATGTTTAGTGTCTT-3′ reverse 5′-TTATGTCTCTTCAAATTGTATATC-3′
PDL-1	forward 5′-AGGATGGCTCCTAGACTCCC-3′ reverse 5′-AGACGATGGTGGCATACTCG-3′
CCR2	forward 5′- ACATGCTGTCCACATCGCA -3′ reverse 5′- GGCGCGCTGTAATCATAGTC -3
STAT1	forward 5′- CTTACCCAGAAAGCCCTGATTA -3′ reverse 5′- CTGTATTCCTCTCGCTCACATC -3
NOS2	forward 5′- GGAAGCAGTAACAAAGGAGATAGA -3′ reverse 5′- CCTCCACCTGGTAGTAGTAGAA -3
IDO1	forward 5′- GTCTGCCTCCTATTCTGGTTTAT -3′ reverse 5′- GCAGTTTGGAGTTGCCTTTC -3
ARG1	forward 5′- GGTGGCAGAAGTCAAGAAGA -3′ reverse 5′- GGTGGGTTAAGGTAGTCAATAGG -3
CX3CR1	forward 5′- GACACATCAGACGTTCCCTTCCCAG -3′ reverse 5′- TGTCCCACAAATCACAGGCTTCA -3
CXCL10	forward 5′- TGGTACTCAAGGAATACCTCTCT -3′ reverse 5′- ATTGCTTTCACTAAACTCTTGATGG -3
CCR7	forward 5′- CCCTGACCTTTAGCAACATACA -3′ reverse 5′- AGCAAGGAGCCGAGATAGA -3
STAT1	forward 5′- CTTACCCAGAAAGCCCTGATTA -3′ reverse 5′- CTGTATTCCTCTCGCTCACATC -3
GATA3	forward 5′- TCTCCTTCCTCTTCTCCTCTTT -3′ reverse 5′- GGTACTTGATGCACTCCTTCTC -3
SOCS3	forward 5′- CAAGACCTTCAGCTCCAAGAG -3′ reverse 5′- GTAGTGATGCACCAGCTTGA -3
NK2D	forward 5′- GTTATTGTGGTCCGTGTCCTAA -3′ reverse 5′- ACTGCCAGGATCCATTTGTTGG -3
NKP30	forward 5′- CTTCTTGCCGTGTTCCTTCAA -3′ reverse 5′- CCAGAACCTCCACTCTGCACA -3
β-ACTIN	forward 5′- ACCAACTGGGACGACATGGAGA -3′ reverse 5′- AGGCATACAGGGACAGGACAG -3

Supplementary Data 1: MRI Images. Representative images of all MRI from the Pitbull, Boxer and Dachshund dogs post contrast T1 and T2 weighted dorsal, transversal and sagittal planes.

Pirata MRI 1 - **DAY 0** - Post contrast T1 weighted dorsal plane
Patient: Pirata (Pitbull dog)

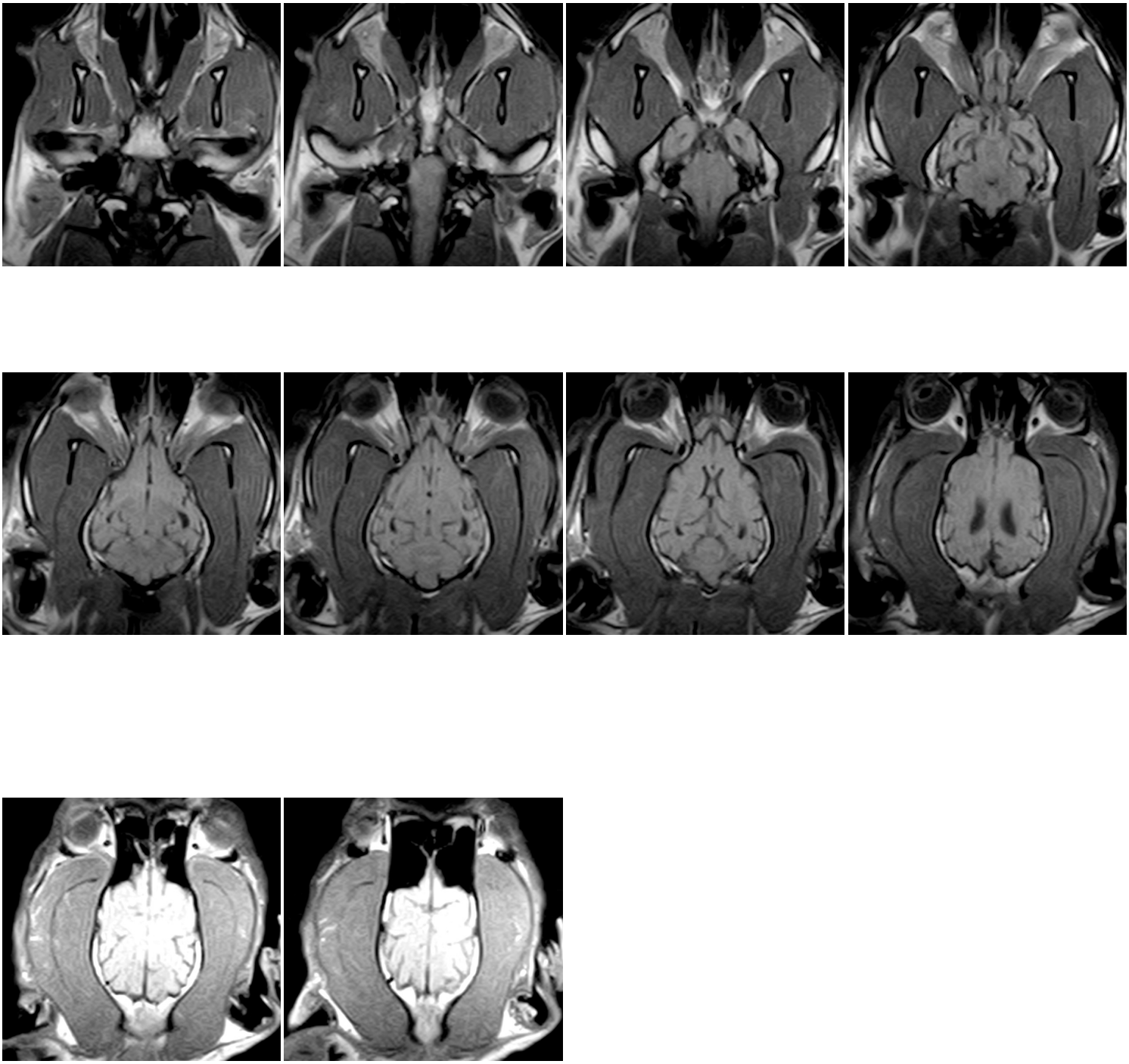

Pirata MRI 1 - **DAY 0** - Post contrast T2 weighted dorsal plane
Patient: Pirata (Pitbull dog)

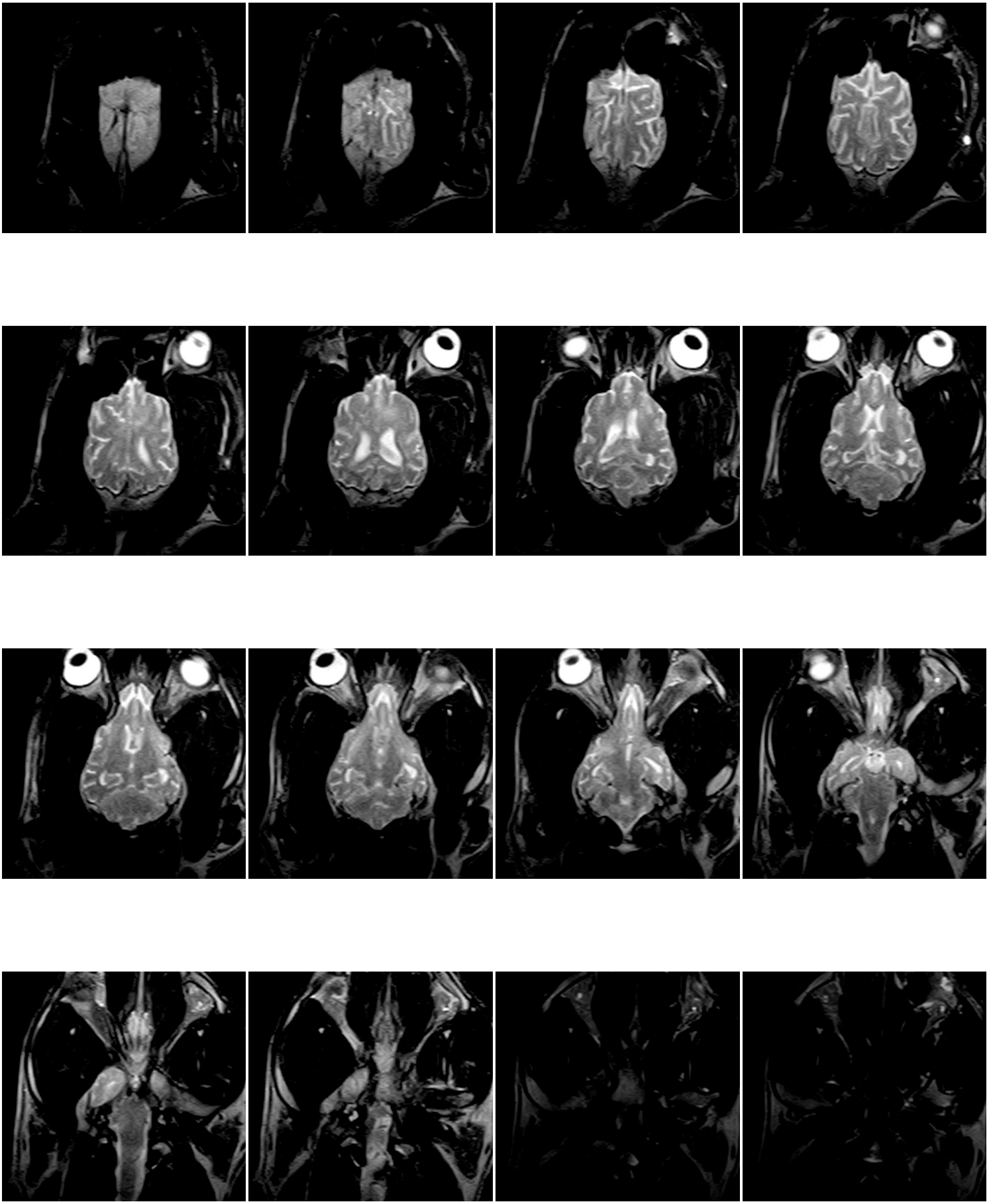

Pirata MRI 1 - **DAY 0** - Post contrast T2 weighted transversal plane
Patient: Pirata (Pitbull dog)

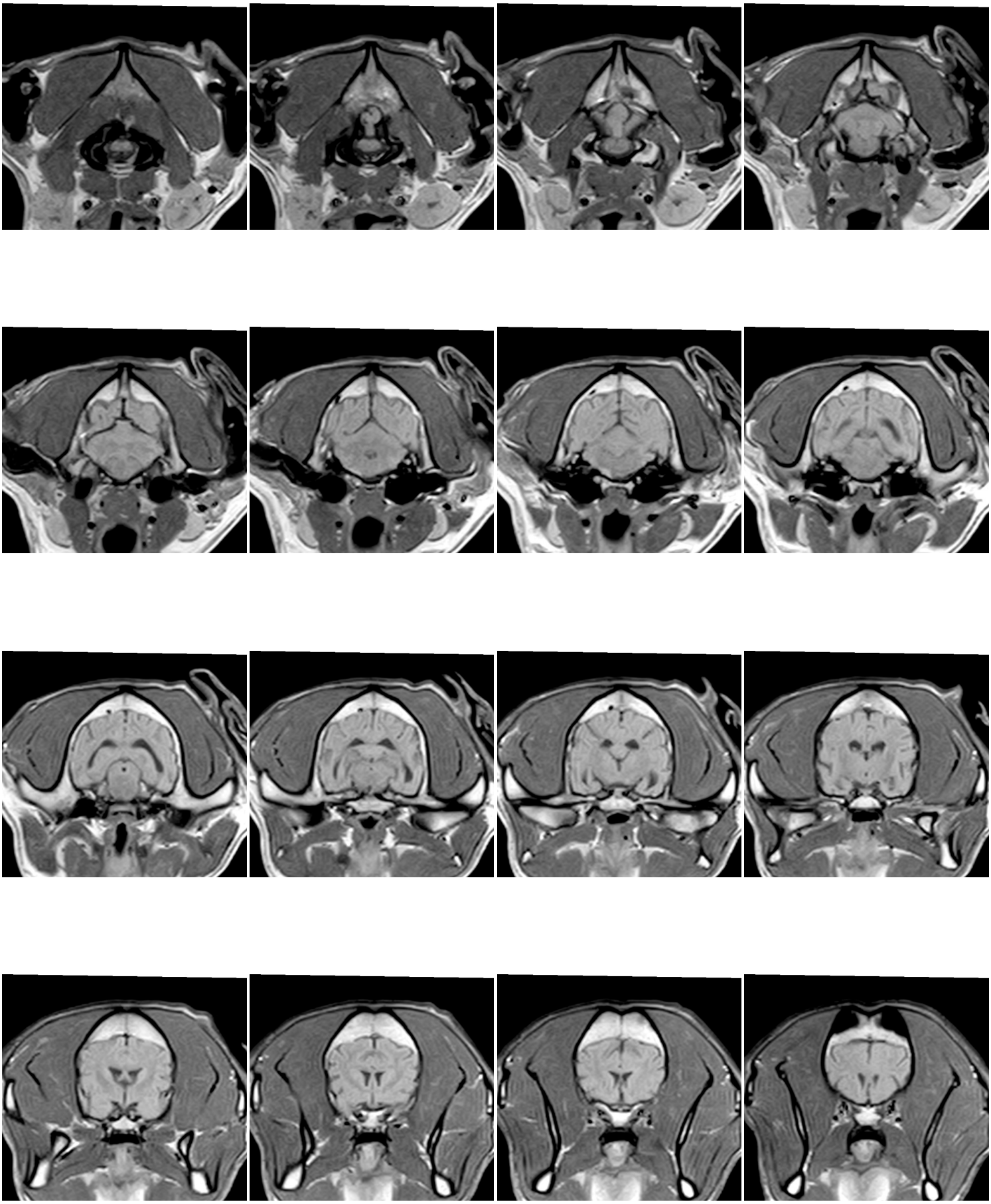

Pirata MRI 2 - **DAY 7** - Post contrast T1 weighted dorsal plane
Patient: Pirata (Pitbull dog)

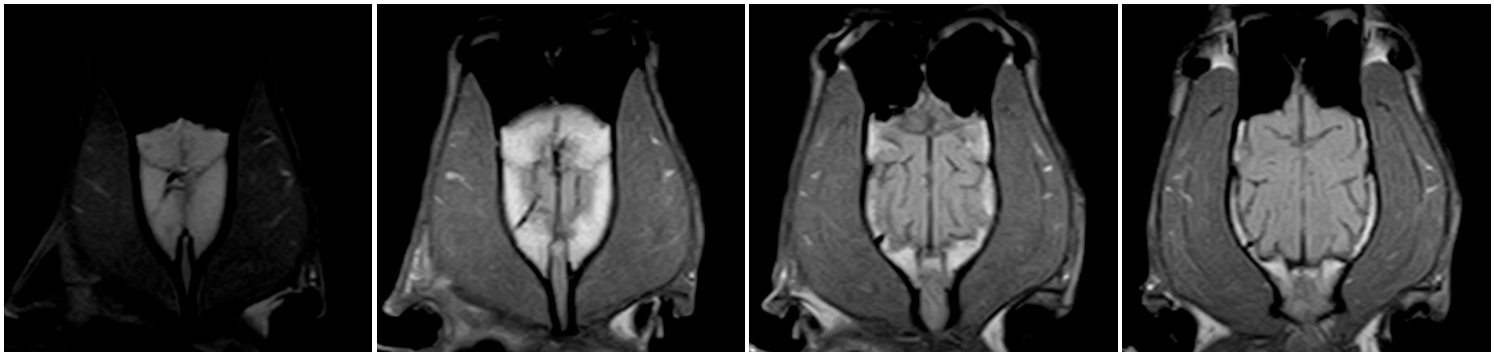

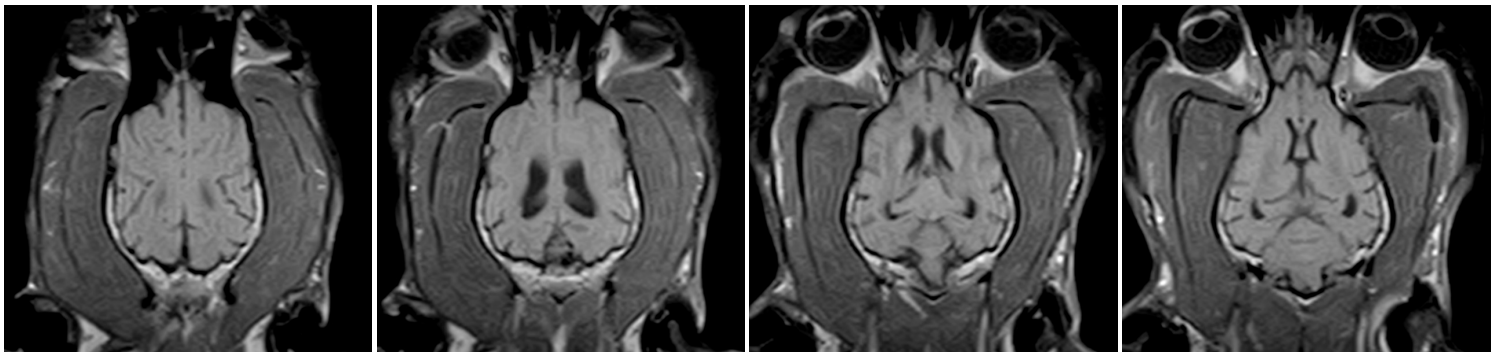

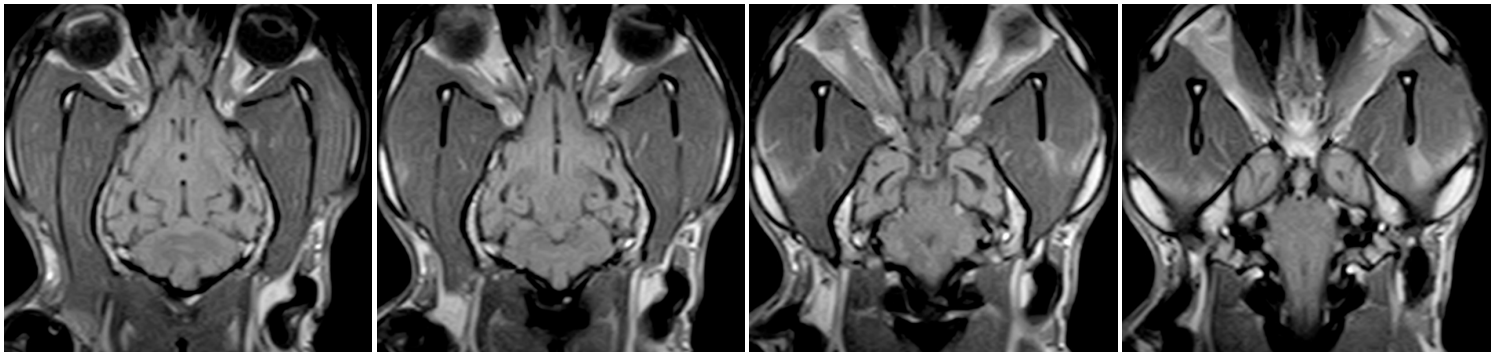

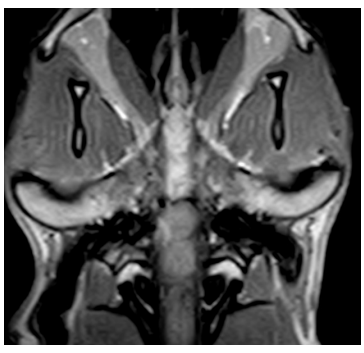

Pirata MRI 2 - **DAY 7** - Post contrast T2 weighted dorsal plane
Patient: Pirata (Pitbull dog)

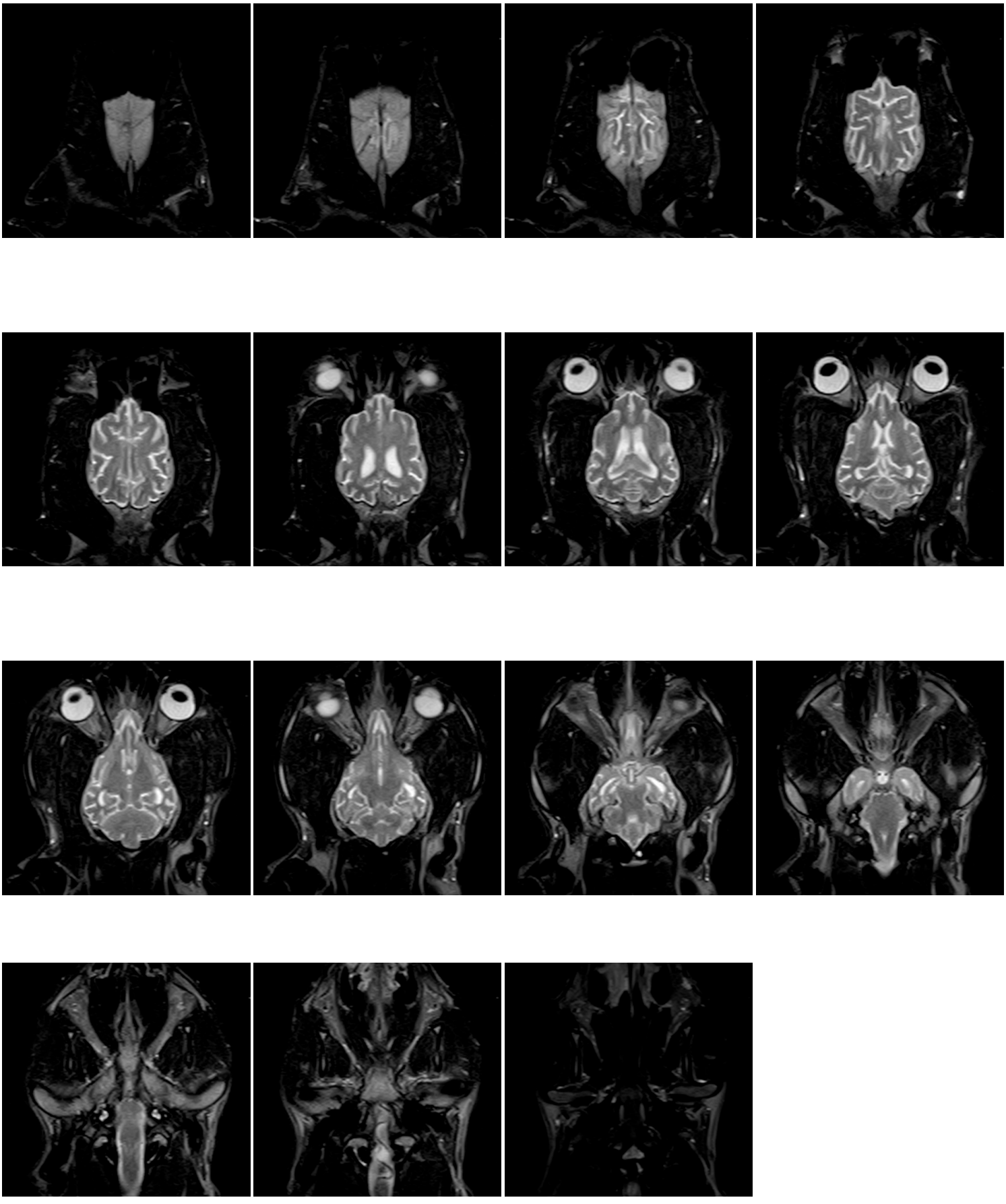

Pirata MRI 2 - **DAY 7** - Post contrast T2 weighted sagittal plane
Patient: Pirata (Pitbull dog)

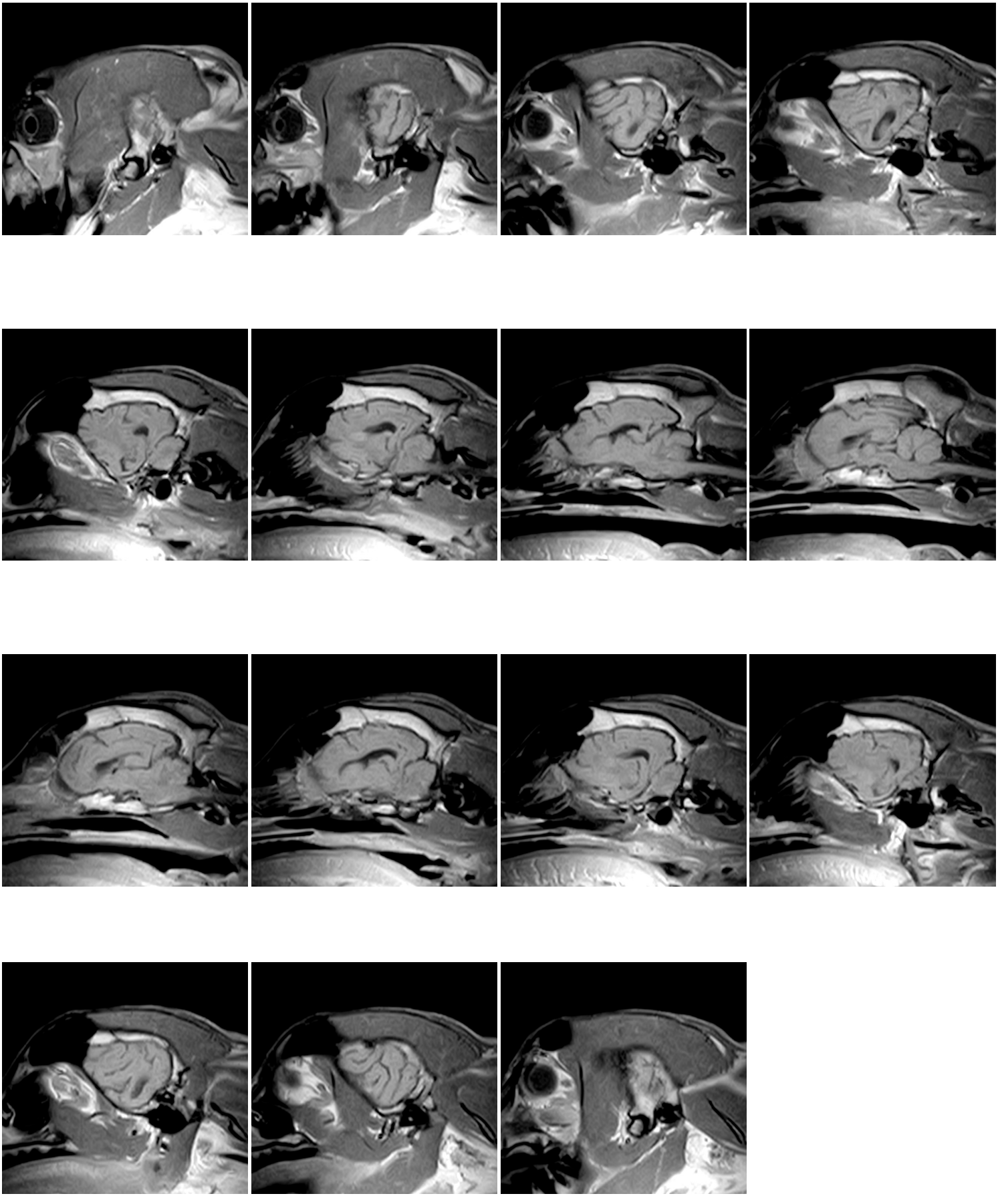

Pirata MRI 2 - **DAY 7** - Post contrast T1 weighted transversal plane
Patient: Pirata (Pitbull dog)

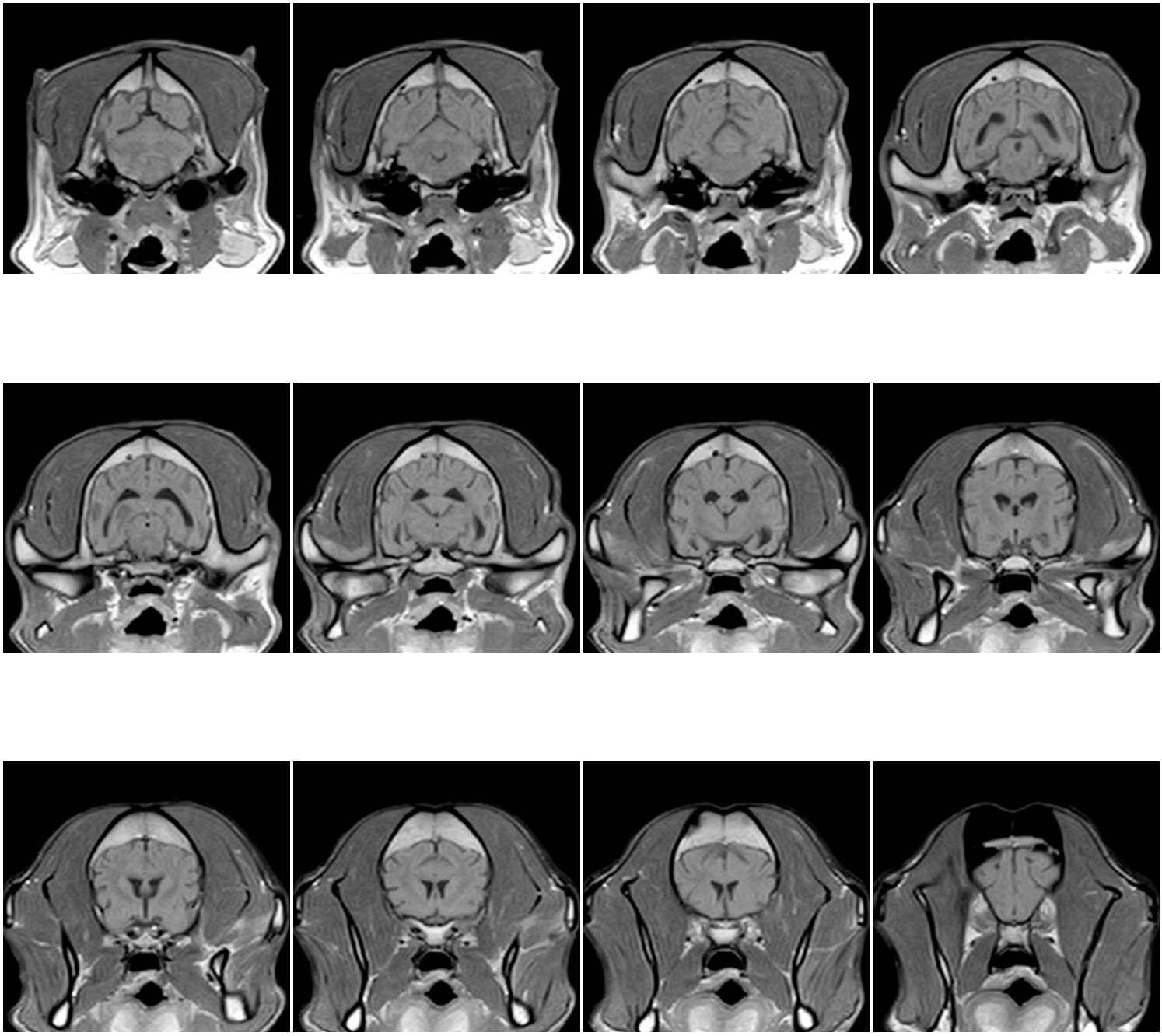

Pirata MRI 2 - **DAY 7** - Post contrast T2 weighted transversal plane
Patient: Pirata (Pitbull dog)

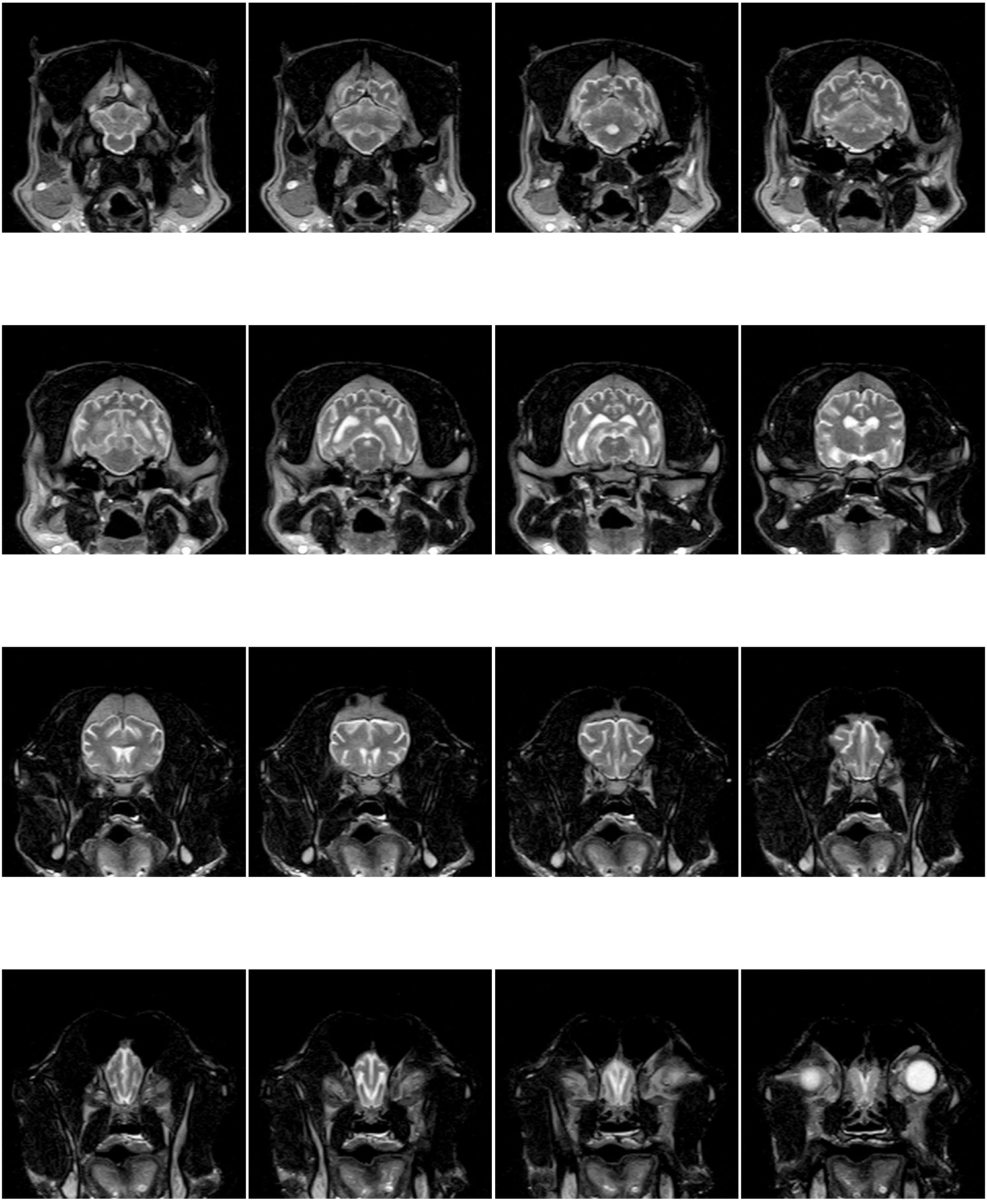

Pirata MRI 3 – **DAY 14** - Post contrast T1 weighted dorsal plane
Patient: Pirata (Pitbull dog)

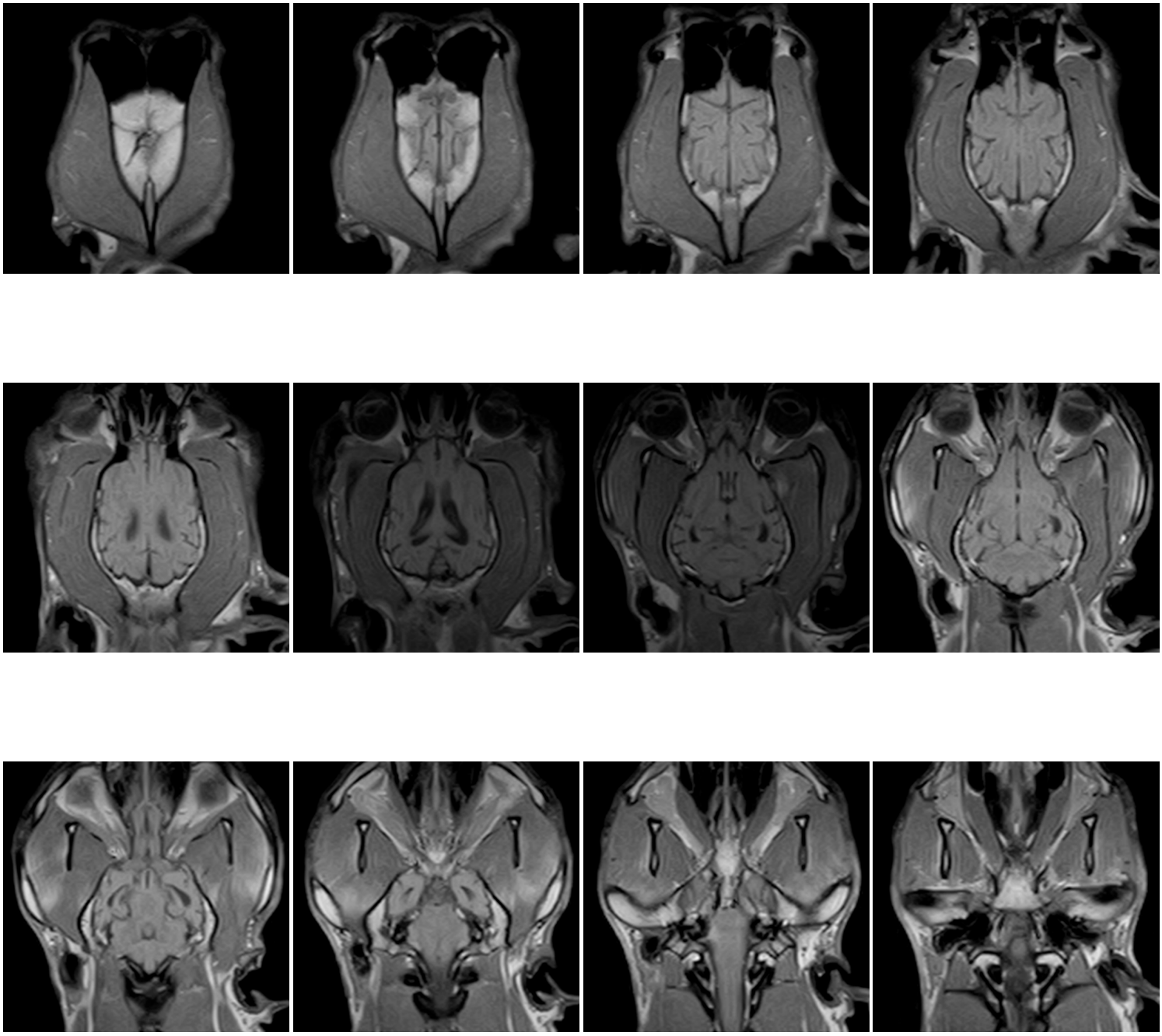

Pirata MRI 3 – **DAY 14** - Post contrast T2 weighted dorsal plane
Patient: Pirata (Pitbull dog)

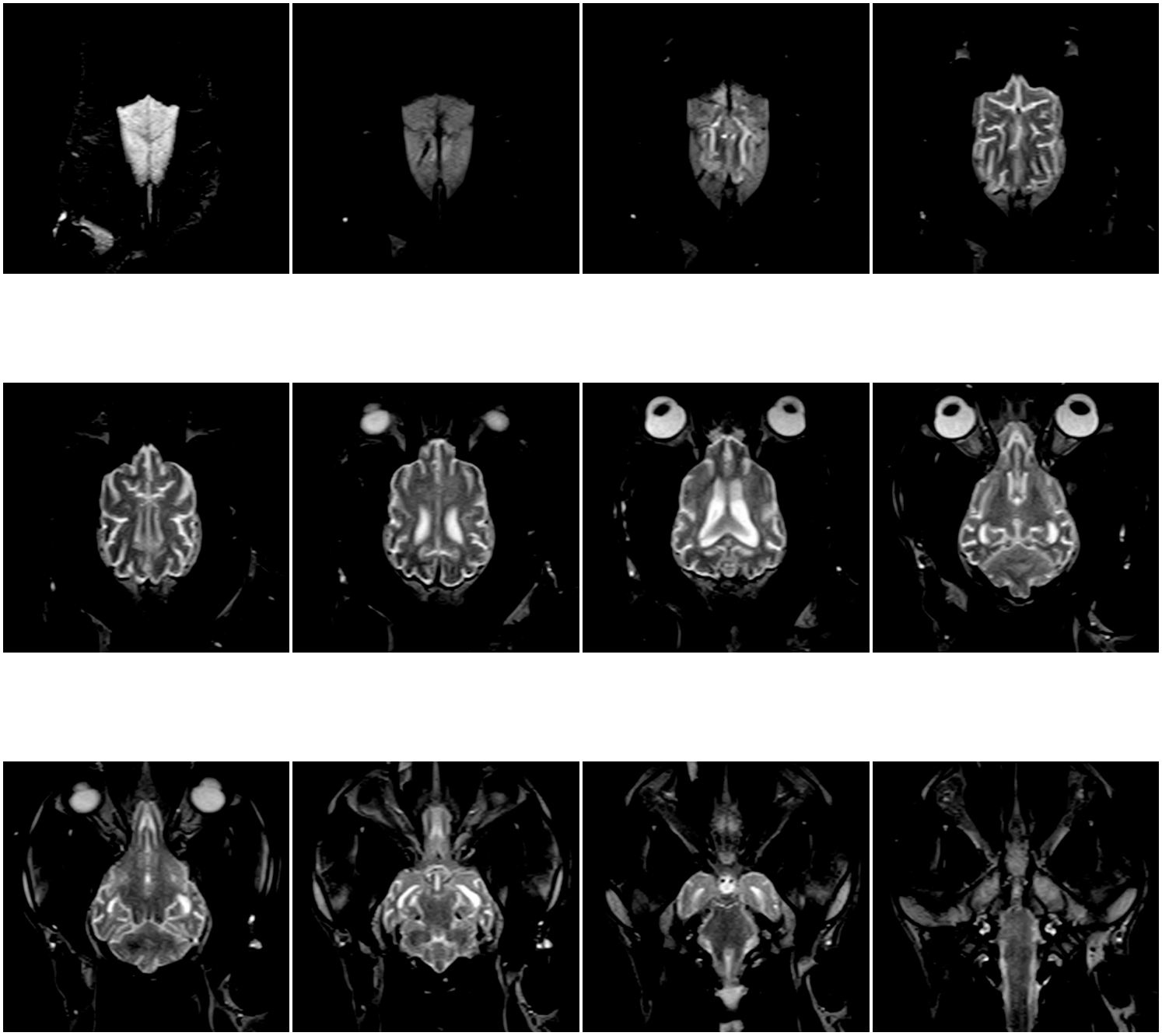

Pirata MRI 3 – **DAY 14** - Post contrast T1 weighted sagittal plane
Patient: Pirata (Pitbull dog)

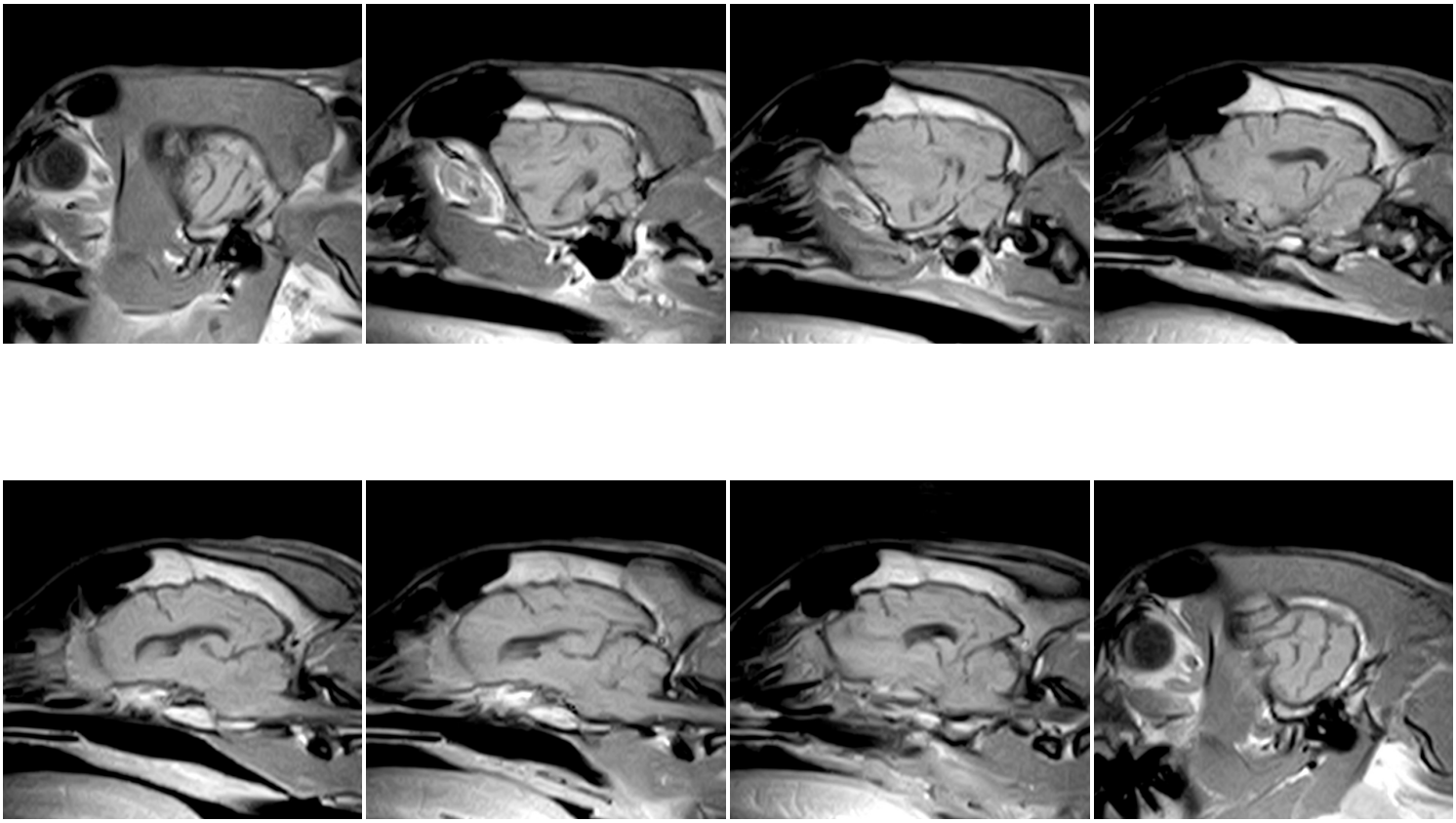

Pirata MRI 3 – **DAY 14** - Post contrast T1 weighted transversal plane
Patient: Pirata (Pitbull dog)

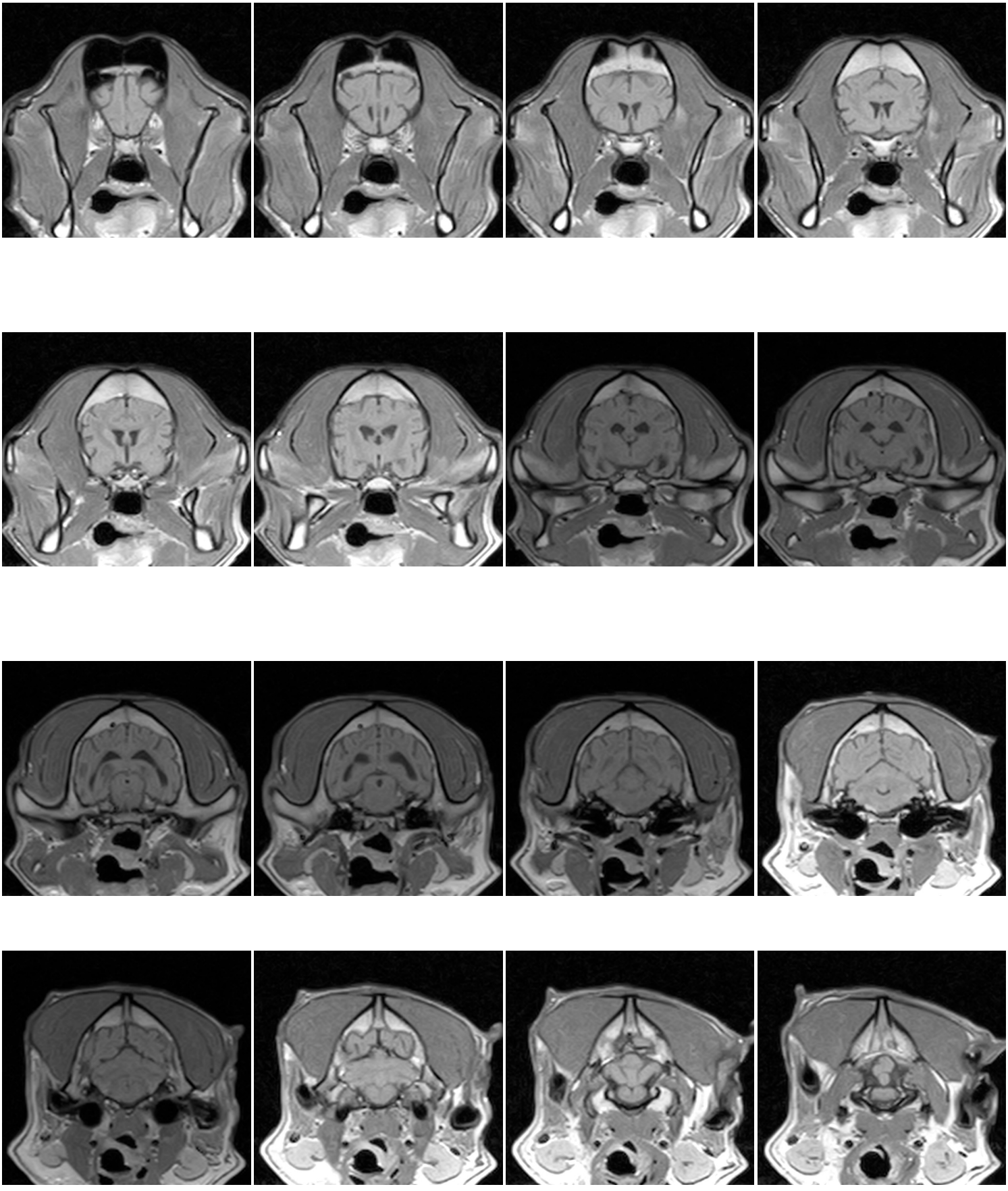

Matheus MRI 1 - **DAY 0** - Post contrast T1 weighted dorsal plane
Patient: Matheus (Boxer dog)

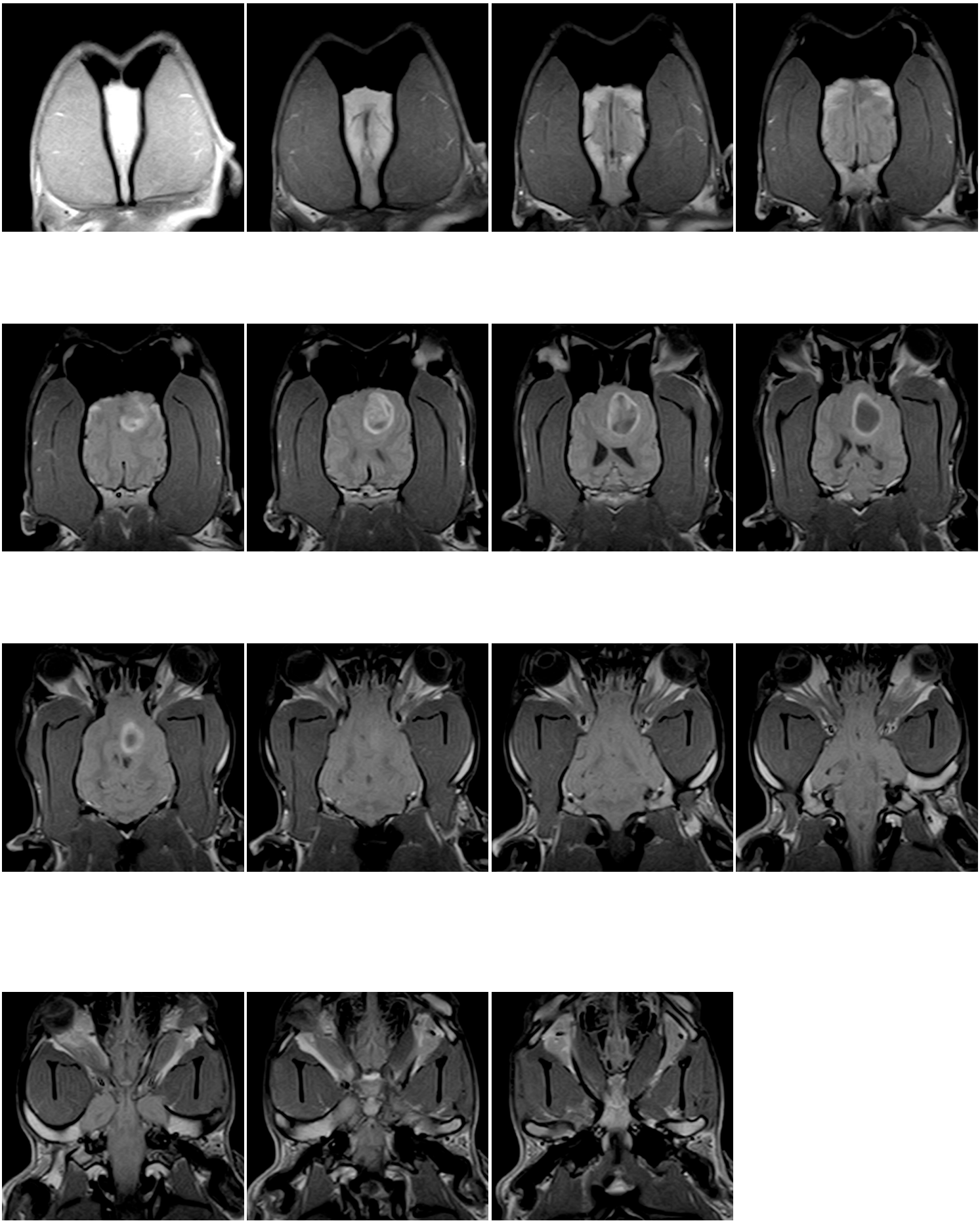

Matheus MRI 1 - **DAY 0** - Post contrast T1 weighted sagittal plane
Patient: Matheus (Boxer dog)

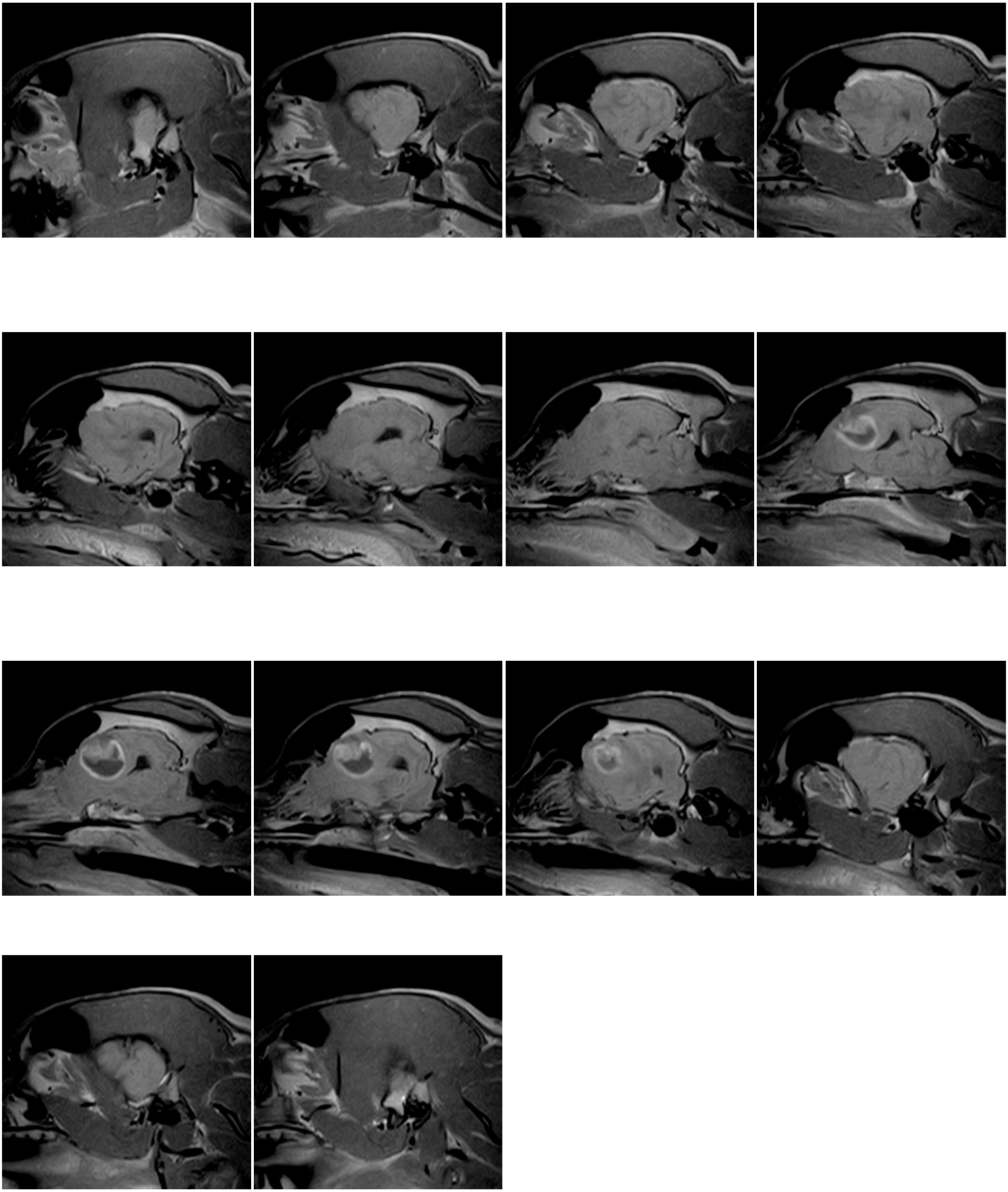

Matheus MRI 1 - **DAY 0** - Post contrast T1 weighted transversal plane
Patient: Matheus (Boxer dog)

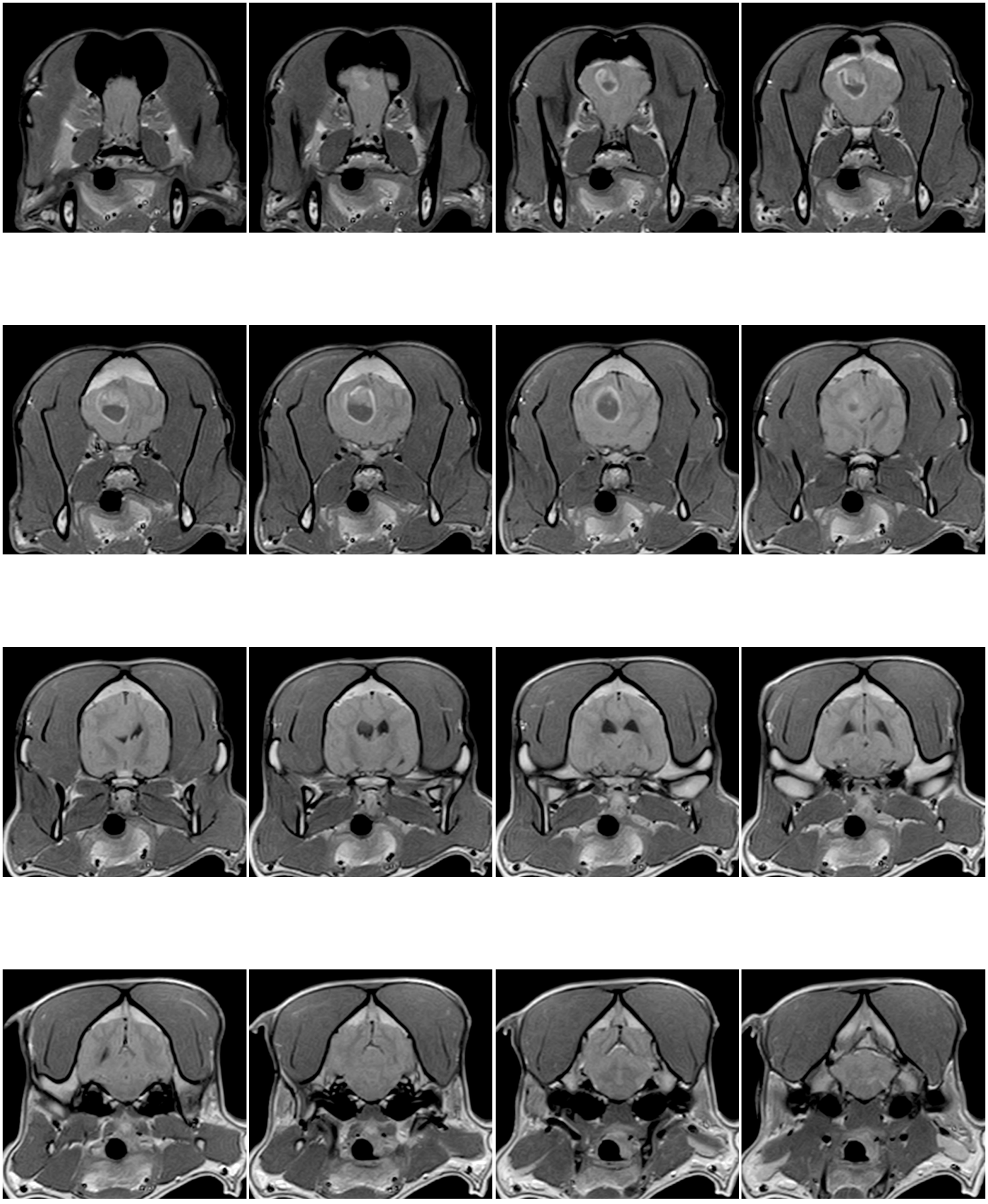

Matheus MRI 2 - **DAY 14** - Post contrast T1 weighted dorsal plane
Patient: Matheus (Boxer dog)

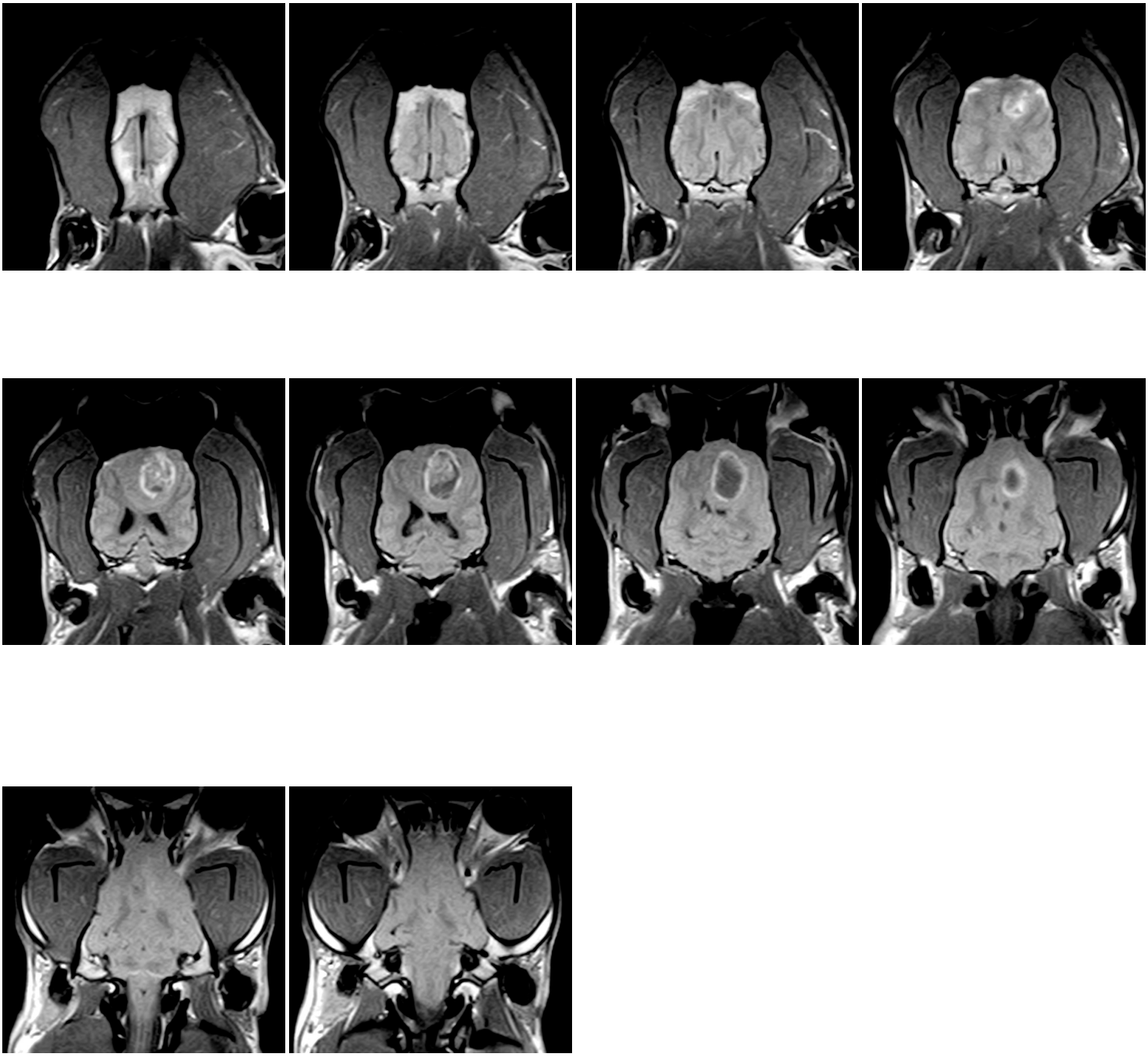

Matheus MRI 2 - **DAY 14** - Post contrast T1 weighted sagittal plane
Patient: Matheus (Boxer dog)

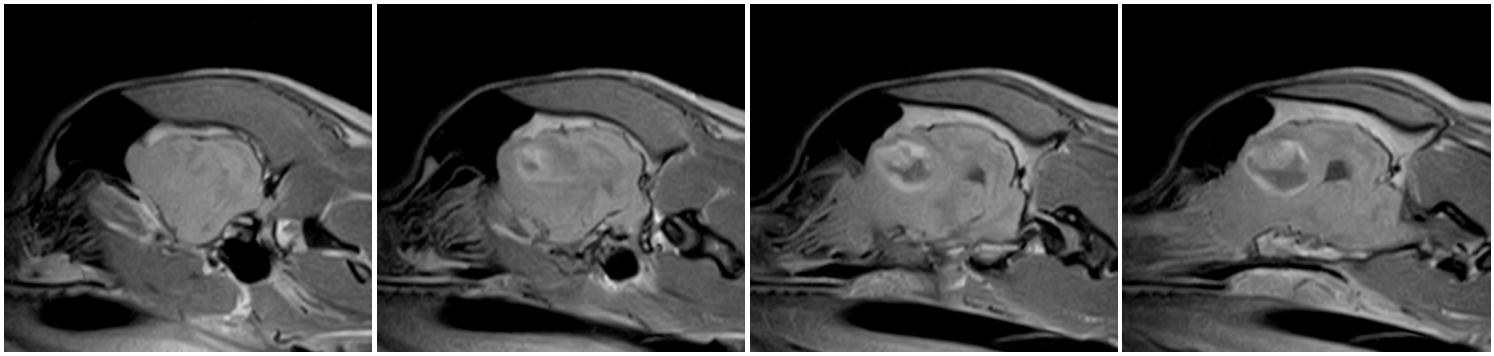

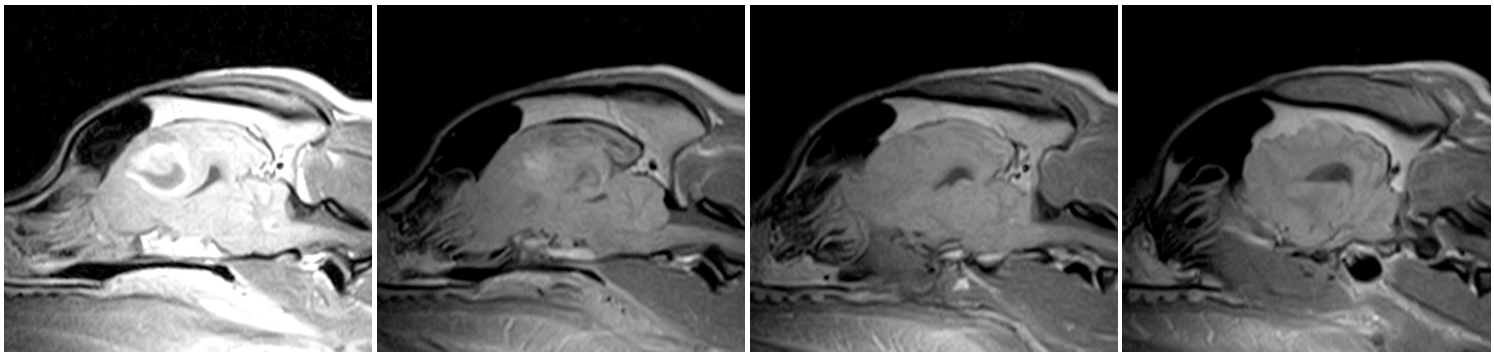

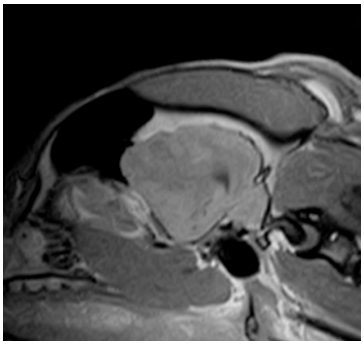

Matheus MRI 2 - **DAY 14** - Post contrast T1 weighted transversal plane
Patient: Matheus (Boxer dog)

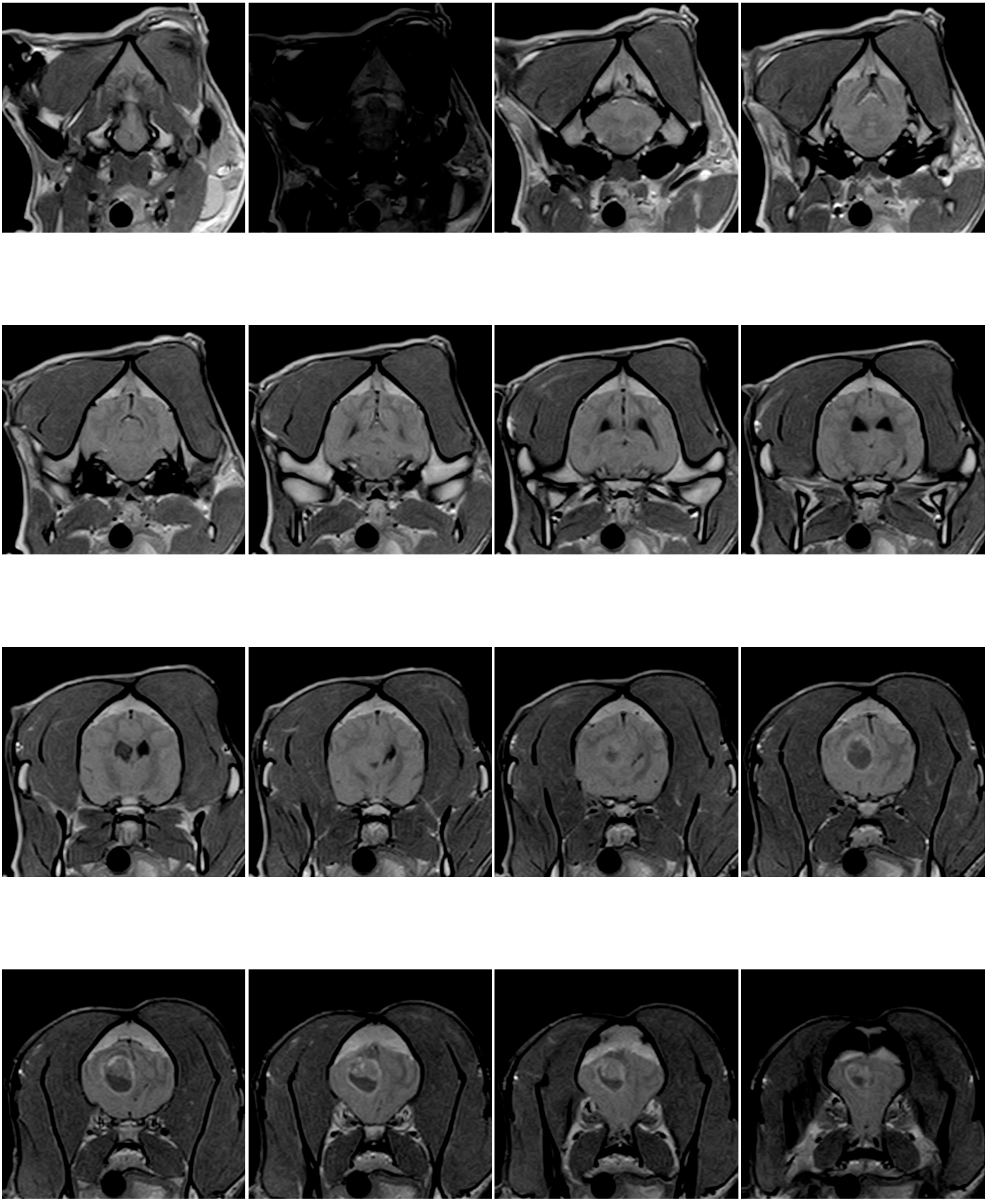

Matheus MRI 3 - **DAY 21** - Post contrast T1 weighted dorsal plane
Patient: Matheus (Boxer dog)

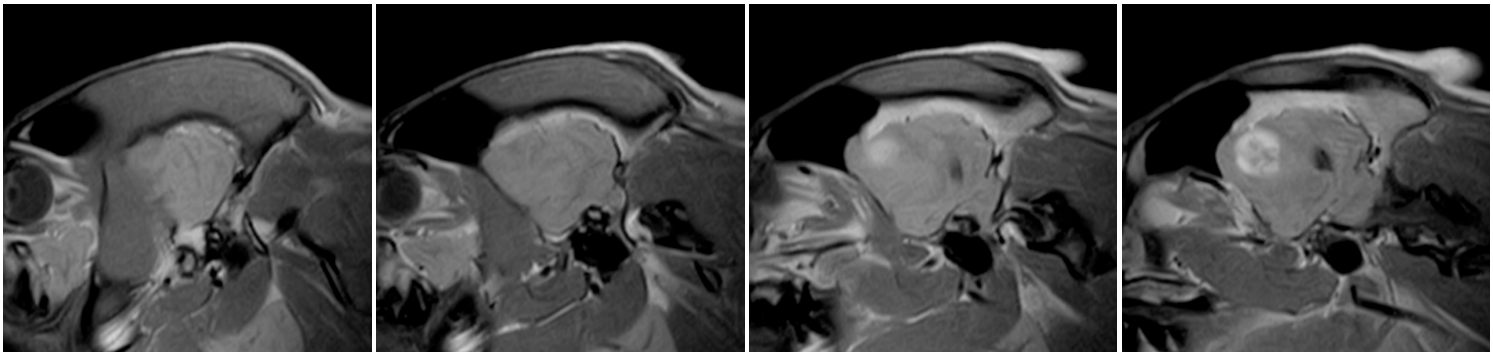

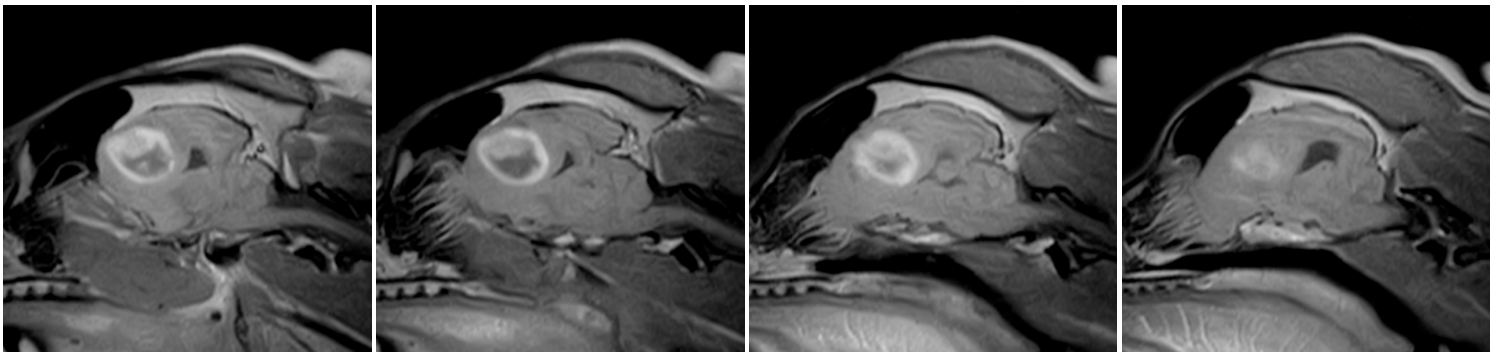

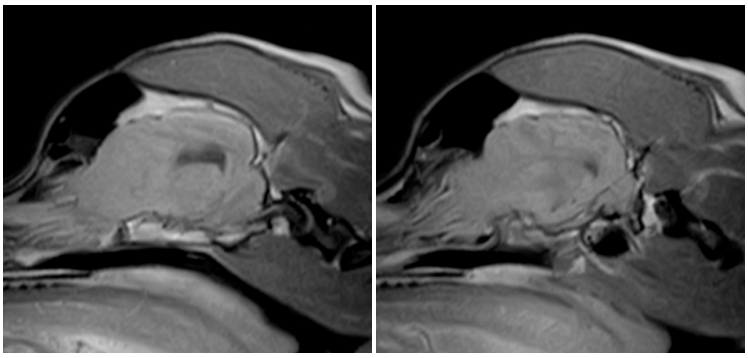

Matheus MRI 3 - **DAY 21** - Post contrast T1 weighted transversal plane
Patient: Matheus (Boxer dog)

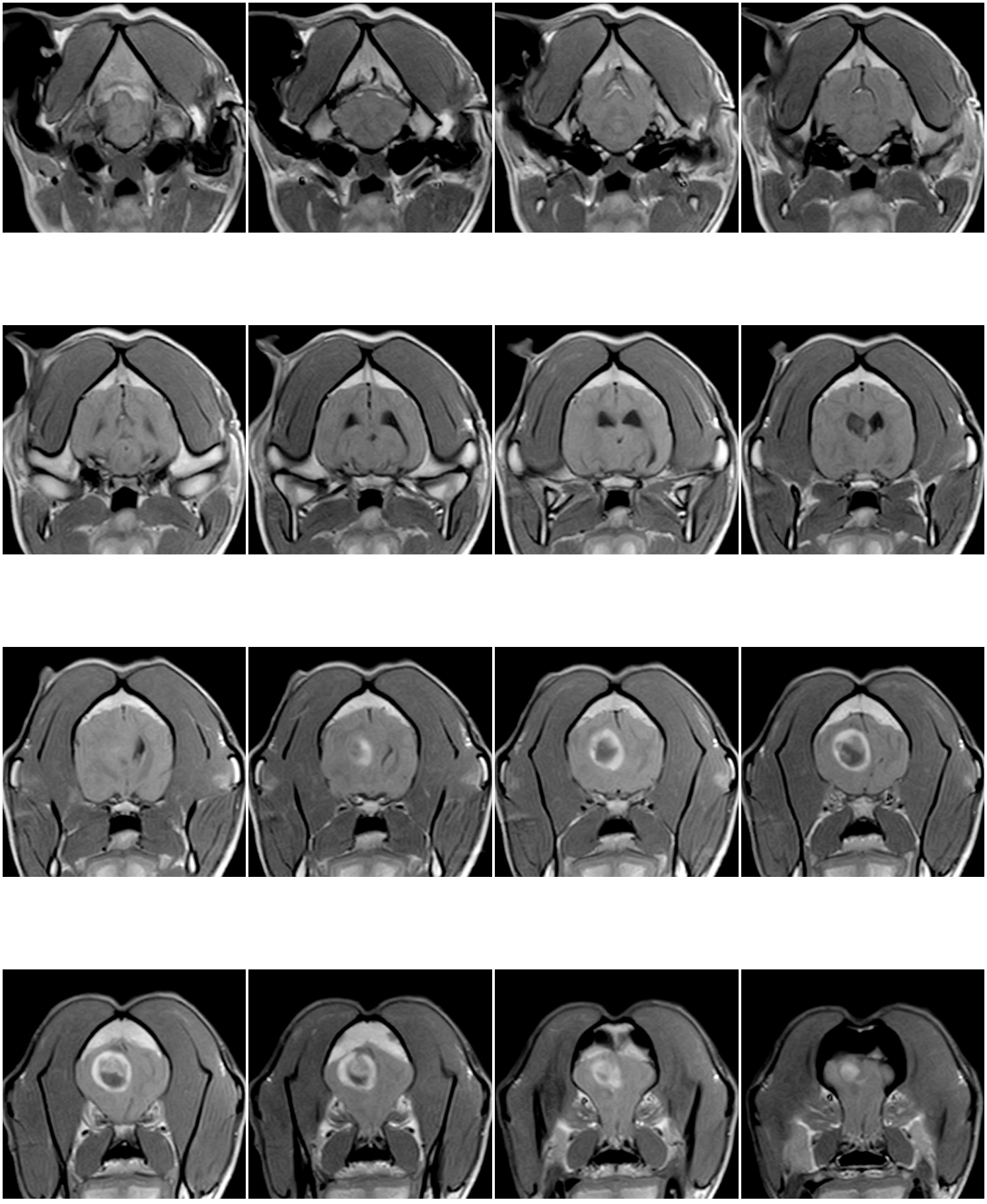

Matheus MRI 4 - **DAY 35** - Post contrast T1 weighted dorsal plane
Patient: Matheus (Boxer dog)

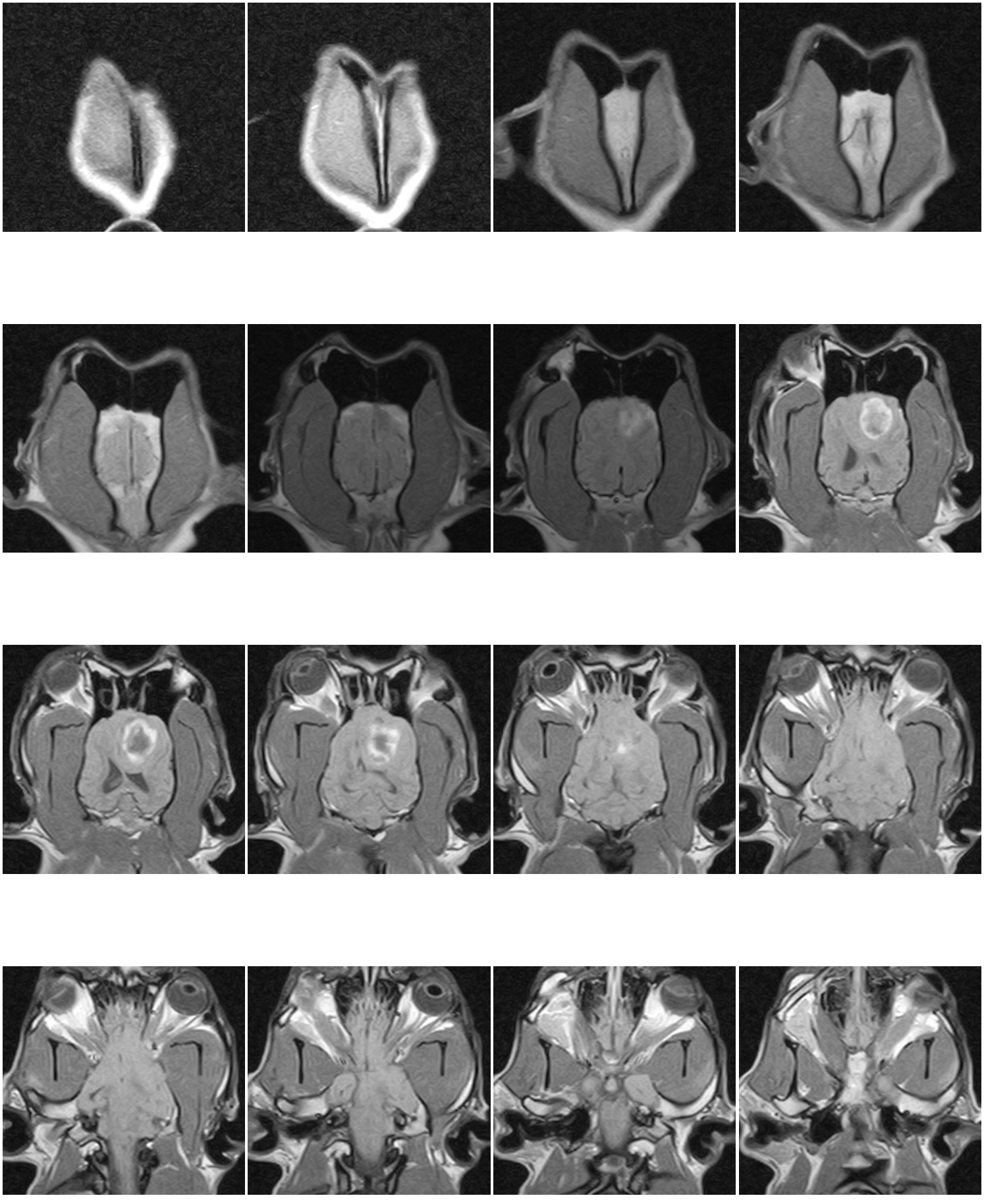

Matheus MRI 4 - **DAY 35** - Post contrast T1 weighted sagittal plane
Patient: Matheus (Boxer dog)

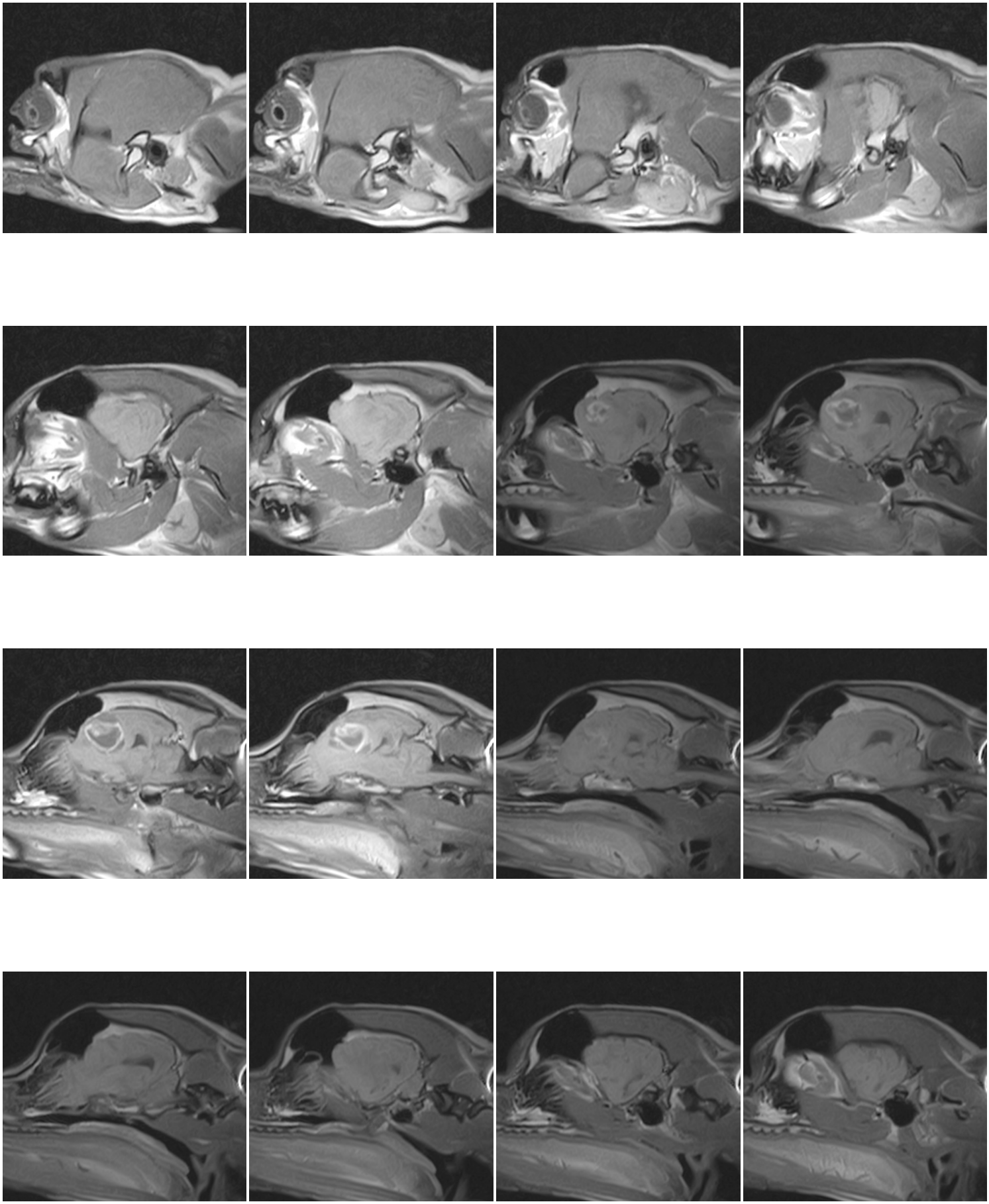

Matheus MRI 4 - **DAY 35** - Post contrast T1 weighted transversal plane
Patient: Matheus (Boxer dog)

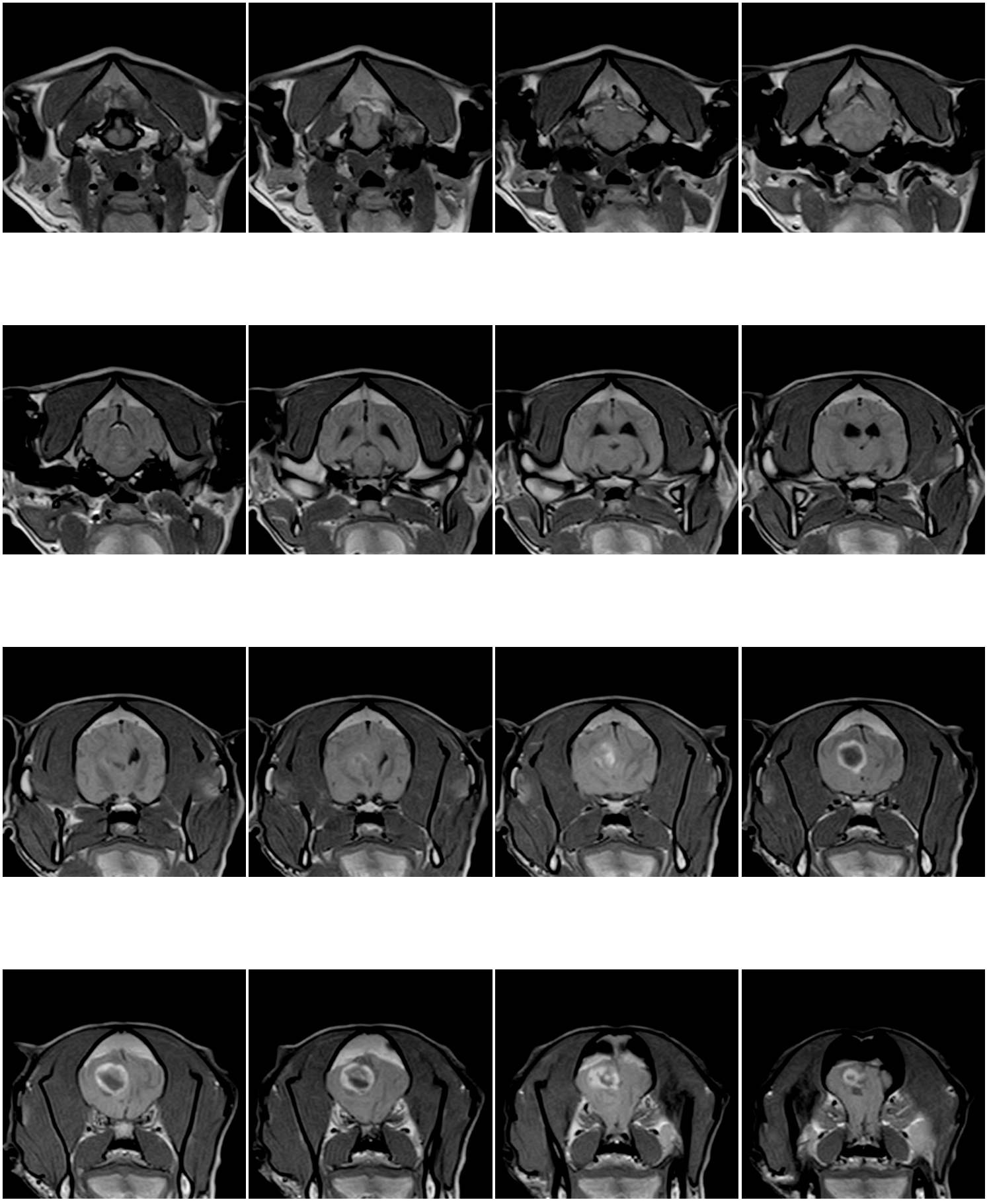

Matheus MRI 5 - **DAY 60** - Post contrast T1 weighted dorsal plane
Patient: Matheus (Boxer dog)

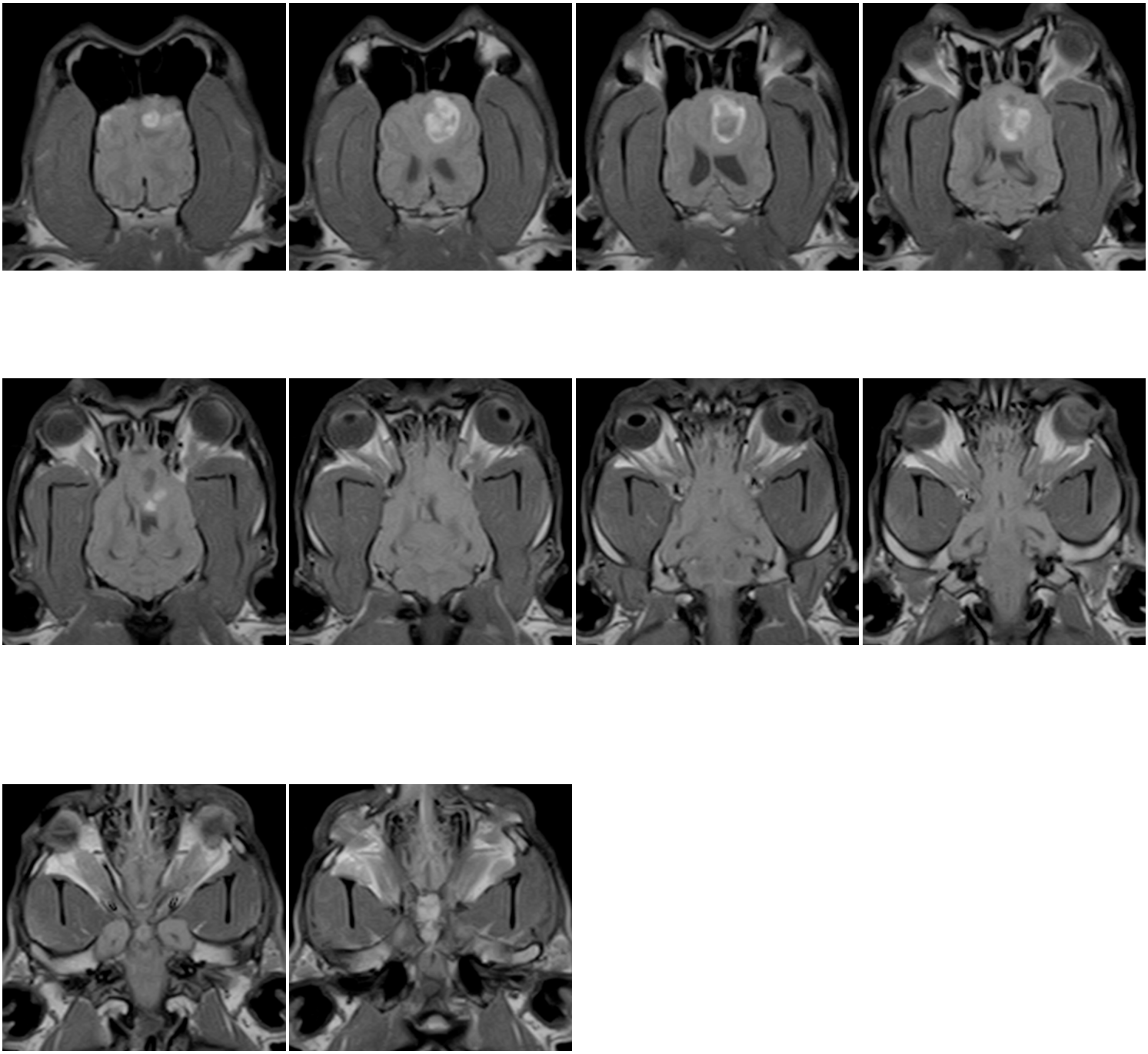

Matheus MRI 5 - **DAY 60** - Post contrast T1 weighted sagittal plane
Patient: Matheus (Boxer dog)

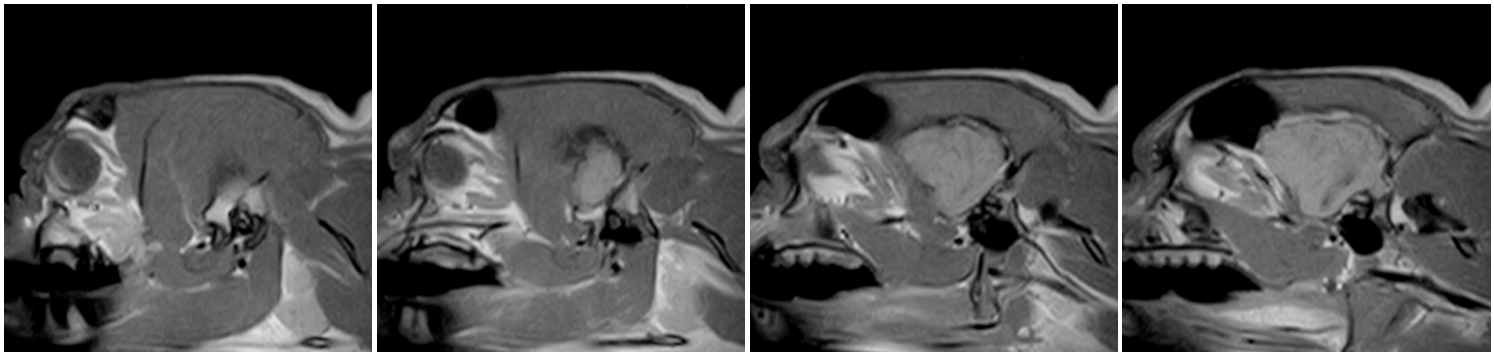

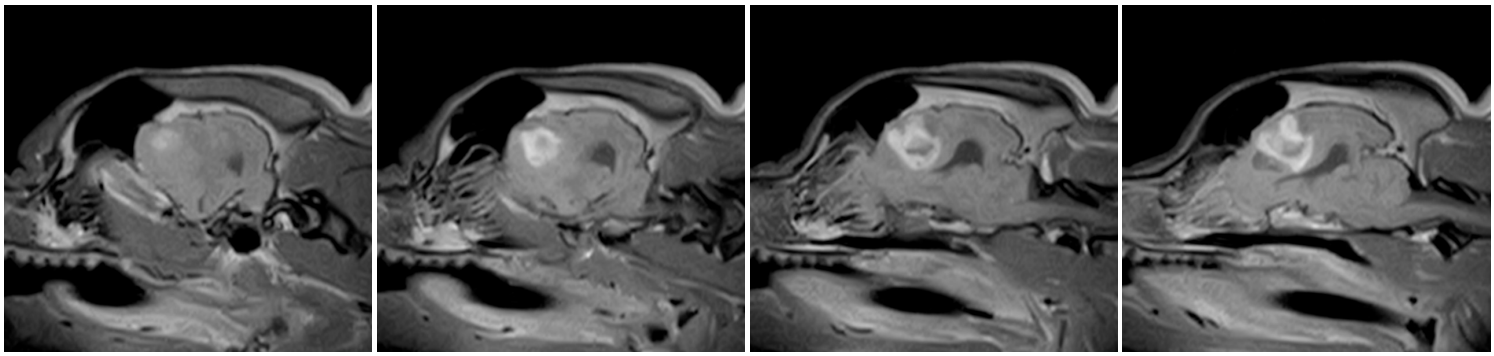

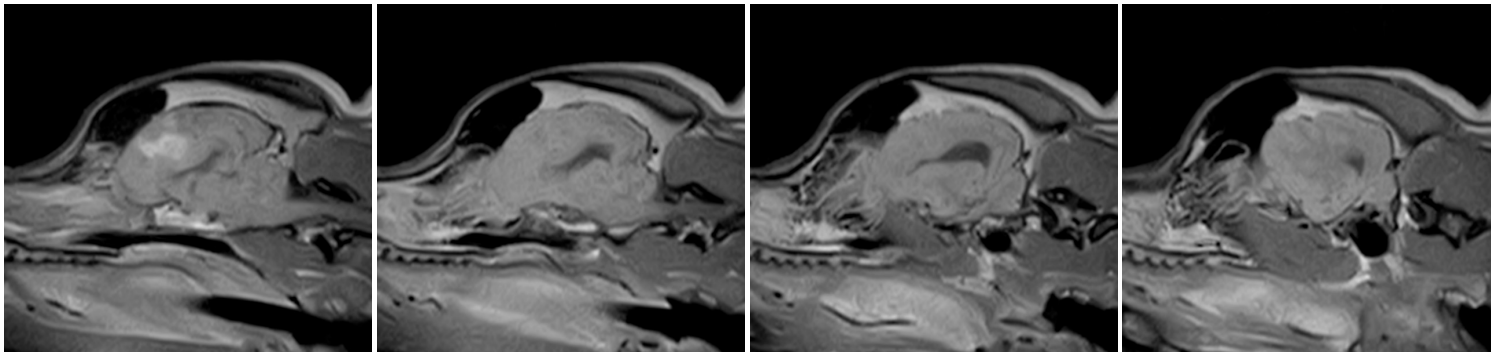

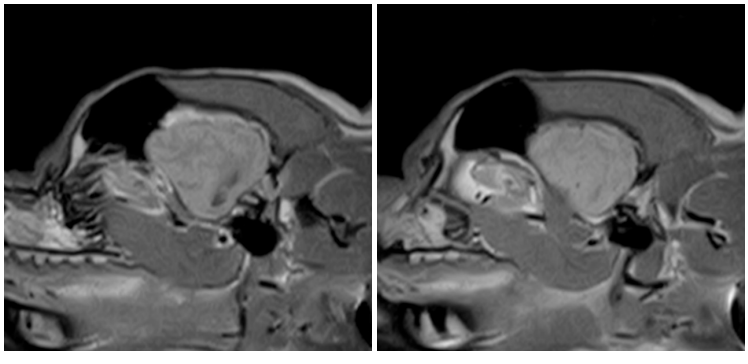

Matheus MRI 5 - **DAY 60** - Post contrast T1 weighted transversal plane
Patient: Matheus (Boxer dog)

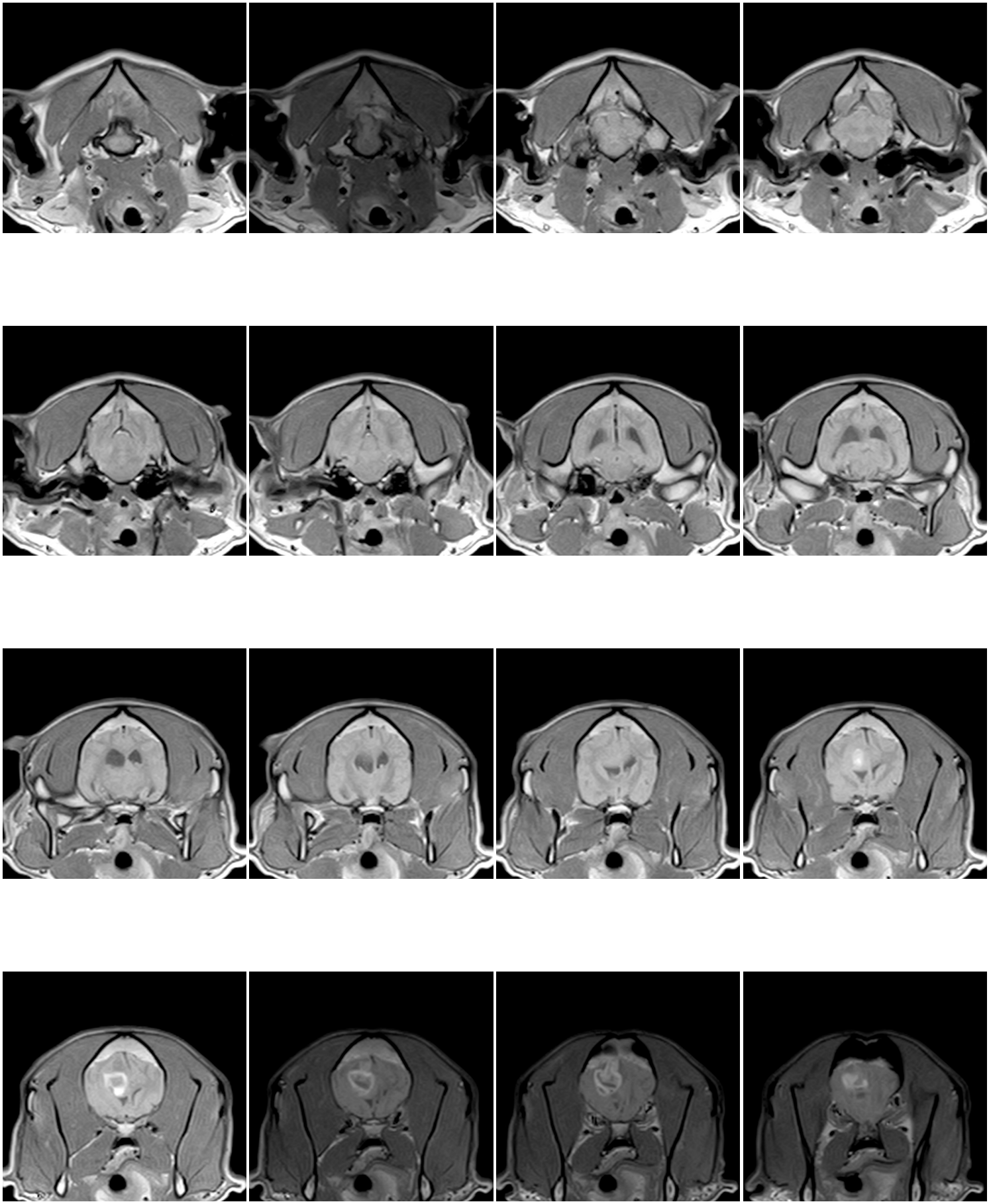

Matheus MRI 6 - **DAY 90** - Post contrast T1 weighted dorsal plane
Patient: Matheus (Boxer dog)

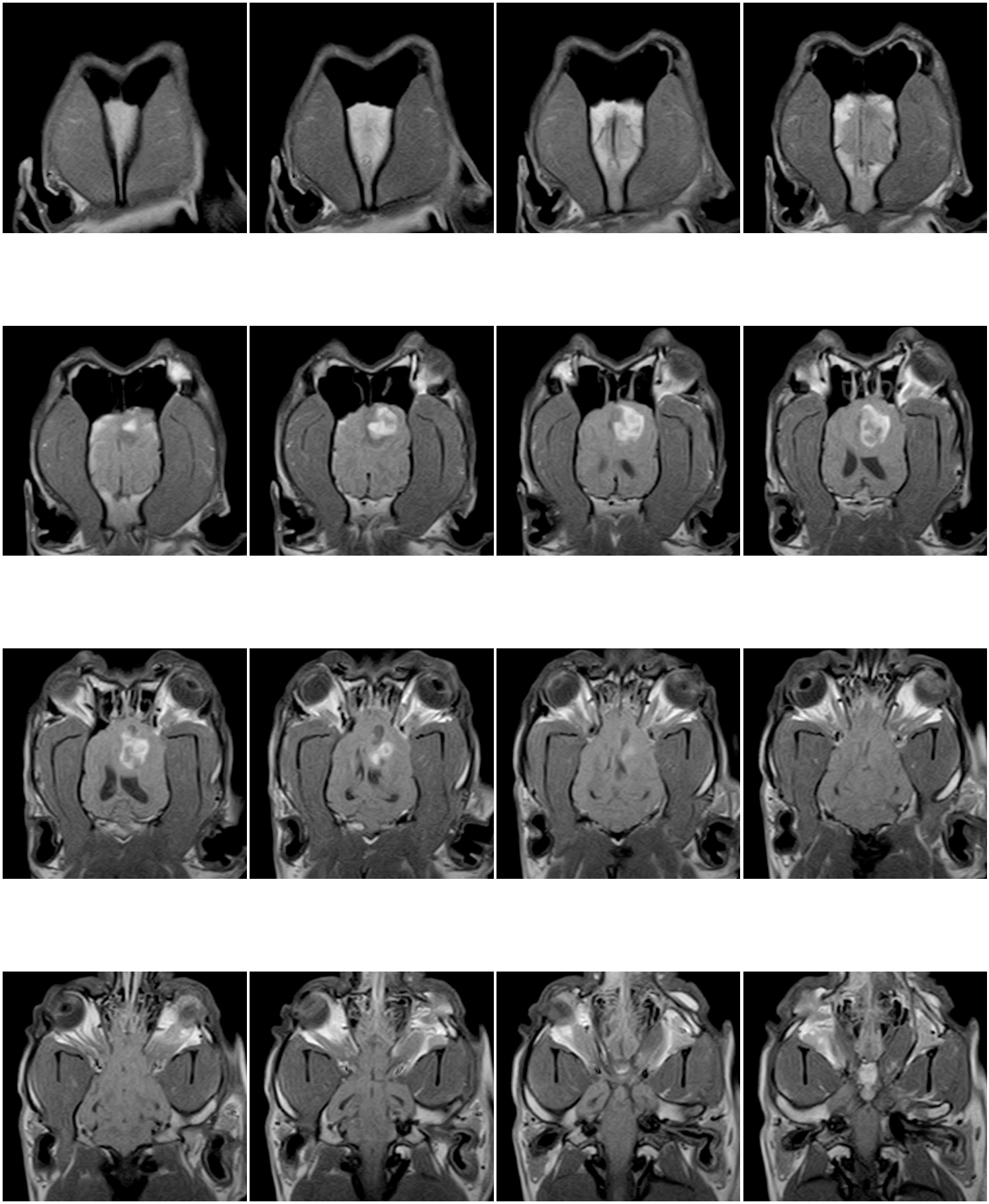

Matheus MRI 6 - **DAY 90** - Post contrast T1 weighted sagittal plane
Patient: Matheus (Boxer dog)

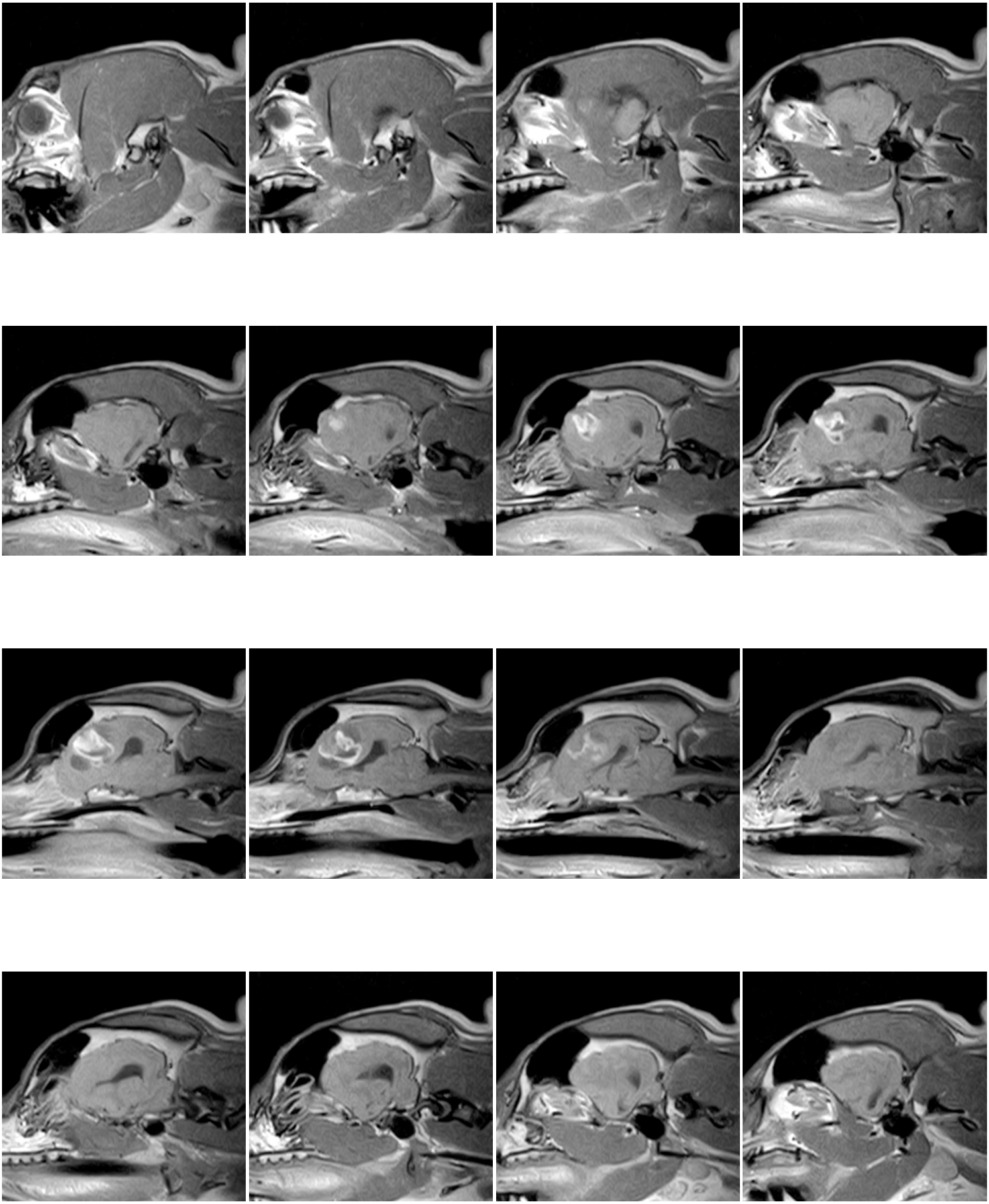

Matheus MRI 6 - **DAY 90** - Post contrast T1 weighted transversal plane
Patient: Matheus (Boxer dog)

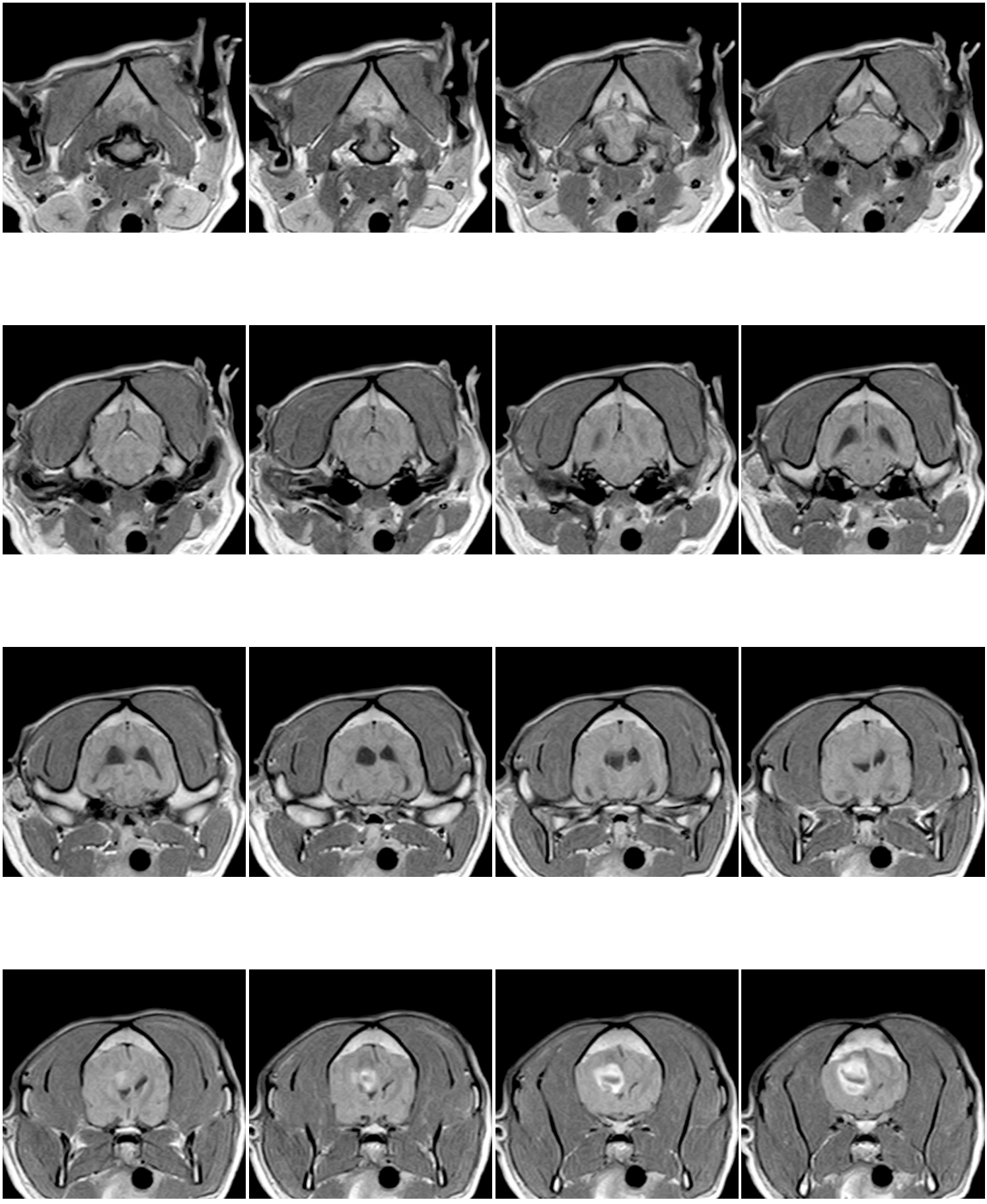

Matheus MRI 7 - **DAY 120** - Post contrast T1 weighted dorsal plane
Patient: Matheus (Boxer dog)

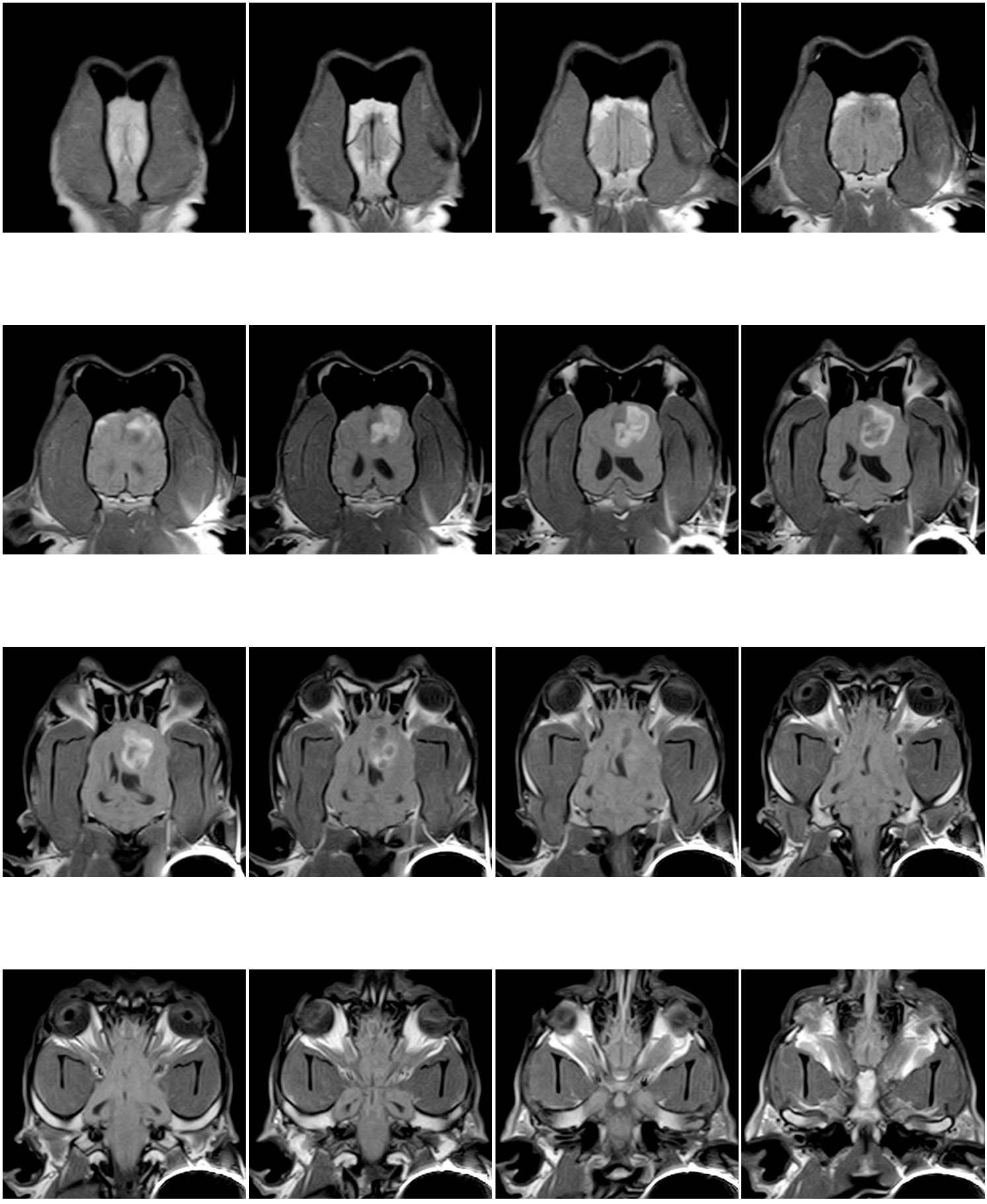

Matheus MRI 7 - **DAY 120** - Post contrast T1 weighted sagittal plane
Patient: Matheus (Boxer dog)

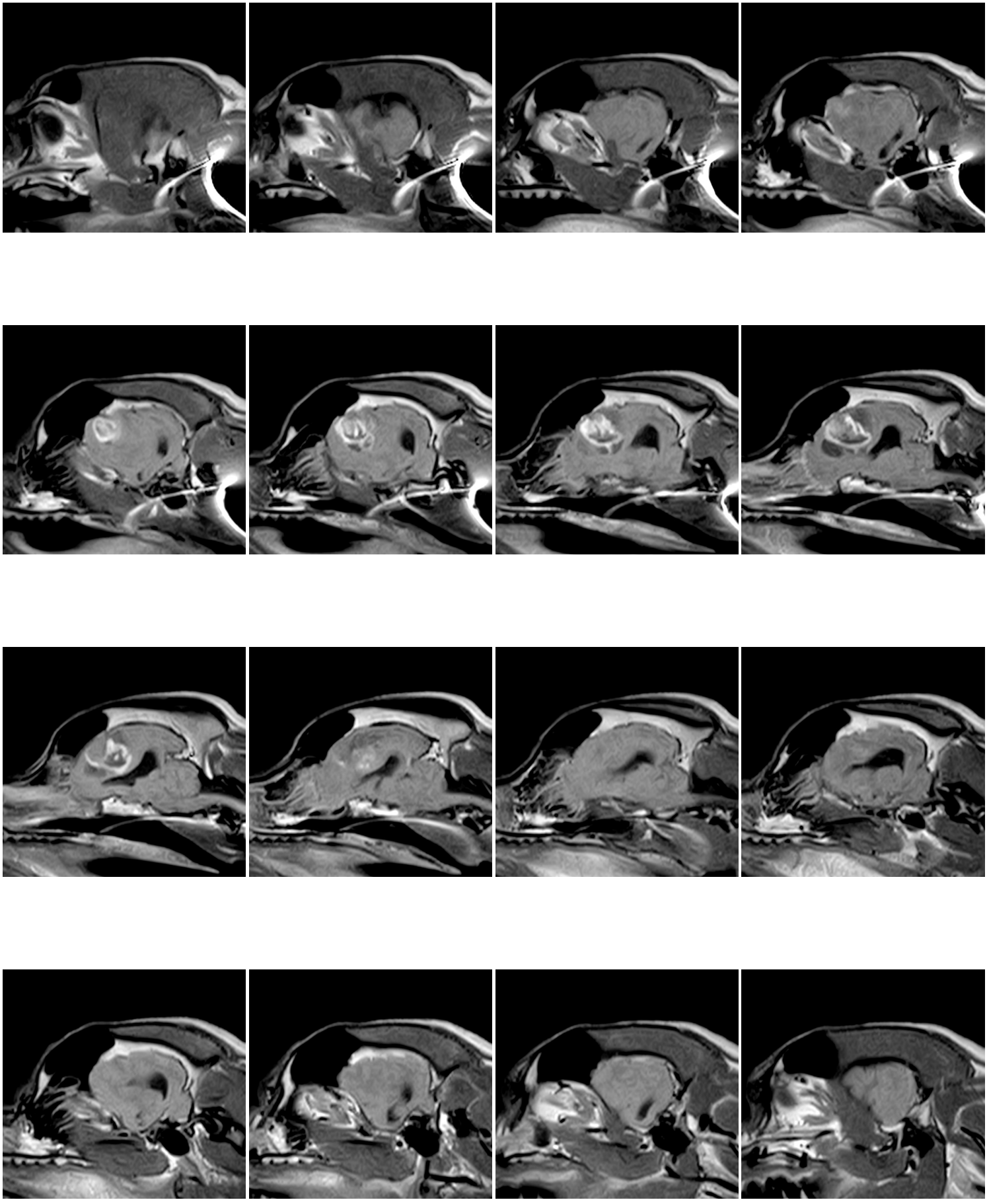

Matheus MRI 7 - **DAY 120** - Post contrast T1 weighted transversal plane
Patient: Matheus (Boxer dog)

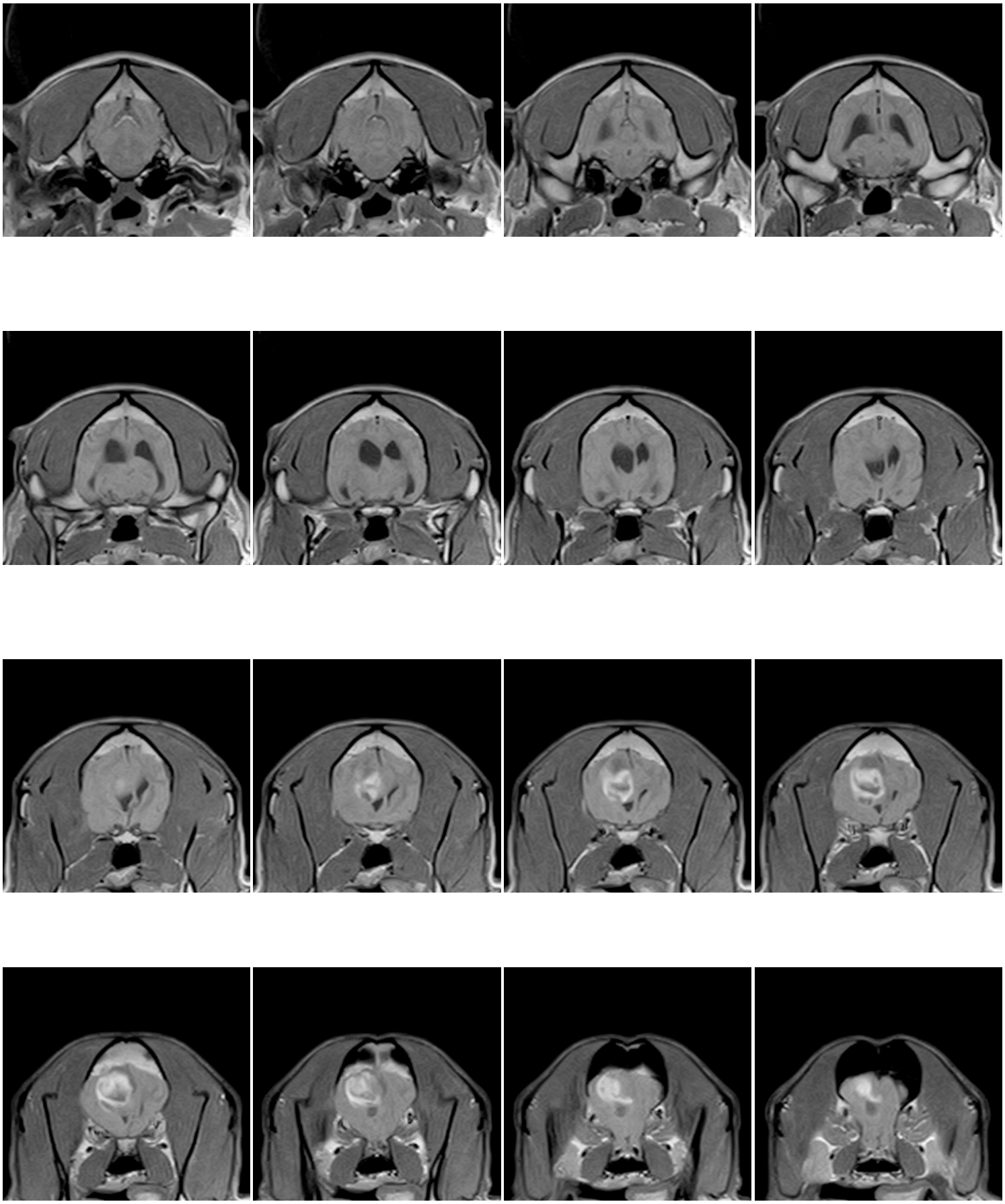

Matheus MRI 8 - **DAY 150** - Post contrast T1 weighted dorsal plane
Patient: Matheus (Boxer dog)

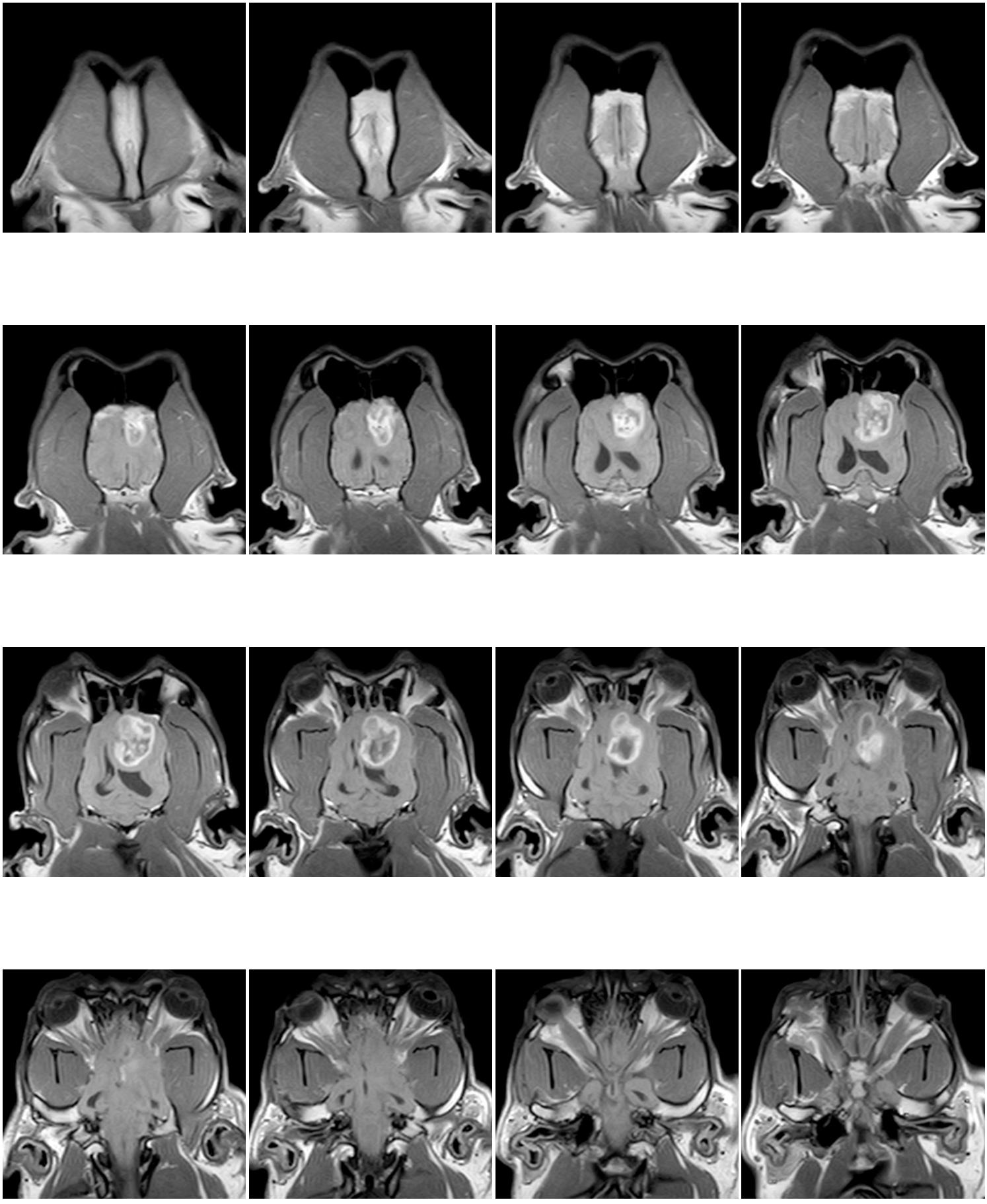

Matheus MRI 8 - **DAY 150** - Post contrast T1 weighted sagittal plane
Patient: Matheus (Boxer dog)

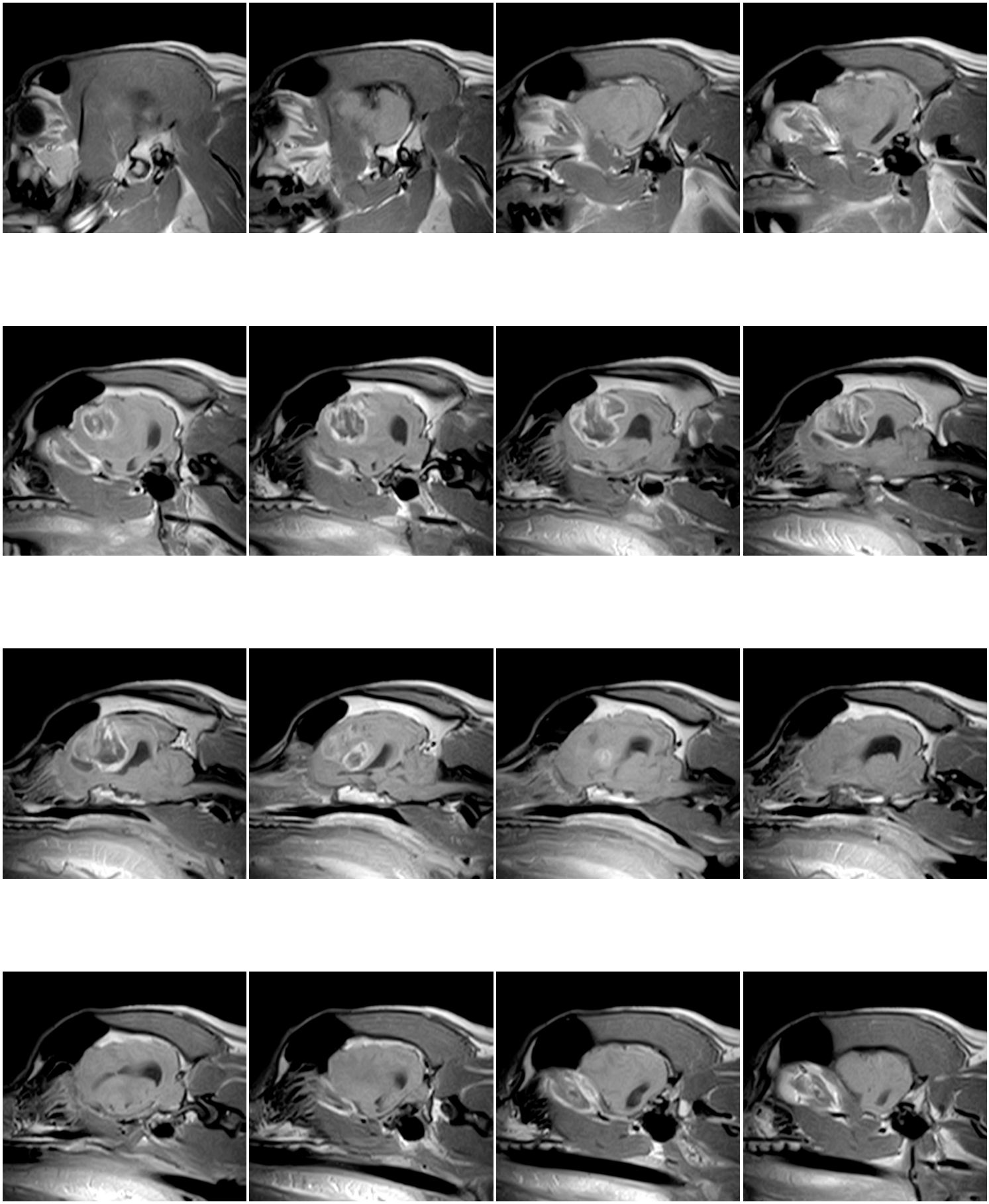

Matheus MRI 8 - **DAY 150** - Post contrast T1 weighted transversal plane
Patient: Matheus (Boxer dog)

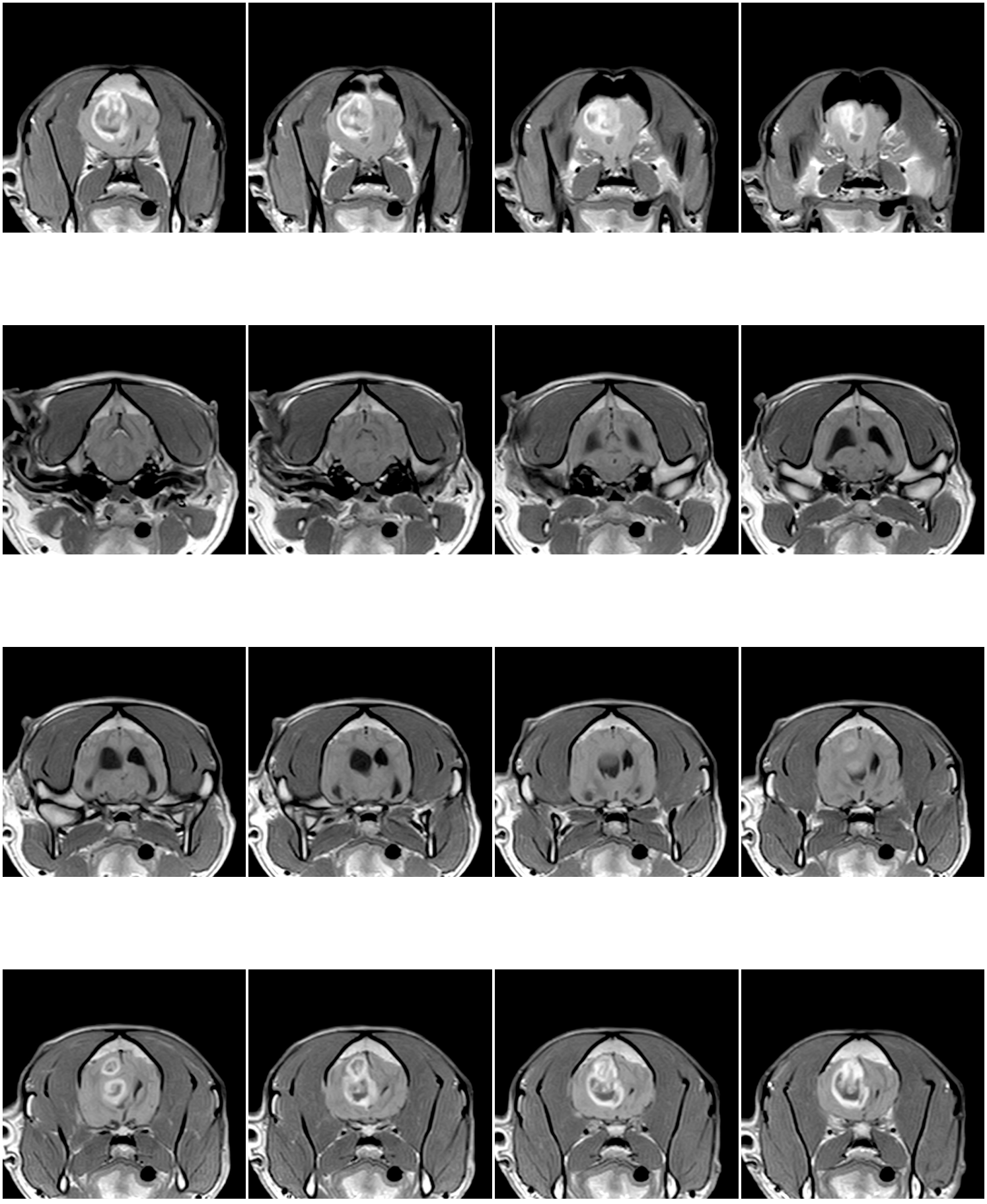

Nina MRI 1 - **DAY 0** - Post contrast T1 weighted dorsal plane
Patient: Nina (Dashchund dog)

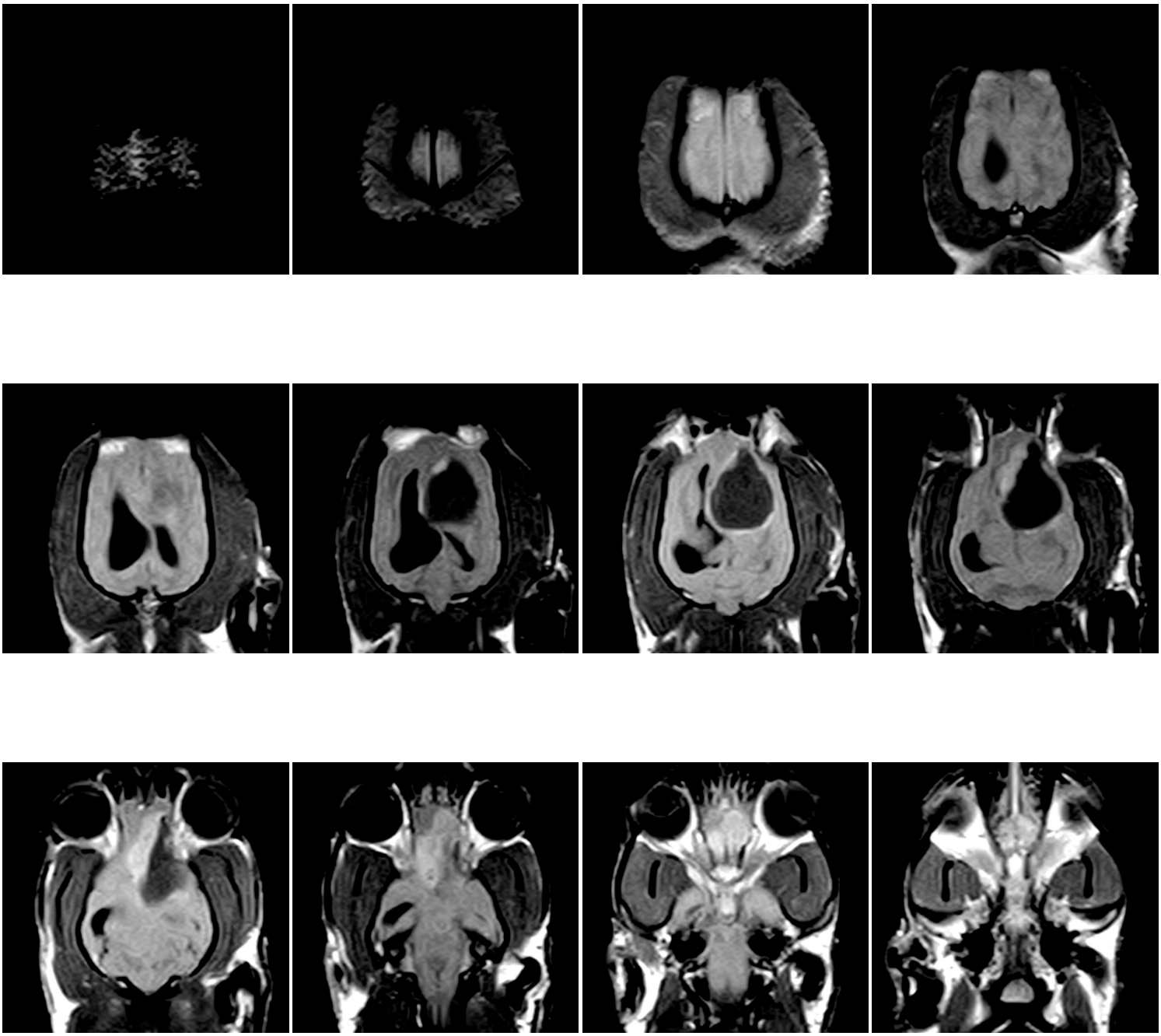

Nina MRI 1 - **DAY 0** - Post contrast T1 weighted sagittal plane
Patient: Nina (Dashchund dog)

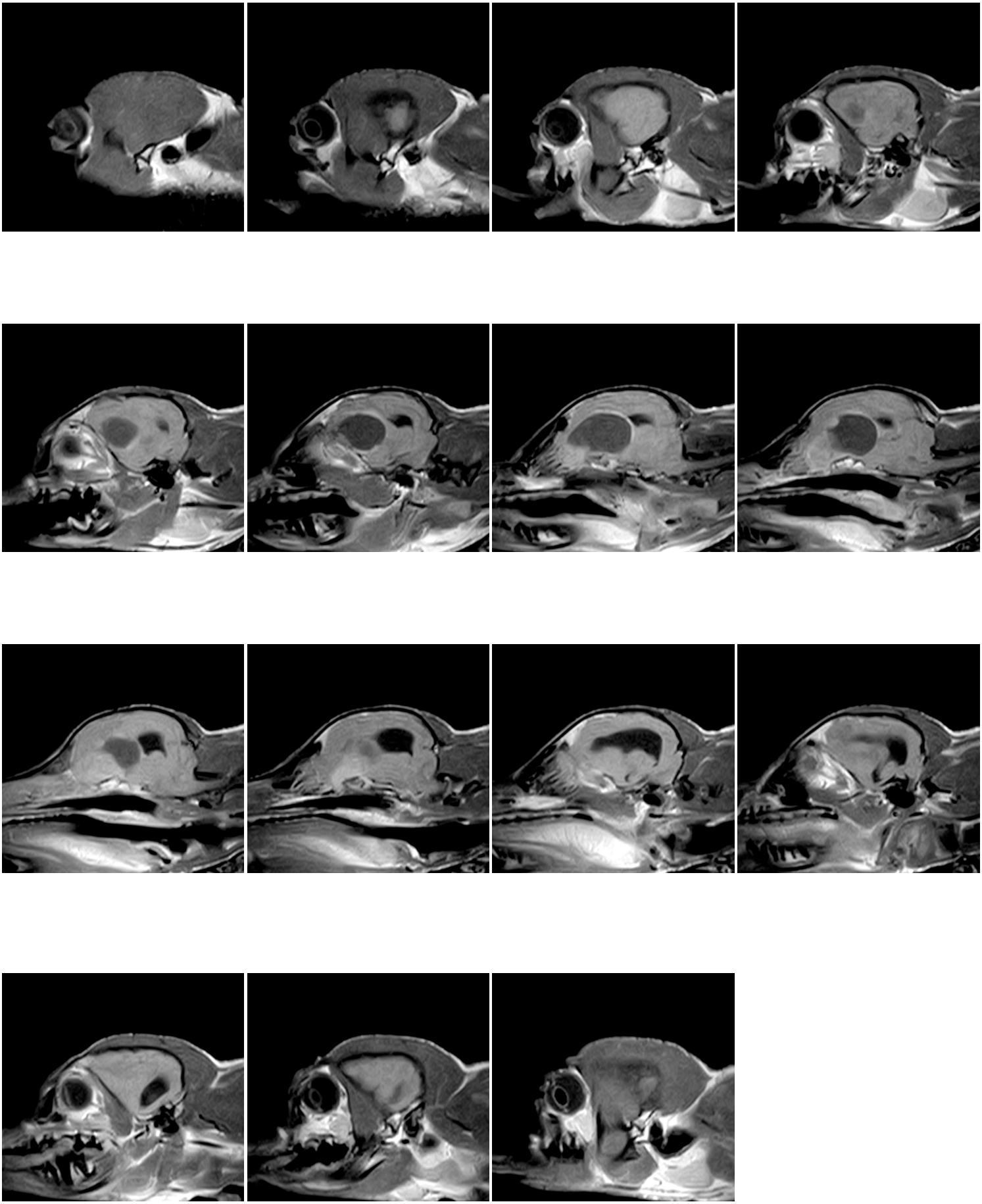

Nina MRI 1 - **DAY 0** - Post contrast T1 weighted transversal plane
Patient: Nina (Dashchund dog)

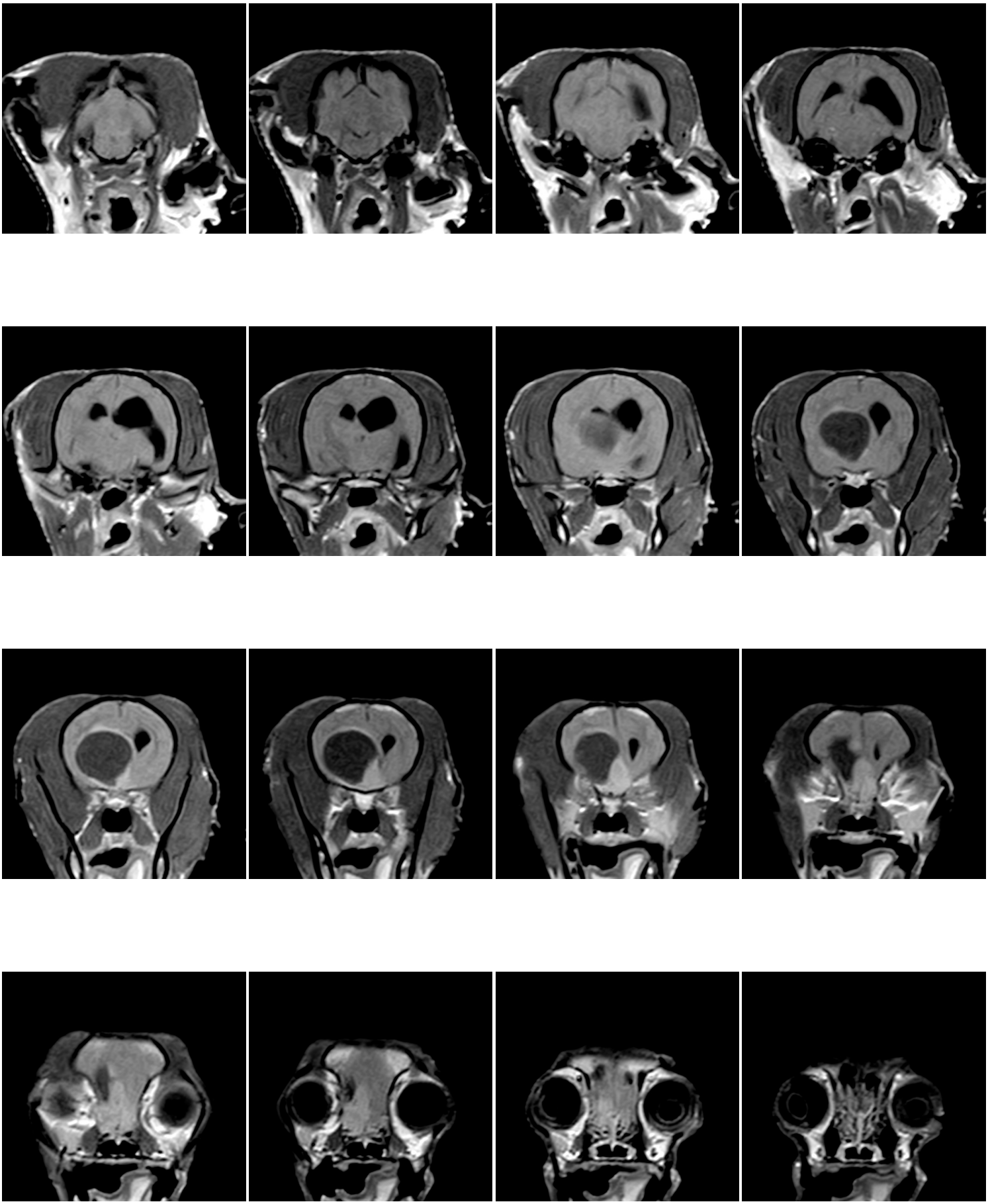

Nina MRI 2 - **DAY 14** - Post contrast T3 weighted dorsal plane
Patient: Nina (Dashchund dog)

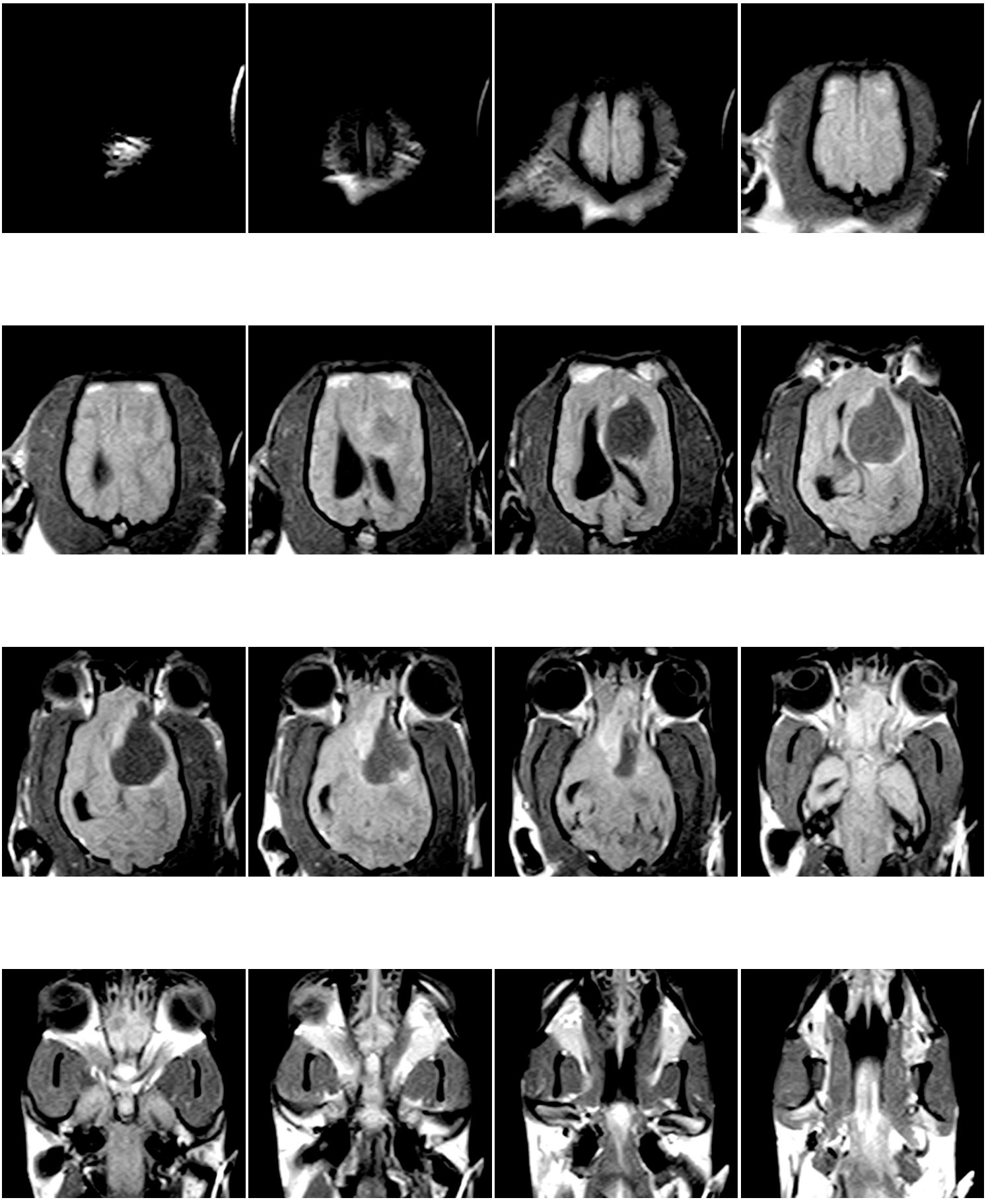

Nina MRI 2 - **DAY 14** - Post contrast T3 weighted sagittal plane
Patient: Nina (Dashchund dog)

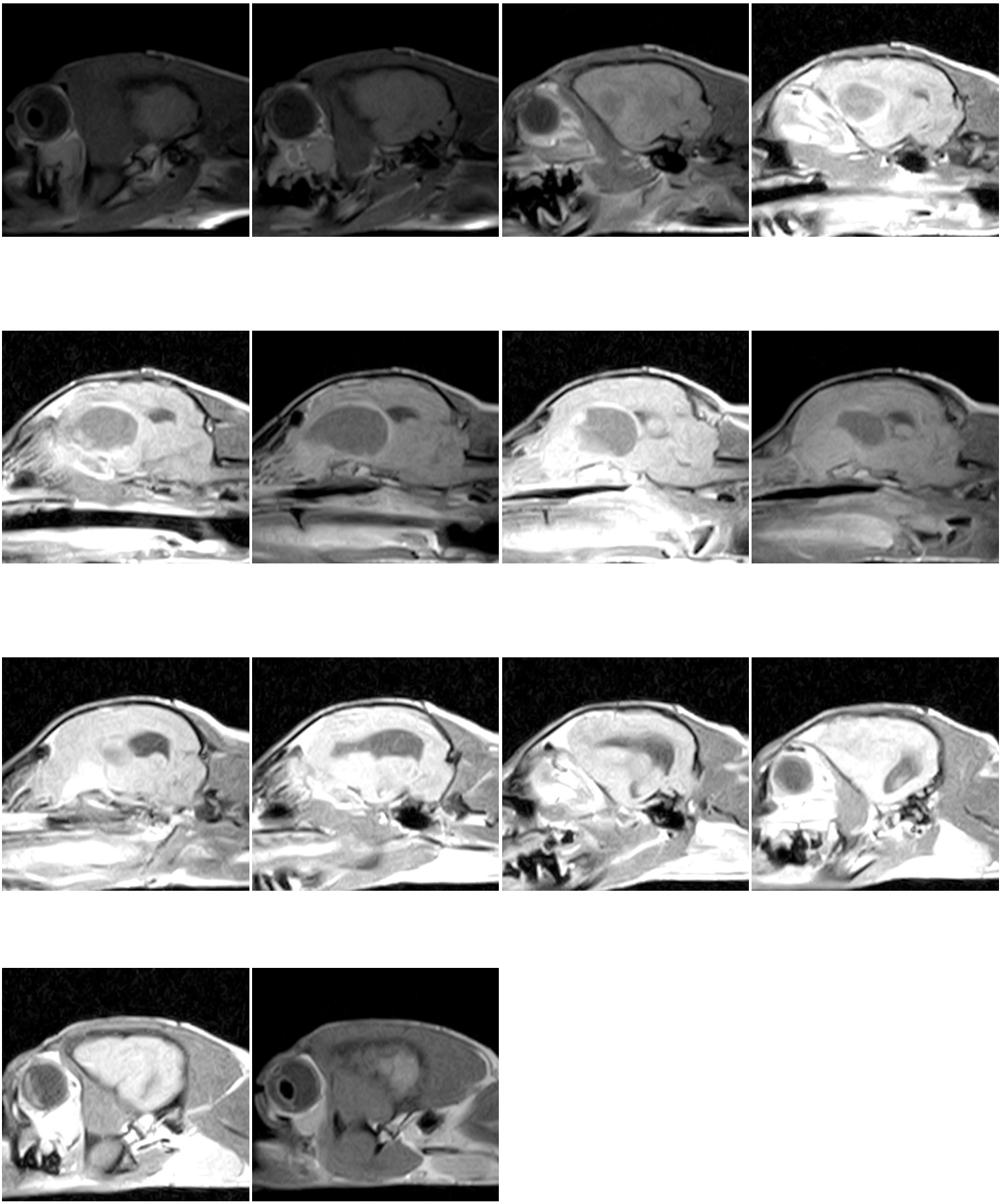

Nina MRI 2 - **DAY 14** - Post contrast T3 weighted transversal plane
Patient: Nina (Dashchund dog)

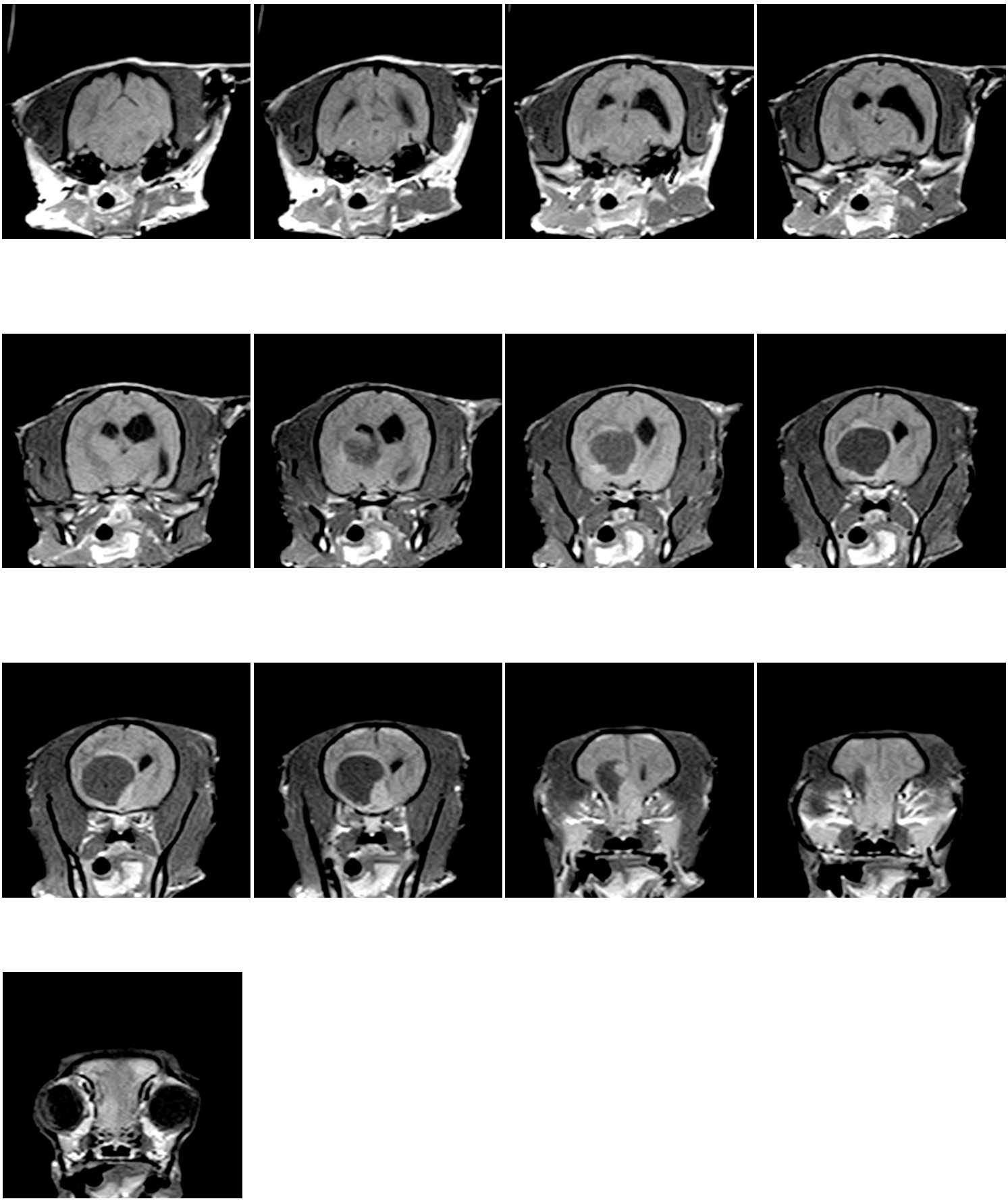

Nina MRI 3 - **DAY 21** - Post contrast T1 weighted dorsal plane
Patient: Nina (Dashchund dog)

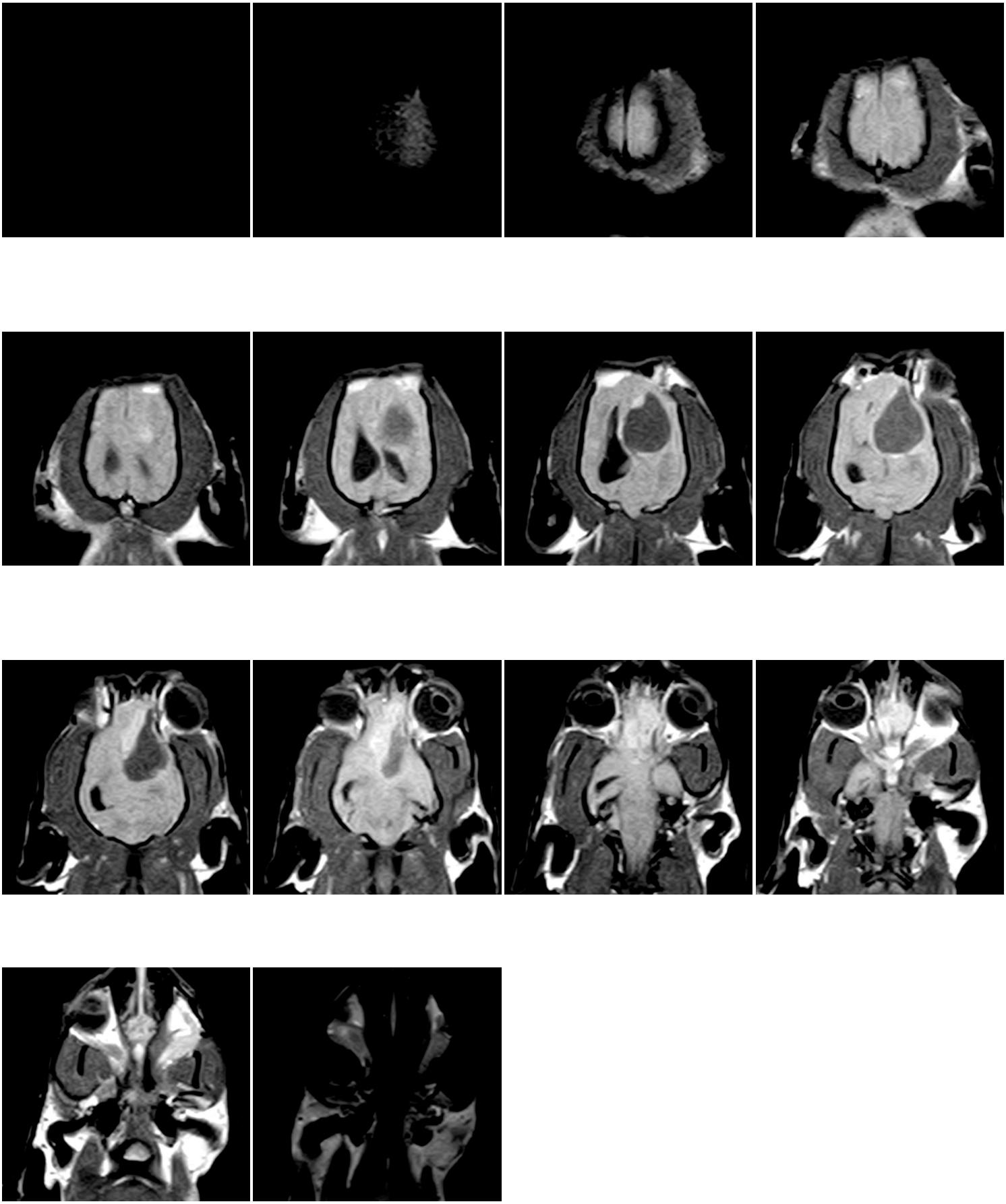

Nina MRI 3 - **DAY 21** - Post contrast T1 weighted sagittal plane
Patient: Nina (Dashchund dog)

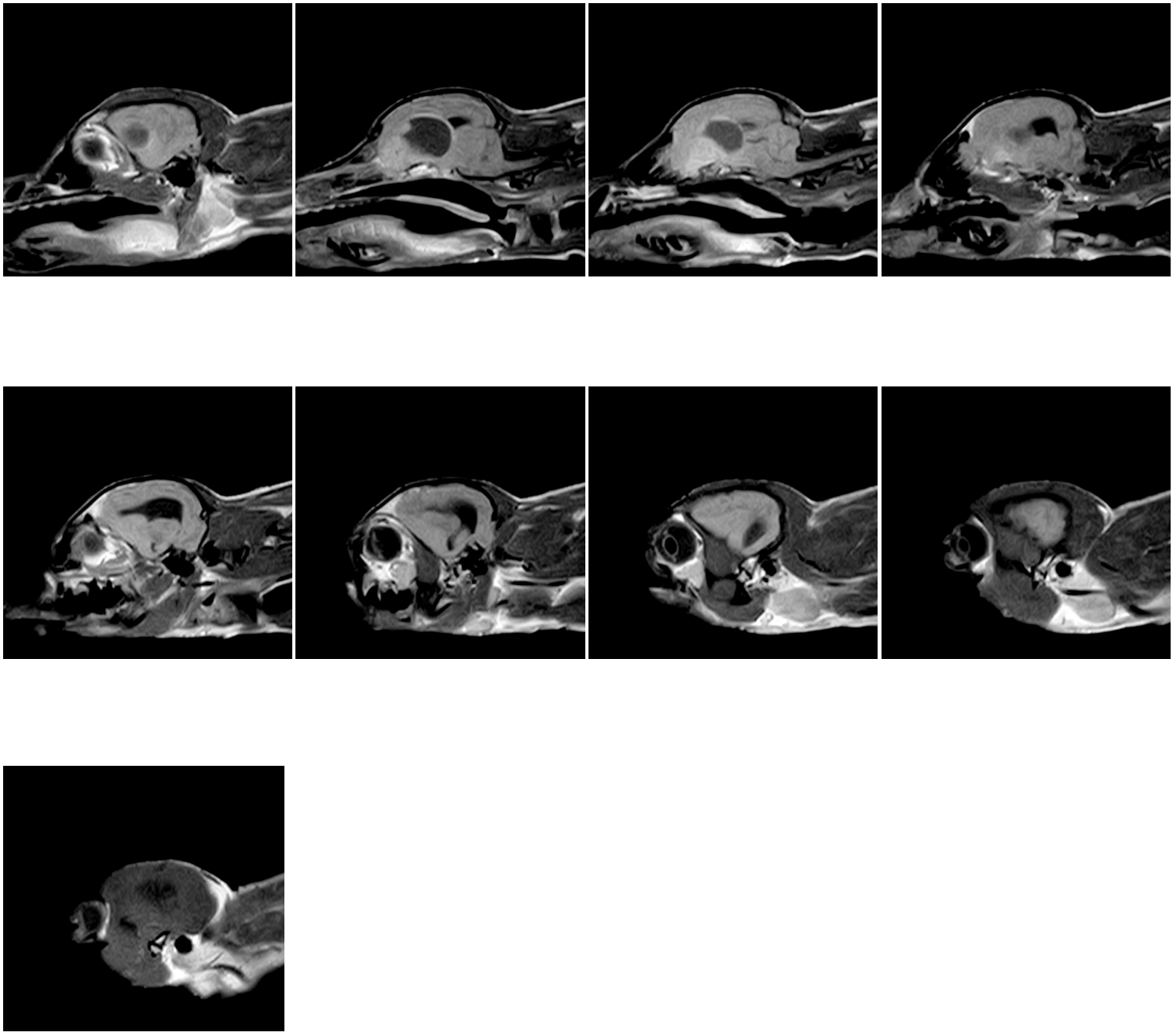

Nina MRI 3 - **DAY 21** - Post contrast T1 weighted transversal plane
Patient: Nina (Dashchund dog)

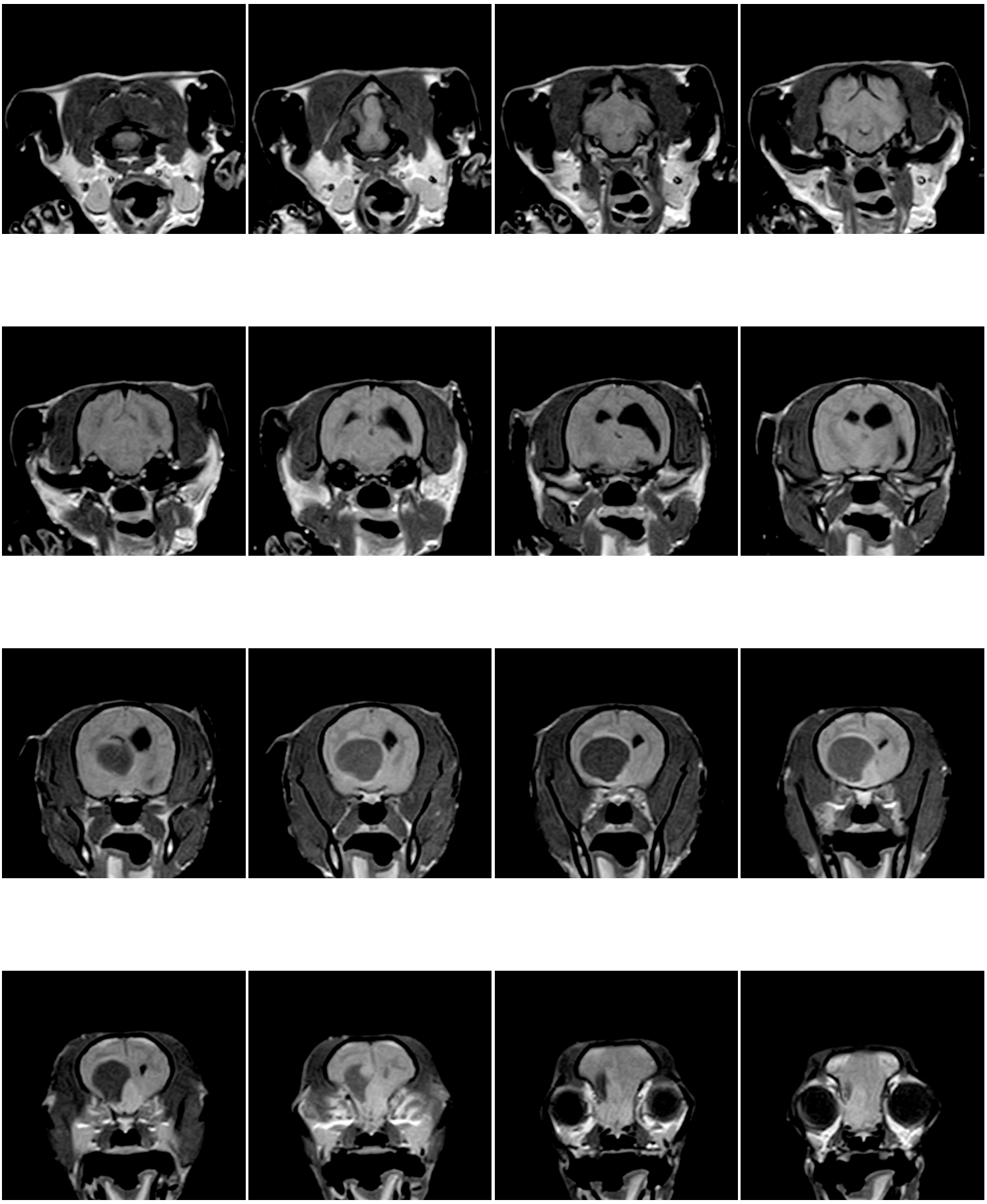

Nina MRI 4 - **DAY 42** - Post contrast T1 weighted dorsal plane
Patient: Nina (Dashchund dog)

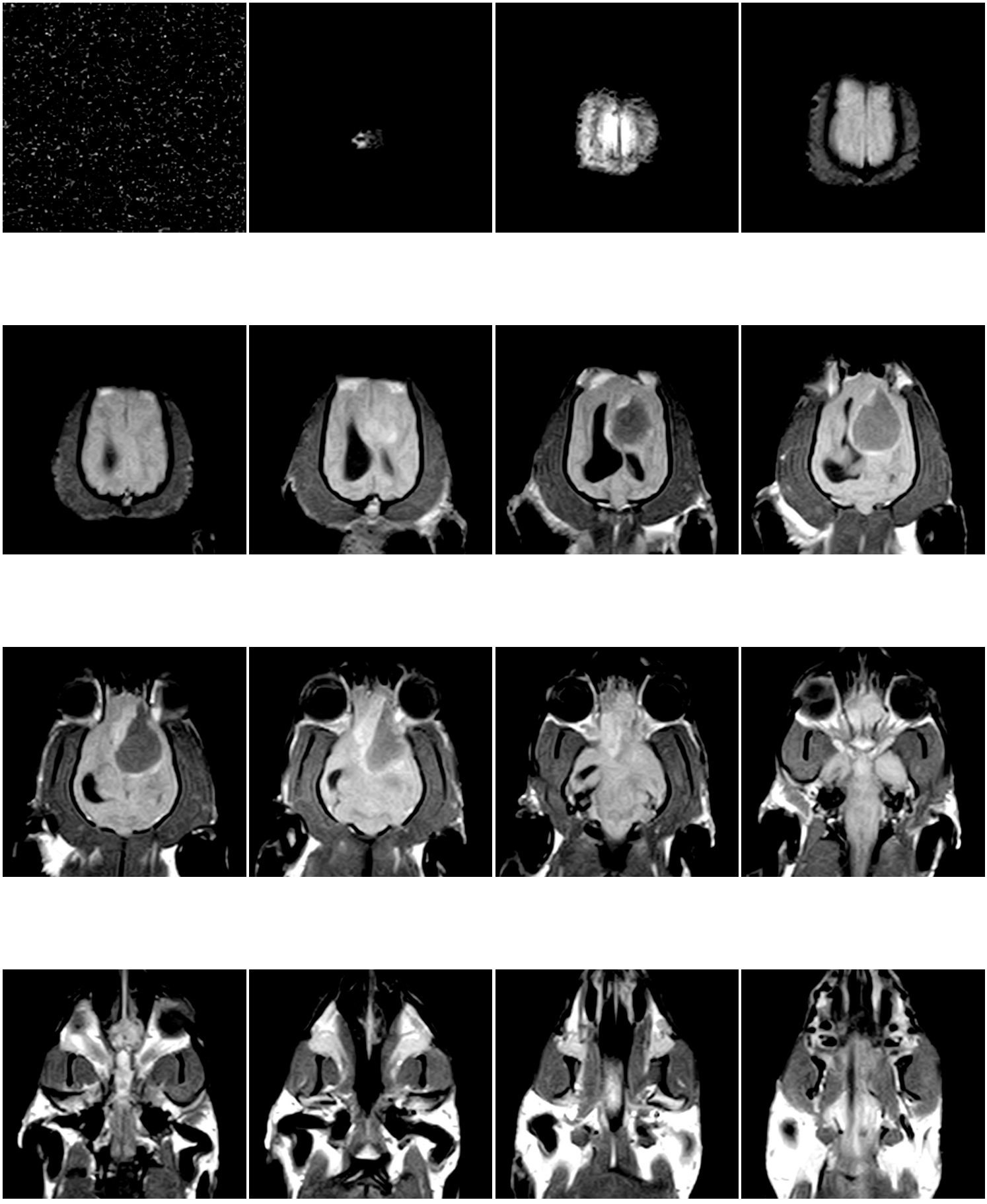

Nina MRI 4 - **DAY 42** - Post contrast T1 weighted sagittal plane
Patient: Nina (Dashchund dog)

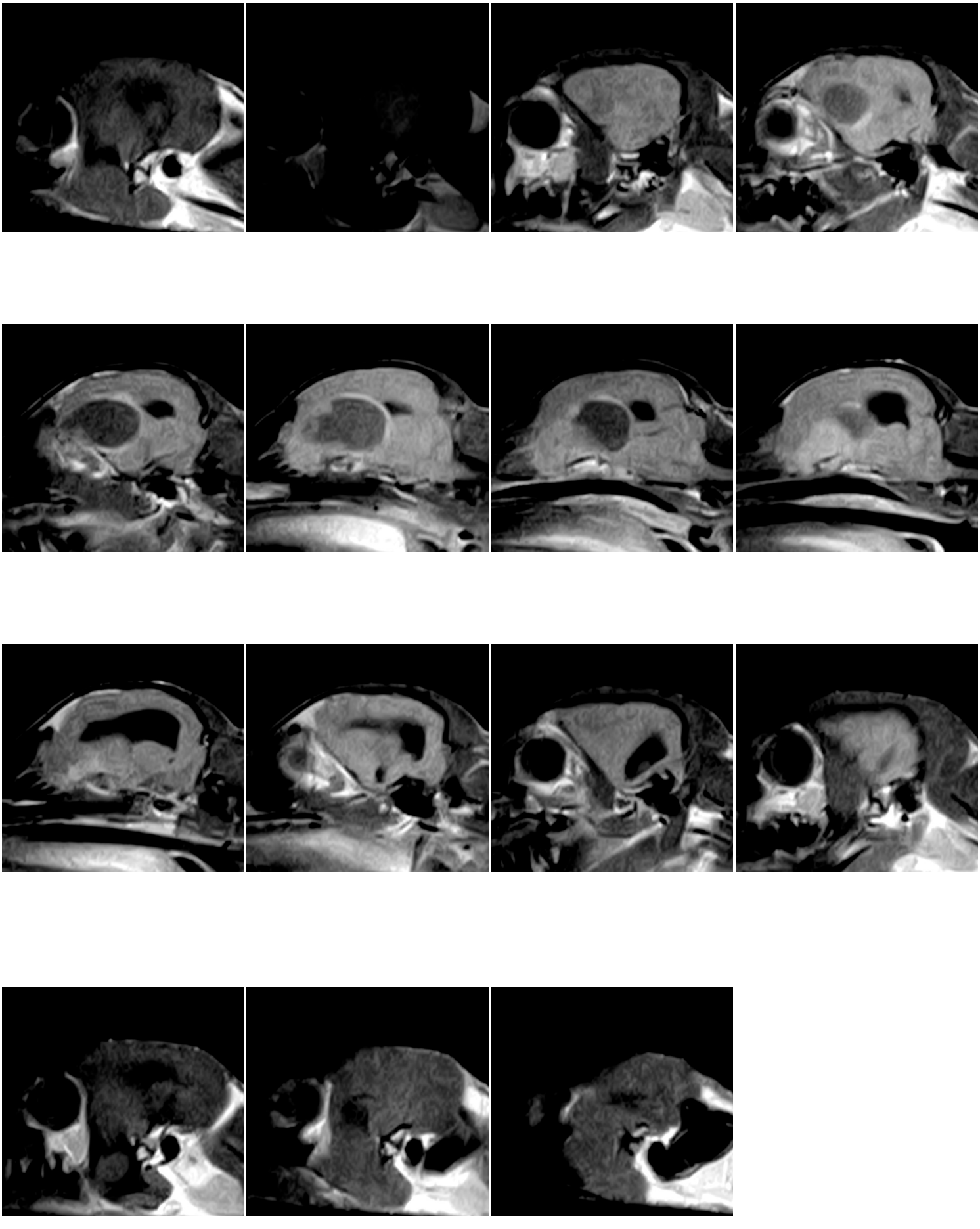

Nina MRI 4 - **DAY 42** - Post contrast T1 weighted transversal plane
Patient: Nina (Dashchund dog)

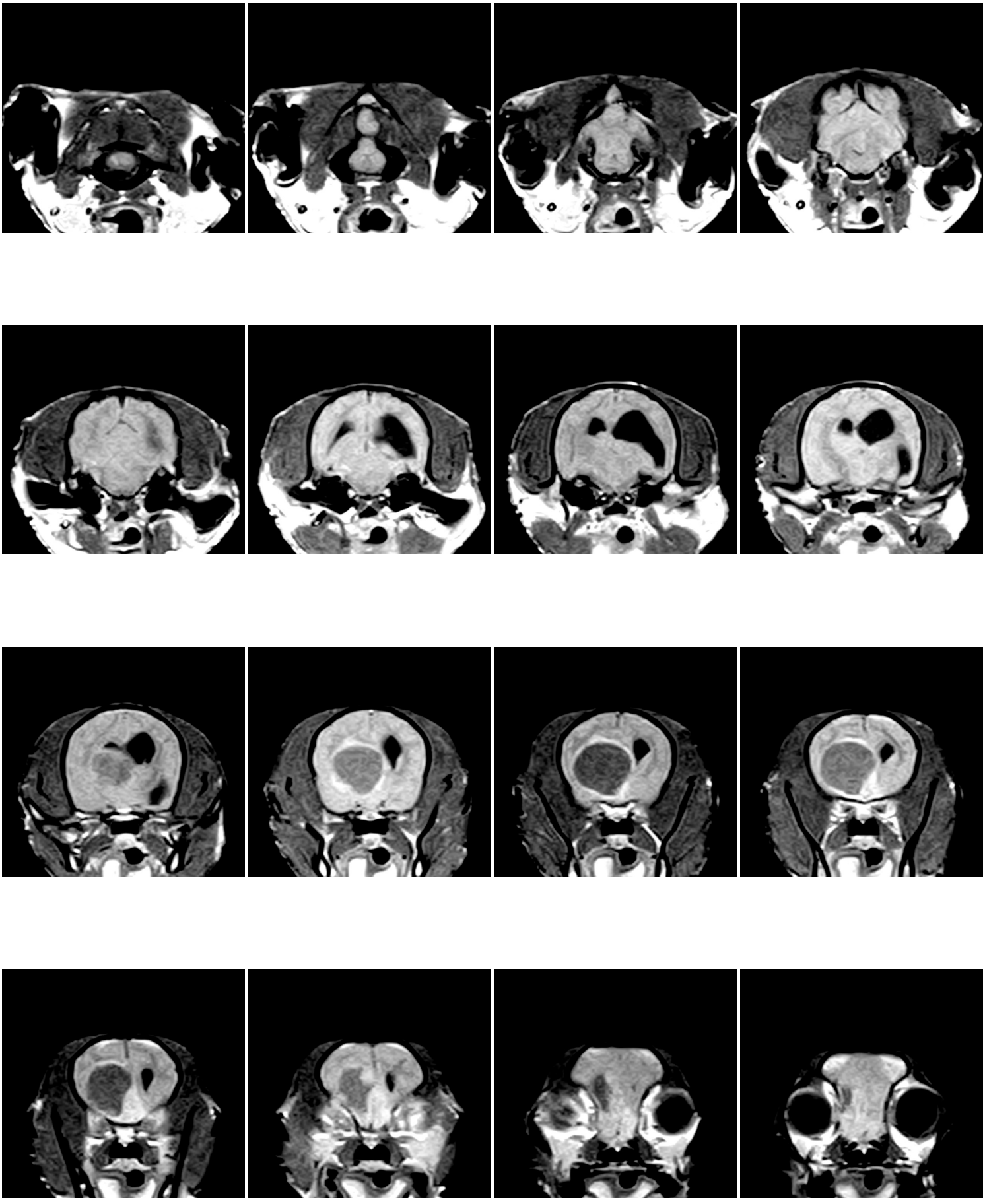

Nina MRI 5 - **DAY 52** - Post contrast T1 weighted dorsal plane
Patient: Nina (Dashchund dog)

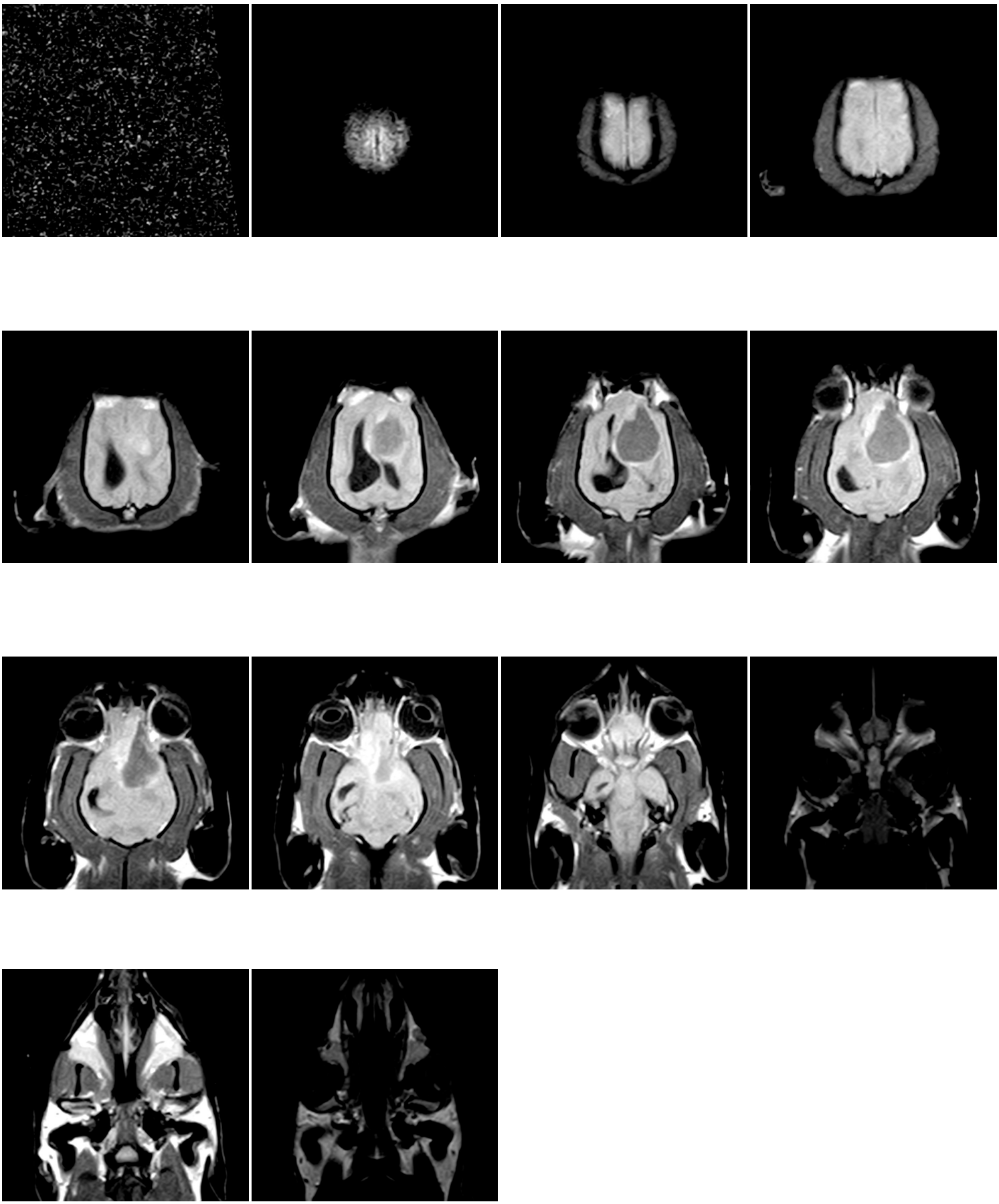

Nina MRI 5 - **DAY 52** - Post contrast T1 weighted sagittal plane
Patient: Nina (Dashchund dog)

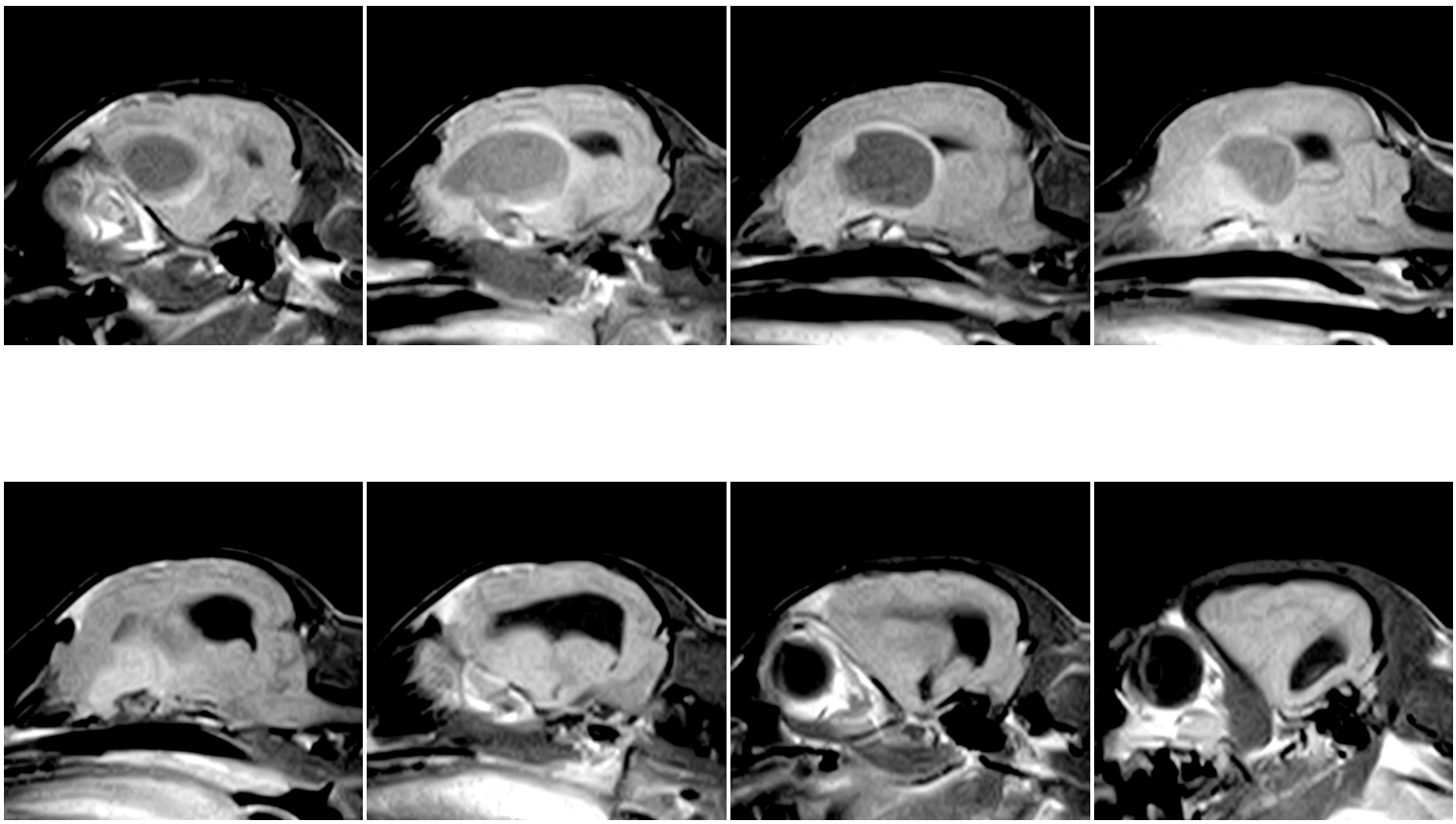

Nina MRI 5 - **DAY 52** - Post contrast T1 weighted transversal plane
Patient: Nina (Dashchund dog)

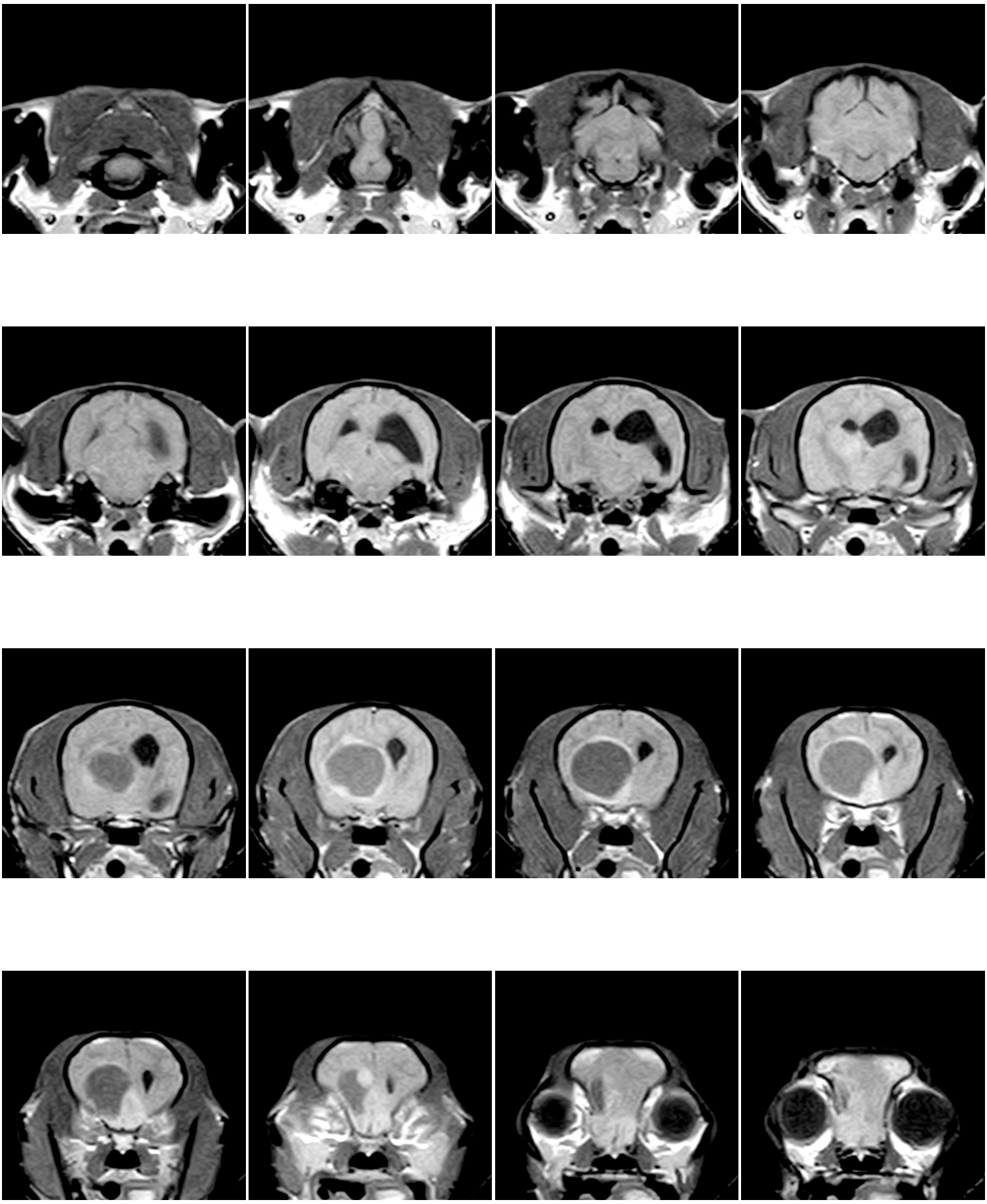

Nina MRI 6 - **DAY 78** - Post contrast T1 weighted dorsal plane
Patient: Nina (Dashchund dog)

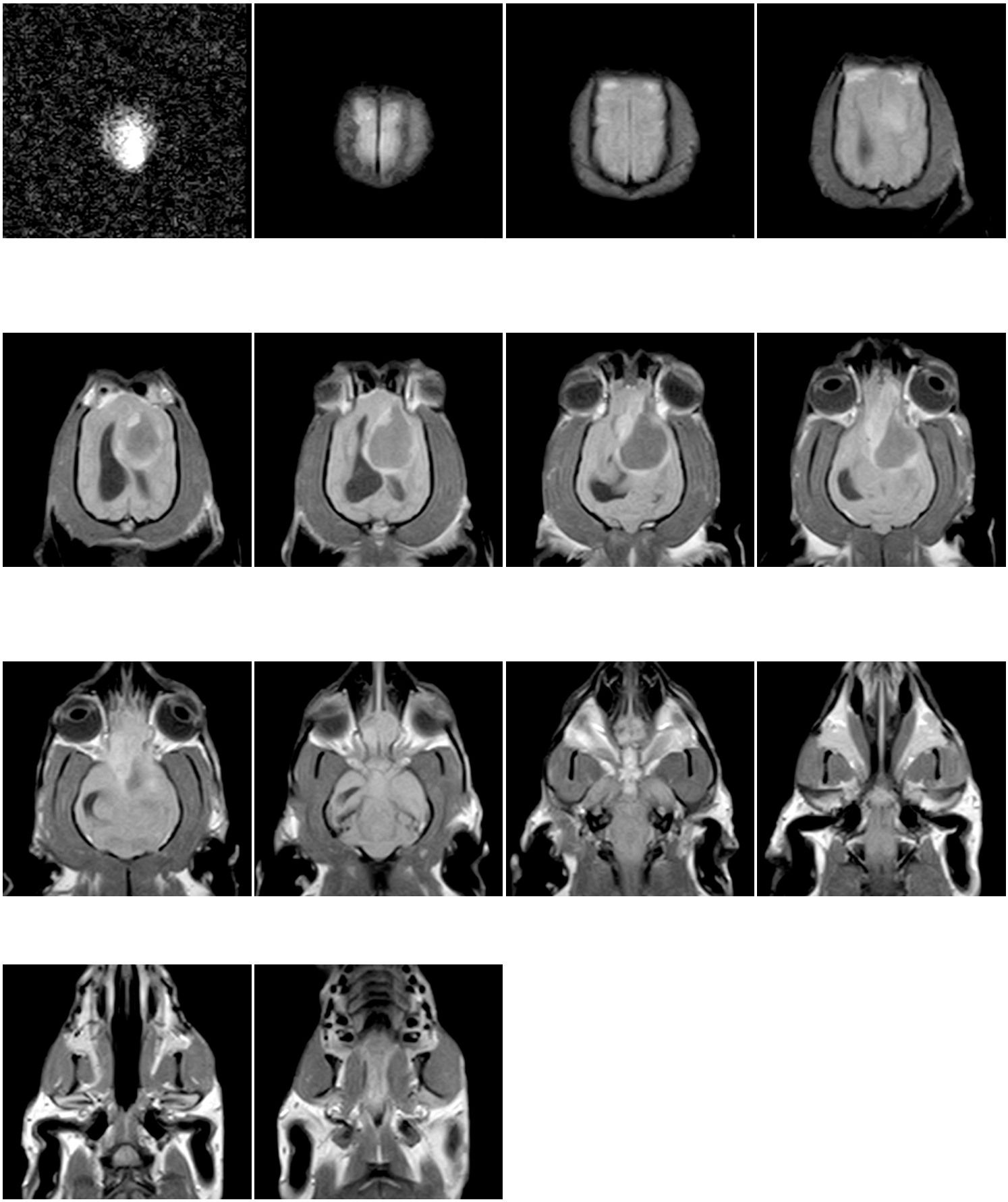

Nina MRI 6 - **DAY 78** - Post contrast T1 weighted sagittal plane
Patient: Nina (Dashchund dog)

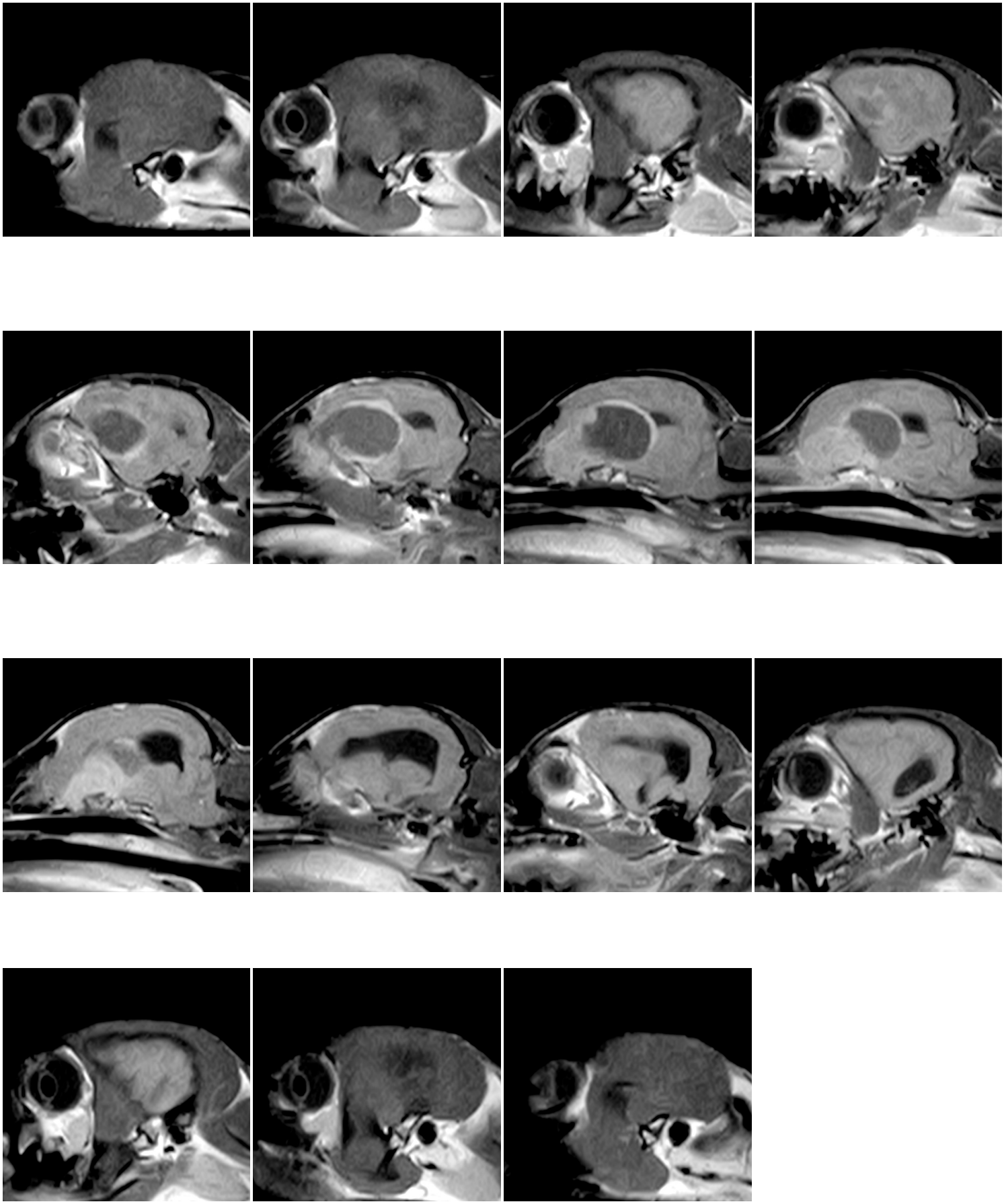

Nina MRI 6 - **DAY 78** - Post contrast T1 weighted transversal plane
Patient: Nina (Dashchund dog)